VARIABILITY AND UNCERTAINTY IN RADIATION DOSES TO MEMBERS OF THE U.S. POPULATION FROM NATURALLY-OCCURRING RADIONUCLIDES IN THE BODY

By

DAVID JUSTIN WATSON

A thesis submitted in partial fulfillment of
the requirements for the degree of

MASTER OF SCIENCE IN ENVIRONMENTAL SCIENCE

WASHINGTON STATE UNIVERSITY
School of Earth and Environmental Science

DECEMBER 2009

To the Faculty of Washington State University:

The members of the Committee appointed to examine the thesis of DAVID JUSTIN WATSON find it satisfactory and recommend that it be accepted.

_____

Daniel J. Strom, Ph.D., Co-Chair

_____

R. Gene Schreckhise, Ph.D., Co-Chair

_____

Paul S. Stansbury, Ph.D.

_____

Bruce A. Napier, M.S.

ACKNOWLEDGMENTS

I would like to thank Dr. Daniel J. Strom, Dr. Paul S. Stansbury, Dr. R. Gene Schreckhise and Mr. Bruce A. Napier for insightful discussions and guidance and Dr. Michael G. Stabin: For providing dose factors and helping me understand various aspects of internal dosimetry.

Mr. Timothy P. Lynch (of Pacific Northwest National Laboratories) graciously provided both ^{40}K and ^{137}Cs whole-body data and guidance on how to interpret them.

Dr. Anthony C. James and Dr. Sergei Y. Tolmachev (of the United States Transuranium and Uranium registries) graciously provided uranium and thorium data and helped me understand the data and the lab techniques behind them.

I would also like to thank Dr. Isabelle M. Fisenne for finding and digitizing one of her hard-to-obtain reports for me, Dr. Samuel E. Glover for insightful discussions, and Dr. Fred A. Mettler for providing UNSCEAR data.

Also, a large debt of gratitude is owed to Mr. Moussa (Moses) Jaraysi (of CH2M Hill Plateau Remediation Company) for authorizing financial support and advocating this work.

Finally, words cannot express the contribution of the subjects of the various studies used in this work. Without them a large body of knowledge would not exist.

VARIABILITY AND UNCERTAINTY IN RADIATION DOSES TO MEMBERS OF THE U.S. POPULATION FROM NATURALLY-OCCURRING RADIONUCLIDES IN THE BODY

Abstract

by David Justin Watson, M.S.
Washington State University
December 2009

Chairs: Daniel J. Strom, R. Gene Schreckhise

The U.S. public's annual effective dose from internally deposited, naturally occurring and anthropogenic radionuclides is calculated using dose factors for seven phantoms (adult male, adult female, newborn, 1-, 5-, 10-, and 15-year-old) from the Radiation Dose Assessment Resource. This study uses 11,741 lines of tissue concentration data from non-occupationally exposed individuals along with information on age, sex, geographic region, body mass index and smoking history, if available. These data–from the literature and from Pacific Northwest National Laboratory's In Vivo Radioassay and Research Facility–contain measurements of 15 radionuclides, including ^{3}H, ^{14}C, ^{40}K, ^{87}Rb, ^{137}Cs, and some members of the natural ^{238}U, ^{235}U, and ^{232}Th decay series. Assumptions about equilibrium with long-lived parents are made for the 28 other radionuclides in these series lacking data. After matching literature data to phantoms based on gender and age, radionuclide concentrations are imputed into all other phantoms' source regions, and the imputed values' uncertainties are increased. Within phantoms, concentration values are grouped into source tissue regions by radionuclide, and imputed into source regions lacking tissue data. Concentrations in the hollow-organ contents source regions are calculated and activities are apportioned to the bone source regions using assumptions about each radionuclide's bone-seeking behavior. Equivalent doses to target tissues from these source regions are estimated, and the target tissues are then mapped to lists of tissues with ICRP tissue weighting factors, or to surrogate tissue regions when there is no direct match. Effective doses, using ICRP tissue weighting factors recommended

in 1977, 1991, and 2007 are calculated from tissue and organ equivalent doses. An upper bound of variability of the effective dose is estimated by calculating the average coefficients of variation (*CV*), assuming all variance is due to variability. The estimate of an adult male's average annual effective dose of 418 μSv (*CV* = 0.68, geometric mean = 346 μSv, s_G = 1.85) using 2007 ICRP tissue weighting factors is higher than both the NCRP's estimates of 390 μSv in 1987 and 285 μSv in 2009, and is 31% higher than UNSCEAR's 310 μSv estimate in 2000. The causes of these differences are discussed.

TABLE OF CONTENTS

LIST OF TABLES

LIST OF FIGURES

Dedication

To Sara, my beautiful wife, who sacrificed too much time and invested so much energy to allow me to finish this degree.

To Justin and Mark, my sons. Now I can be a full-time father again.

To the memory of my grandparents, Oswald J. and Phyllis M. Wick, both of whom passed away while I was completing this degree. I wish they could have seen this.

VARIABILITY AND UNCERTAINTY IN RADIATION DOSES TO MEMBERS OF THE U.S. POPULATION FROM NATURALLY- OCCURRING RADIONUCLIDES IN THE BODY

David J. Watson and Daniel J. Strom*

Description of This Thesis

This thesis is comprised of a single manuscript in the style required by *Health Physics*, to which the manuscript will be submitted for publication.

Introduction

Estimates of effective doses to the American public from internally-deposited naturally-occurring and anthropogenic ubiquitous radionuclides provide benchmarks for comparison with other sources of ionizing radiation exposure. These estimates provide bases for regulatory bodies to set radiation protection standards and also help educate professionals and the general public. Internal deposition of naturally-occurring and anthropogenic radionuclides comprises a significant portion of an individual's annual effective radiation dose (NCRP 2009). On the average, the effective dose from internally-deposited naturally-occurring and anthropogenic radionuclides was recently estimated to be about seven times less than that from radon, but only slightly less than that from external cosmic radiation and only slightly more than that from external terrestrial radiation (NCRP 2009).

A complete estimate of the U.S. public's annual effective dose from naturally occurring and anthropogenic ubiquitous radionuclides in the environment includes cosmogenic and primordial radionuclides found in tissues. Cosmogenic radionuclides are created through interaction of cosmic rays with stable atoms, typically with low atomic numbers. Naturally occurring cosmogenic radionuclides include ^{3}H and ^{14}C (Cember and Johnson 2009). Primordial radionuclides originated during the formation of the earth and have not completely decayed due to their long half lives. The naturally occurring primordial radionuclides include ^{40}K, ^{87}Rb, and the uranium, actinium, and thorium series (Cember and Johnson 2009). Anthropogenic radionuclides are those created through human activity. These radionuclides from the nuclear fuel cycle and atmospheric nuclear weapons testing are globally-distributed and include ^{90}Sr, ^{129}I, and ^{137}Cs. The list of radionuclides considered in this study excludes natural and anthropogenic radioactive materials in the body resulting from occupational or medical intakes. Inhaled radon, thoron and their short-lived decay products in the respiratory tract are also excluded from this study. Note that ^{210}Pb and ^{210}Po are not included in the so-called short-lived decay products of ^{222}Rn that contribute to potential alpha energy exposure to the respiratory tract. Most of the radionuclides are part of natural background (U-, Th-, and Ac- series; ^{40}K; ^{87}Rb). Some are part of

unnatural background (^{137}Cs + ^{137m}Ba, ^{129}I, ^{90}Sr + ^{90}Y). Some are part of both natural and unnatural background (^{3}H, ^{14}C). In this study, ubiquitous naturally-occurring and anthropogenic radionuclides are referred to as ubiquitous radionuclides.

Radiation doses to humans from environmental levels of ubiquitous radionuclides have been estimated using tissue concentration studies of one or more naturally occurring radionuclides. The National Council on Radiation Protection & Measurements (NCRP) and the United Nations Scientific Committee on the Effects of Atomic Radiation (UNSCEAR) have published their estimates of effective doses to humans from naturally occurring radionuclides in the environment (NCRP 1987, UNSCEAR 2000). These estimates are based on concentration data for fewer than 10 tissues and, in the case of UNSCEAR, the data may not be limited to United States subjects.

This study calculates the effective dose to the U.S. public from ubiquitous radionuclides deposited in the body's tissues. Dose factors provided by Stabin and Siegel (2003) are used for calculating equivalent doses using a data set comprised from an extensive review of the literature. Only data from U.S. subjects, non-occupationally exposed to ubiquitous radionuclides, are used. This study also examines the relationship of age and gender on annual effective dose. In addition, it explores the changes in annual effective dose estimates arising from the differences between International Commission on Radiological Protection (ICRP) tissue weighting factor recommendations from 1977, 1990, and 2007. Data are too sparse for meaningful examination of effective dose on geographic location or physical characteristics such as body mass index. Variance in the data arises from both measurement uncertainties and inter- and intra-individual variability. Disaggregating uncertainty and variability is beyond the scope of this study. Instead, an upper bound of variability is estimated by calculating the average coefficient of variation (*CV*) for the total effective dose, and assuming all variance is due to variability and no variance is from uncertainty.

This study reviews historical papers from the literature and retains their original non-SI units for radionuclide activity or radionuclide activity concentration in tissue. When SI units in parenthesis follow historical units, the values associated with historical units are directly from the literature.

Literature Review

The sparse data available in the oft-referenced UNSCEAR (2000) and NCRP (1987) reports did not fit the objectives of this study, so a literature search was conducted to collect tissue concentration data for United States subjects. Data collection focused on tissues from non-occupationally exposed U.S. subjects, with data on age, sex, geographic region, body mass index, and smoking history, if available. While UNSCEAR (2000) and NCRP (1987) both report non-occupational tissue concentrations for selected tissues, the data are not correlated with age or sex and fewer than 10 tissues are reported in either report.

Tritium and carbon-14

An UNSCEAR (1982) report estimated tritium and ^{14}C activity concentrations in testes, lungs, red bone marrow, thyroid, bone lining cells and other tissues. The UNSCEAR report assumed the concentrations of ^{3}H per mass of H matched that of continental surface waters prior to above-ground nuclear weapons testing. Its estimate of 0.4 Bq tritium kg^{-1} tissue was assumed to be uniform across all human tissues. For its ^{14}C estimates, the concentration of ^{14}C in the body was assumed to be 227 Bq kg^{-1} and used reference man carbon tissue concentrations from ICRP (1975).

Potassium-40 and rubidium-87

Anderson and Langham (1959) measured whole-body potassium content of 1,590 males and females from one to 79 years old. Subjects were measured with a 4π liquid scintillation gamma counter. Data were presented as plots of mass concentration of potassium per kilogram of body mass against age. The authors reported a standard deviation of a single measurement in the age range of 5 to 68 years old as 7 to 15 percent, while the standard deviation of the mean for the same age group was 1 to 4 percent. The authors found both sexes exhibit similar concentration changes with age. There is a rapid increase in concentration from infancy to about age 9. There follows an equally rapid decrease in concentration from the peak age to age 13 for females and age 12 for males. Males exhibit a second peak at age 16, followed by a rapid decrease until about age 20. Both sexes then exhibit a less rapid decrease in potassium

concentration for the remainder of their lives. The rate of concentration increase and decrease is almost the same for both sexes in all cases except the males' second concentration peak in puberty.

Novak et al. (1970) measured the whole-body potassium content of 31 male and 33 female infants, each 32 days old. Subjects were counted while sleeping with a whole-body counter consisting of ten 18 × 18 × 6 inch (45.7 × 45.7 × 15.2 cm) plastic scintillators, each connected to 4 photomultipliers. Results were presented as mean mass concentration of potassium per kg of body mass. Uncertainty was presented as one standard deviation. The authors found slightly lower absolute total body potassium for females than males, but the difference was not statistically significant. The mean mass concentration of potassium was the same between genders (1.8 g kg^{-1}).

Novak (1973) followed up on Novak et al.'s (1970) study by measuring the whole-body potassium content of the same subjects. The same counter and techniques were used as the previous study. Data were presented as mass concentration of potassium per kilogram of body mass at 1, 4, 9 and 12 months old. Uncertainty was presented as one standard deviation. The author found an overall increase of total body potassium with age for both boys and girls. The author also found that boys had statistically significantly higher total body potassium levels than girls at each age. The author found the mass concentration of potassium remained generally the same for both sexes throughout the first year of life. Both sexes exhibited a decrease in concentration at 4 months, and girls has a slight increase between 9 and 12 months, but in all cases the concentration differences were not statistically significant.

Novak et al. (1973) also measured the whole-body potassium content of 111 adolescent males and 100 adolescent females. All subjects were aged between 11 and 15 years old. The authors used the same whole-body counter described in their previous study (Novak et al. 1970). Results were presented as mass concentrations of potassium per kilogram of body mass. The authors found a difference in patterns of concentrations by age between the sexes. Girls from ages 11 to 15 showed an overall decrease in concentration from 2.14 to 1.99 g K kg^{-1}, with a significant decrease in concentration at age 13. Boys showed a slight decrease in potassium concentration until age 13 from 2.26 to 2.21 g K kg^{-1}, then a significant increase to 2.32 g K kg^{-1} by age 15.

Cohn et al. (1977) examined ^{40}K concentration differences among races by measuring the total body potassium content of 26 black women and 21 black men and comparing the results to those of 40 white women and 27 white men matched by age. The subjects were counted in the Brookhaven National Laboratory's whole-body counter. Results were presented as total body potassium by sex and age group for the black subjects. Uncertainty was presented as coefficient of variation. Average body weight and height were also presented for each age group. White subjects' total body potassium results were presented by sex and age group as a ratio to the results of the black subjects. White subjects' average body weights and heights by age group were also presented as ratios to the black subjects results. Uncertainty was presented as coefficient of variation only for the average of all subjects. For each age group, the authors found no significant difference between total body potassium values between the races for either sex.

An UNSCEAR report (1982) added a thyroid estimate to its 1977 activity concentration estimates for ^{40}K and ^{87}Rb in testes, lungs, red bone marrow, bone lining cells and other tissues. The report presented ^{40}K tissue concentrations that were calculated using the average mass concentration of elemental potassium per tissue as reported by Kaul (1974, as referenced in UNSCEAR 1982), ICRP (1975) organ mass recommendations, and the isotopic ratio and specific activity of ^{40}K. The UNSCEAR report calculated ^{87}Rb concentrations using a similar methodology, but with ICRP (1975) reference-man rubidium mass concentrations, along with the isotopic ratio and specific activity of ^{87}Rb. The NCRP's 1987 report presented UNSCEAR's (1982) ^{40}K and ^{87}Rb estimates and added its own calculations for kidney and liver. The NCRP report calculated potassium and rubidium mass concentrations in liver and kidney by dividing ICRP's (1975) potassium and rubidium quantities by its tissue mass recommendations. They then used the resulting mass concentrations and specific activities of ^{40}K and ^{87}Rb as appropriate to calculate activity concentrations in tissue. The NCRP report (1987) also presented plots of UNSCEAR (1972) whole-body elemental potassium concentration data to age, with separate plots for sex.

Fisenne and Perry (1986) measured the potassium content of the lungs, liver, kidneys, and thoracic vertebrae of 58 deceased New York City residents. Samples were obtained from disease-free

cadavers at autopsy. Subjects were both male and female between 15 and 82 years of age. Tissues were wet ashed with nitric acid and diluted to 100 mL with nitric acid and measured by atomic absorption spectrophotometry. The authors provided results in mean mass concentration of potassium and found no statistical difference in the potassium concentrations of any tissue based on gender or age. Uncertainty was presented as standard deviation. The average potassium concentration for all ages and both genders was 1937 ± 467 μg K g^{-1} wet tissue in lung, 2734 ± 998 μg K g^{-1} wet tissue in liver, 2616 ± 1717 μg K g^{-1} wet tissue in kidney and 1863 ± 524 μg K g^{-1} wet tissue in vertebrae.

Strom et al. (2009) collected ^{40}K whole-body mass concentration data at the Pacific Northwest National Laboratory's in vivo Radioassay and Research Facility in Richland, Washington, U.S.A. Subjects were workers at the U.S. Department of Energy's Hanford site and were counted using an array of five germanium coaxial detectors. Mass concentrations of ^{40}K were determined by calculating the mass of potassium from the activity measurement and dividing by the worker's body mass recorded at the facility. Measurements were correlated to age and sex.

Cesium-137

Lynch supplied ^{137}Cs whole-body mass-concentration data collected at the Pacific Northwest National Laboratory's in vivo Radioassay and Research Facility in Richland, Washington, USA. Subjects were workers at the U.S. Department of Energy's Hanford Site and were counted using an array of five germanium coaxial detectors. All whole-body counts are baseline measurements on workers with no known occupational exposure to ^{137}Cs. Activity concentrations of ^{137}Cs were determined by dividing the worker's body mass recorded at the facility by the activity measurement. Measurements were correlated to age and sex.

Uranium series isotopes

Table 1 shows the radionuclides and tissues included in the articles containing usable data. Each study's parameters are listed in Table 2.

Hursh and Gates (1950) determined the radium content in the bodies of 25 adults and 6 stillborn infants. The bodies were thermally ashed, and 20-g aliquots of the ash were acid digested and dried

repeatedly until a clear solution was obtained. The solution was placed in a flask; the headspace flushed of radon, and allowed to sit for 11 to 12 days. The radon progeny in the flask's headspace was transferred to a counting chamber and alpha counted. Data were presented as mass concentration per gram of body ash. Uncertainty was presented as standard error. The authors found that the average whole-body radium content was about 100 times less than that found in a German study by Krebs (1942, as referenced in Hursh and Gates 1950), which was attributed to geographical differences or to technical difficulties with the analysis. The authors also noted that the first five bodies had higher radium contents, which was attributed to contamination of the bodies from being ashed on the crematorium floor, which contained radium-bearing fire-brick and mortar. Subsequent ashing was performed on a stainless steel bed. The authors reported that, among adults, the average whole-body radium content was 6.4×10^{-14} g Ra g^{-1} ash for all subjects and 5.0×10^{-14} g Ra g^{-1} ash for bodies ashed on stainless steel. The average whole-body radium content in stillborn children was 3.6×10^{-14} g Ra g^{-1} ash.

Hursh (1957) attempted to demonstrate that the large difference between his (1950) study and Krebs (1942, as referenced in Hursh 1957) results were not due to different separation technique and counting method. Hursh re-analyzed the ashes from 14 of the 25 subjects in his (1950) study, using Krebs' co-precipitation technique to separate the radium and place it on a glass plaque as radium-barium-sulfate for counting in a 2π proportional counter. The authors found, with one exception, that the results of each sample did not differ between analysis techniques "...by more than the uncertainty of the measurement" (Hursh 1957).

Palmer and Queen (1958) cremated 50 cadavers, and aliquots of the resulting ash were dissolved in hydrogen peroxide and nitric acid and dried. The resulting residue was dissolved in nitric acid and centrifuged. Samples were stored until radon-radium equilibrium was reached and were alpha counted. The authors found an average whole-body value of 0.47×10^{-10} g radium, which was consistent with previous studies.

Walton et al. (1959) dissolved previously ashed samples in hot hydrochloric acid, then filtered and thermally re-ashed them. The samples were then re-dissolved in hydrochloric acid, diluted with

distilled water, and placed in a vacuum apparatus. Residual radon was flushed out by bubbling nitrogen through the solution, which was then pressurized and allowed to stand for three days. The radon decay products were flushed into an ionization chamber with nitrogen and counted for 16 hours with a "low level radon counting apparatus" (Walton et al. 1959). The authors found an average skeletal concentration of 8×10^{-15} g radium g^{-1} bone ash.

Hursh (1960) measured ash from cadavers that had been ashed eight years before the analysis and, therefore, assumed equilibrium between ^{210}Po and ^{210}Pb. Ten-g aliquots of ash were digested in acid, from which ^{210}Po was plated onto silver foil and counted by a low background, gas-flow proportional counter. The Pb-210 content was calculated from the ^{210}Po results assuming that the lead resided in the skeleton during life, the wet skeleton mass was a factor of three times that of the whole-body ash, and all of the radon formed from decay during storage had escaped the storage container. The author found an average of 0.015 pCi (555 μBq) ^{210}Pb g^{-1} of wet bone in this study.

Black (1961) reported ^{210}Po concentrations in the ribs, sternum and lungs of 10 individuals as part of the development of a method to measure background levels of ^{210}Po and ^{210}Pb. The author wet ashed samples with nitric acid, then plated ^{210}Po on copper foil, and counted with an alpha scintillation counter. Results were presented as activity concentration of ^{210}Po per gram of wet bone weight. No uncertainty was reported.

Holtzman (1963) wet ashed bone samples and electroplated ^{210}Po on silver disks, which were then counted by proportional alpha counter to determine ^{210}Po content. For half of the subjects, ^{226}Ra measurements were made on the same samples as the polonium measurements. Radium measurements on the other half were made on different samples from the same subject. Radium was measured by radon determination method while calcium was precipitated from solution and weighed. Calcium mass was used in conjunction with calcium to ash ratios from previous studies to calculate the mass of ash in each sample. The Pb-210 content was calculated by measuring the daughter ^{210}Po in the samples three or more months later and using the results to calculate ^{210}Pb content. The Po-210 results were not reported. The average ^{210}Pb concentrations were determined to be 0.161 pCi (5.96 mBq) g^{-1} bone ash in men and 0.119

pCi (4.40 mBq) g^{-1} bone ash in women. Pb-210 concentrations were higher in trabecular bone than in cortical bone. The Ra-226 was uniformly distributed in the skeleton, and ^{210}Pb skeletal concentrations were inconsistent between subjects.

Hursh and Lovaas (1963) pooled samples from 10 subjects by tissue type for analysis, while the other subjects' tissues were analyzed individually. For individual analyses, radium was extracted from ashed tissue samples through a series of precipitations and then transferred to a stainless steel planchet. Individually analyzed bone samples "received preliminary treatment to remove calcium", after which the resulting ash was dissolved, and the radium separation continued using the procedure used for the pooled tissue samples. Pooled samples of each tissue type were combined after thermal ashing and dissolved in nitric acid. Radium was extracted from the samples through a series of precipitations. The precipitate was washed, dissolved in distilled water, and transferred to a planchet. All planchets were stored until daughter products reached equilibrium, and then the planchets were counted two or more times using either a gas-flow alpha counter or a scintillation detector. The authors found the clavicle had the highest radium concentration (averaging 3.4×10^{-14} g Ra g^{-1} wet tissue mass), followed by vertebrae (averaging 1.1×10^{-14} g Ra g^{-1} wet tissue mass) and liver (0.18×10^{-14} g Ra g^{-1} wet tissue mass). The authors calculated a whole-body burden of 2.64×10^{-11} g ^{226}Ra, of which 80 per cent was found in the skeleton.

Hallden et al. (1963) dry ashed bone samples, added a barium carrier, and then dissolved the samples in HCl. A multi-step process yielded $BaRaSO_4$ precipitate, which was removed, dissolved in an acid solution, and held for five hours to allow build up of the ^{222}Rn daughter product. The sample was then gamma counted twice for 14 hours and the two results averaged. The mean concentration of ^{226}Ra was found to be 0.026 pCi (0.962 mBq) g^{-1} Ca in subjects from San Francisco and 0.032 pCi (1.184 mBq) g^{-1} Ca in subjects from New York City.

Segall (1963) correlated the natural radioactivity in New England bedrock to skeletal ^{226}Ra, ^{224}Ra, and ^{210}Po concentrations. Teeth were analyzed using a newly developed technique described by Hunt et al. (1963). No significant correlation between tooth ^{226}Ra and ^{210}Po concentrations and bedrock radioactivity were found.

The role of natural concentrations of ^{226}Ra, ^{228}Ra and ^{210}Pb in osteogenic sarcoma was investigated by Lucas et al. (1964). Samples were obtained from non-occupationally exposed patients with osteogenic sarcoma. Each sample was obtained from bone adjacent to the tumor, cleaned of soft tissue and dried at 100°F (37.8°C). The samples were analyzed as described in Lucas et al. (1963). When compared to previous studies of individuals without cancer, the authors found significantly higher ^{226}Ra and ^{228}Ra concentrations in the sarcoma patients, while lead-210 concentrations were not significantly different. They attributed the elevated radium tissue concentrations to higher radium concentrations in Midwestern drinking water.

Ferri and Baratta (1966) presented ^{210}Po concentrations in the lung, liver, kidney, heart and psoas muscle (a muscle on both sides of the lumbar region of the backbone, connecting it to the femur) of both smokers and non-smokers. The analysis was part of a larger study examining the ^{210}Po content in tobacco from various cigarette brands and the ^{210}Po content of cigarette smoke. The authors did not describe their analytical procedure for the human tissue, nor did they identify the geographical region from which the tissues came. Results were presented in pCi g^{-1} of wet tissue and no uncertainty was reported. The authors found ^{210}Po present in both tobacco leaves and tobacco smoke, and also found that ^{210}Po concentrations in tissues of smokers was consistently higher than those of non-smokers, except for the psoas muscle.

Blanchard (1966) presented ^{210}Pb and ^{90}Sr concentrations in bones from 14 infants from Cincinnati, Ohio. The author was examining correlations between ^{90}Sr and ^{210}Pb concentrations in bone because of their similar deposition patterns in the body. After ashing and dissolving the bone samples in hydrochloric acid, ^{210}Po was deposited on a nickel planchet for alpha counting. The ^{210}Pb activity was then calculated from the counting results and used to calculate the concentration in bone. Results were reported as activity concentrations per gram of calcium in bone and no uncertainty was reported. The author reported a correlation between ^{210}Pb and ^{90}Sr in the skeleton.

Baratta and Ferri (1967) reported ^{210}Po concentrations were highest in bone, with the highest soft tissue concentration in liver after examining several tissues from a number of deceased subjects in the Boston area. Organs were wet ashed and counted for ^{137}Cs. The Po-210 was then electrodeposited on

silver for counting, after which, the ^{90}Sr was "determined by routine methods". The Cs-137 was evenly distributed throughout the body and total ^{137}Cs body burden was extrapolated to be 20 nCi (740 Bq). Twice as much ^{90}Sr was found in male subjects' organs as female subjects. Vertebral ^{90}Sr concentrations were extrapolated to total skeleton burdens of 0.47 nCi (17.3 Bq) in males and 0.40 nCi (14.8 Bq) in females. The Po-210 concentrations were found to be the same order of magnitude as previous studies and were higher in the lungs, blood and psoas muscle of smokers when compared to non-smokers. The authors did not find a difference between ^{210}Po concentrations in other organs between smokers and non-smokers.

Pb-210 and ^{210}Po tissue concentrations were also reported by Blanchard (1967). Organs were wet ashed and ^{210}Po was electrochemically deposited on a silver disc for alpha counting by a low background ZnS(Ag) scintillation counter. After storing the remaining solution for 4 to 6 months, ^{210}Po was again electrochemically deposited on a silver disc, which was counted and considered to represent the amount of ^{210}Pb in the sample. The author found substantial variance in the radionuclide content of each tissue group, particularly the liver and kidney. He also found the largest percentage of ^{210}Pb and ^{210}Po was in the skeleton, and that ^{210}Po tends to accumulate in the liver and kidney, while ^{210}Pb accumulated in the lung. Factoring the subjects' smoking histories into the study, the author found a statistically significant increase of ^{210}Po concentrations in all smokers' tissues and of ^{210}Pb concentrations in smoker's livers.

Lovaas and Hursh (1968) determined the suitability of using teeth as an analog for bone for bioassay purposes by studying the correlation between tooth and bone concentrations of ^{226}Ra and ^{210}Po. The authors used 10 to 20 grams of wet bone and all available teeth from each cadaver. Samples were wet ashed and "...lead-210 values were obtained by electrodeposition of an equilibrium quantity of ^{210}Po on silver foil...". The silver foil was counted using a gas flow proportional counter and the results decay corrected to account for the five to seven years between time of death and counting. Radon was separated from the sample using helium entrainment, dried, collected in a liquid nitrogen cooled copper trap, and transferred to a scintillation chamber for counting. Mean bone concentration fell within 50% of the mean

tooth concentration at the 95% confidence interval when the tooth value was at or above 0.019 pCi (703 μBq) g^{-1} ash.

In 1969, Baratta et al. expanded Baratta and Ferri's 1967 study to include subjects throughout the United States and analysis for ^{210}Pb. The ^{137}Cs and ^{210}Po were analyzed as described in Baratta and Ferri (1967) and ^{210}Pb was determined by counting its ^{210}Bi daughter product after separation using an ion-exchange precipitating technique. The ^{137}Cs tissue concentrations were decreasing compared to the authors' previous study's (Baratta and Ferri 1967) results and concentrations were highest in the liver and lowest in the ilium. The authors calculated an average ^{137}Cs total body burden of 7.48 nCi (277 Bq) in 1966 and 3.63 nCi in (134 Bq) 1967, using their analytical results. The Po-210 was found concentrated in the lung and liver, while ^{210}Pb was found concentrated in the muscles. Each set of results was noted to be log-normally distributed.

Martin (1969) used bones from 75 skeletons to determine ^{226}Ra activity concentrations in bone. The subjects for the study resided in various parts of the United States, but had died in the state of Wisconsin. The author did not describe the methods used in his study. He found that the log mean of 33 fCi (1.22 mBq) ^{226}Ra g^{-1} Ca was in agreement with other ^{226}Ra bone concentration studies performed at the time.

Hunt et al. (1970) measured ^{90}Sr, ^{137}Cs, and ^{210}Po in various human tissues obtained at autopsies in the Boston area. Samples were wet ashed, then diluted to provide suitable counting geometry. The Po-210 was "spontaneously plated" on a silver disk; however, the author does not indicate what was done to the sample following that step. He found that the highest polonium concentration was in the bone, and the highest soft tissue concentration for females was in the liver and for males was the kidney. The author also noted that tissue concentrations "did not differ markedly" between smokers and non-smokers.

Bogen et al. (1976) measured ^{210}Pb in vertebrae from 13 individuals from New York City. Samples were analyzed using procedures in Harley (1972). Results were provided in activity concentrations per gram of bone ash. No uncertainty was reported in the results. The author reported an average ^{210}Pb content of 0.20 pCi (7.4 mBq) g^{-1} ash.

Fisenne et al. (1981) estimated the average skeletal alpha dose by country by combining ^{226}Ra bone concentration results from several studies, including original work. Vertebral samples were dry ashed, and analyzed for calcium by atomic absorption spectrophotometry or by potassium permanganate titrations. Radium was extracted by coprecipitation as sulfate with stable barium carrier, after which the sulfate was dissolved in alkaline ethylenediaminetetraacetic acid (EDTA). The radium content was determined using the radon emanation method and the results were normalized to the stable calcium results. The authors found the median ^{226}Ra concentration in bone for the 26 countries in the study was 30 fCi (1.11 mBq) g^{-1} of calcium with a geometric standard deviation (s_G) of 2.0. The authors used the median concentration to calculate a median annual alpha dose for the global population of 0.4 mrad (4 μGy) y^{-1} (assuming critical dose was 10 μm from the bone surface) with a 70-year median lifetime dose of 28 mrad (280 μGy).

Wrenn et al. (1981) presented ^{230}Th tissue concentrations in a study of thorium concentrations in humans described below.

Broadway and Strong (1983) studied ^{90}Sr, $^{238,239-240}$Pu, ^{234}U, ^{235}U and ^{238}U activity concentrations in bone. Their subjects died in various geographical regions of the United States between 1972 and 1975 (although uranium data were only available for 1975). Samples were thermally ashed and counted with silicon surface-barrier detectors to establish the plutonium and uranium radionuclide concentrations. The ^{90}Sr was measured through beta counting. The authors found a decrease in $^{239–240}$Pu and ^{90}Sr bone concentrations compared to previous studies' results. The authors couldn't correlate age and uranium bone concentration. They found enrichment of ^{234}U in bone, but rejected artificially enriched uranium uptake as a source, noting that ^{234}U enrichment was common in nature.

Singh et al. (1985) analyzed rib, sternum, and vertebrae samples of Colorado and Pennsylvania subjects to determine uranium, thorium, and plutonium concentrations in bone. Samples were spiked with ^{232}U, ^{229}Th, and ^{242}Pu tracers and wet ashed. Uranium, thorium, and plutonium separated from solution using a multi-step precipitation and back extraction process. All the radionuclides were electroplated onto platinum discs for alpha-spectrometer counting. Activity concentrations of radionuclide per kilogram of

wet bone weight were presented with standard deviation but were not correlated to age or sex. No statistical difference was found between the two populations for the radionuclides analyzed, except for ^{234}U, ^{238}U, and ^{230}Th being more abundant in the ribs of the Colorado population. In the different types of bone, ^{234}U had the highest concentrations, followed by ^{228}Th, ^{238}U, ^{230}Th, ^{239,240}Pu, ^{232}Th, ^{235}U, and ^{238}Pu. The concentrations of all radionuclides analyzed were highest in the sternum, except for ^{230}Th, which was most abundant in the ribs.

Singh et al. (1989) determined plutonium and uranium concentrations in vertebrae, ribs, and femoral head samples. Femoral head samples were obtained from a population undergoing hip surgery, while the ribs and vertebrae samples were collected at autopsy from former Utah residents. The samples were wet ashed, then uranium and plutonium were extracted separately using with a sequential process of precipitation, acid dissolution, back extraction and electrodeposition on a platinum disc for analysis with an alpha-spectrometer. Mean activity concentrations of ^{239,240}Pu, ^{238}U, and ^{234}U per kg of wet weight were presented and separated by bone type. Uncertainty was presented as one standard deviation. Age and sex of the subjects were not noted. The authors found that uranium and plutonium concentrations in the femoral head were not significantly different from those in the vertebrae and ribs, offering an alternative sampling method for measuring actinide skeletal burden.

Harley and Fisenne (1990) used bones from a previous study by Martin (1969) to examine bone content of ^{234}U, ^{235}U, ^{238}U, ^{230}Th, ^{232}Th, and ^{226}Ra. The previously ashed samples were re-blended and dissolved in HCl. Uranium was extracted through precipitation and alpha counted. Thorium was extracted from the waste solution through precipitation and measured by alpha spectrometry. Radium was extracted from the waste solution through precipitation and measured by radon emanation into pulse ionization chambers. Activity concentration of the radionuclides per kg of bone ash and were correlated to age and sex. The authors found the radionuclides studied were homogeneously distributed throughout the skeleton.

Non-occupational concentrations of ^{230}Th in several tissues were provided by the United States Uranium and Transuranium Registry (USTUR)[‡], which analyzed a whole-body donation from a worker

who had been occupationally exposed to plutonium and americium (USTUR case 0212). Tissue samples were thermally ashed, then wet ashed using HNO_3 and H_2O_2 and dissolved in 8M HCl. Selected aliquots were then analyzed for plutonium and americium content using an ion exchange and solvent extraction method, while other aliquots were analyzed for thorium using both alpha spectrometry and neutron activation methods.

USTUR[§] also provided tissue concentration data for ^{234}U, ^{235}U, and ^{238}U from the analysis of a whole-body donation from a subject occupationally exposed to plutonium but without any known exposure to uranium (USTUR case 0425). Tissue samples were thermally ashed, and then wet oxidized using HNO_3 and H_2O_2, and finally dissolution in 6–8M HCl. Aliquots were taken from the sample set and analyzed for ^{234}U, ^{235}U, and ^{238}U using alpha spectrometry and kinetic phosphorescence analysis. Results were presented as activity concentration per kg of wet tissue and uncertainty was reported as standard deviation.

Momcilovic and Lykken (2007) published data on whole-body activity of ^{214}Bi in 385 women and 175 men in North Dakota. While they did not publish the mean and standard deviations of the data, they published equations that predict whole-body activity variations over the year. These equations can be averaged over a year to approximate the average annual value of the data. For both sexes, the "95% prediction interval" on a natural log scale seems to vary over about 4, implying a lognormal distribution and that A(97.5 percentile)/A(2.5 percentile) ~ exp(4) = 54.6, which corresponds to a geometric standard deviation (s_G) of 2.774 for both sexes. The arithmetic means and standard deviations due to variability inferred from this s_G are 490 ± 770 Bq for men and 393 ± 720 Bq for women, with geometric means of 250 Bq and 233 Bq, respectively. These data, while intriguing, are not used in the present work as they cannot be apportioned to individual tissues and organs. Most of the ^{214}Bi is probably due to inhaled ^{222}Rn and its decay products. Only a small part of this translocates out of the respiratory tract to other tissues. Some ^{214}Bi is produced from the decay of ^{226}Ra in the body.

Thorium series isotopes

Table 3 relates radionuclides and tissues to the articles containing usable thorium series data. Each study's parameters are listed in Table 4 and the analytical methods and results are described in the text following the tables.

Lucas et al. (1970) examined the natural concentrations of ^{232}Th in rib bones obtained at autopsy or during surgery. Soft tissue was removed from the samples and they were dried at 110°F (43.3°C) and stored at –10°C prior to analysis. Samples were thermally ashed, placed in quartz tubes, and irradiated along with thorium standards in a nuclear reactor. After seven days, the samples were removed from the tubes and dissolved in hydrochloric acid. The ^{233}Pa, the activation product of ^{232}Th, was extracted from solution using an ion exchange column, eluted from the column and counted with a 4 × 2 inch (10.2 × 5.1 cm) sodium iodide detector combined with a multichannel analyzer, utilizing an iterative least squares computational method. The standard deviation of the results determined by "the standard method from the counting statistics and the deviation from duplicate standards". The authors found a general increase in ^{232}Th concentration in bone with age.

Singh et al. (1985) presented ^{228}Th and ^{232}Th activity concentrations in bone along with the uranium series results previously summarized.

Wrenn et al. (1981) determined the concentration of several thorium isotopes in human tissues. Samples were wet ashed with nitric acid after addition of ^{229}Th tracer. Bone samples were heated and digested with nitric acid to remove organics. Other tissues were heated with nitric acid and treated with H_2O_2 to remove organics. Calcium and thorium were extracted from bone solution using a multi-step precipitation process. Plutonium and thorium were co-precipitated from soft tissue solutions with a multi-step precipitation and back extraction process. Thorium was electrodeposited onto a platinum disk after organics removal. The disk was counted by an alpha spectrometer consisting of a 300-mm^2 silicon detector with a multichannel analyzer. The concentration of ^{230}Th was higher than that of ^{232}Th in all tissues. Tissue concentrations of ^{232}Th and ^{230}Th were highest in the lymph nodes, followed by the lung, bone, kidney, and liver. Tissue concentrations of ^{228}Th were highest in the lymph nodes, followed by the

bone, lung, kidney, and liver. The concentration of thorium in the pulmonary system of New York subjects was in equilibrium with air. The thorium isotopes' relative distribution was different among the organs analyzed and ^{228}Th was more abundant in bone than ^{232}Th which was attributed to decay of ^{228}Ra independently taken up by bone.

Non-occupational concentrations of ^{232}Th and ^{228}Th in several tissues were provided by the USTUR, which analyzed a whole-body donation from a worker who had been occupationally exposed to plutonium and americium using methods previously described.

Actinium series isotopes

Actinium series isotopes were often analyzed along with uranium and thorium series isotopes. Uranium-235 tissue concentrations were reported by Broadway and Strong (1983), Singh et al. (1985), and Harley and Fisenne (1990), whose articles have been previously summarized. Table 5 presents the parameters of these studies.

Elemental rubidium

No studies of rubidium-87 tissue concentrations were found in the literature search. Since ^{87}Rb concentrations can be calculated from its natural isotopic ratio and elemental rubidium tissue concentrations, part of the literature search focused on obtaining elemental rubidium tissue concentration data. In general, trace element studies tended to focus on non-U.S. populations or, more often, did not include rubidium. Table 6 relates tissue to article for usable rubidium elemental concentration data and the analytical methods and results are described in the text following the table.

UNSCEAR (1972) presents mass concentrations of elemental rubidium originally from Spier (1968).

Iyengar et al. (1988) compiled human tissue element concentrations from data in the literature. Data were obtained using a variety of techniques and had been previously published. Since the authors drew from studies around the world, only data from U.S. sources were carried forward into this study.

Elemental uranium

Three studies focused on elemental uranium concentrations in tissue. Data from these studies were collected with the intent of using isotopic ratios of uranium radionuclides to calculate their tissue concentrations. The tissues analyzed in each study are related to article in Tables 7 and 8 show the parameters of each study. The analytical procedures are described in the text following the table.

Fisenne et al. (1988) compiled a number of studies on uranium concentrations in human tissue. The authors found that muscle and fat were possibly major repositories for uranium and that the median skeletal burden was 30µg. The authors calculated the average alpha doses based on United States data were 0.5 µGy y^{-1} for lungs, 0.13 µGy y^{-1} for liver, 0.36 µGy y^{-1} for kidney, and 0.25 µGy y^{-1} for bone surfaces (10 µm from bone surface).

Fisenne and Welford (1986) measured elemental uranium concentrations in various human tissues. Dry ashing was chosen for soft tissues and most vertebrae samples to provide comparison values with previous dry ash studies. A ^{232}U tracer solution was then added to all samples, which were then wet ashed by acid dissolution. Uranium and iron were separated from the solution by anionic-exchange column chromatography, after which the iron was removed through electrolysis. The mass of uranium in the resultant solution was determined fluoroscopically and the chemical yield of the uranium was established by alpha-counting the ^{232}U tracer. The mean skeletal uranium burden in New York City residents between the ages of 14 and 73 was 6.6 µg while the soft tissue uranium burden was 8 µg, which was lower than the ICRP reference man estimate of 67 µg for the same tissues studied (ICRP 1975).

Kathren (1997) measured elemental uranium concentration in the tissues of two non-occupationally exposed USTUR whole-body donations (USTUR cases 0213 and 0242). Both subjects had recorded occupational exposure to plutonium but no known exposure to uranium. Tissue preparation followed a procedure described by McInroy et al. (1985) and resulting solutions were analyzed for uranium using kinetic phosphorescence analysis (KPA). The author found that uranium primarily concentrated in bone and found agreement between the results (4.8 ng g^{-1} net weight and 5.8 ng g^{-1} net weight) and the reference man (ICRP 1975) value (5.9 ng g^{-1}). Concentrations between bone types varied,

and concentration variability in soft tissues was noted with the highest concentrations found in the pulmonary lymph nodes and the lowest in the liver. Notably, one case had an abnormally high thyroid concentration.

Materials and Methods

Seven distinct lists of organs, tissues, and/or anatomical regions were used in this study, as enumerated in the list of acronyms in Table 9.

Tissue concentration data were obtained from studies in the open literature and other sources of non-occupationally exposed U.S. subjects. The resulting data set contained 11,741 lines of data, compiled from 42 studies published between 1950 and 2008 as well as uranium and thorium data provided by the USTUR and whole-body ^{137}Cs activity data from Pacific Northwest National Laboratory's In Vivo Radioassay and Research Facility. An individual datum in the set of data collected from the literature is called a tissue (in vivo or autopsy) datum (TIVAD). The TIVADs are further subdivided between the original literature data (LitTIVADs) and the set of data that has been aggregated or disaggregated from the LitTIVADs and which represent measurements of individuals in the original sample population (intermediate TIVADs, iTIVADs).

General description of method

Forty naturally occurring (primordial and cosmogenic) and three anthropogenic radionuclides were considered in this study (Table 10). Strontium-90 and ^{129}I were not considered further because of an absence of recent data for these radionuclides. Strontium-90 taken in as a result of atmospheric nuclear weapons test has undergone over 1.5 physical half-lives of radioactive decay and significant translocation and elimination. Radon exposures by inhalation were excluded due to their short half-lives and lack of tissue concentration bioassay results.

Figure 1 illustrates the general methods used in this analysis. The methods are described in the following text.

Dose factors

The analysis used radionuclide-specific dose factors, F_D, from the Radiation Dose Assessment Resource (RADAR)** as described by Stabin and Siegel (2003). These dose factors were used for assessing a target organ's equivalent dose from a source region within the body. The RADAR used seven phantoms (i.e., 1) newborn, 2) 1-year-old, 3) 5-year-old, 4) 10-year-old, 5) 15-year-old, 6) adult male and 7) adult female) to calculate the dose factors. The RADAR dose factors allowed dose assessment to be conducted among 25 separate target tissues from nuclear transitions in 28 different source regions. The dose factors incorporated a radiation weighting factor of 20 for alphas. The specific absorbed fraction (SAF) for calculating alpha dose to organ walls of hollow-organs used an International Commission on Radiological Protection (ICRP [1975]) recommended value as described by

$$SAF = \frac{0.01}{2m_c}, \tag{1}$$

where, m_c is the mass of the contents of an organ. RADAR dose factors are medically oriented, so certain, gender-related combinations had dose factors of 0 mSv MBq-s^{-1} (e.g., testes to ovaries, testes to uterus, ovaries to testes, uterus to testes, etc.).

Differences among studies, coupled with sparse U.S. tissue concentration data, resulted in considerable gaps in the final data set where tissue concentrations of a given radionuclide were missing for a particular age range or gender. Filling these gaps required developing methods for imputing missing tissue, age, and sex data for each radionuclide. Imputation is a method whereby missing values in a data set can be replaced by plausible values drawn from similar or related data sets (Fox-Wasylyshyn and El-Masri 2005). The current analysis used “hot deck” imputation, where the missing data was filled in using values from the set of tissue concentration values for the same radionuclide (Fox-Wasylyshyn and El-Masri 2005, Gelman and Hill 2006), attempting to first use data from the closest surrogate tissue, and then using other imputation methods. Tissue concentrations obtained in the literature review were matched by age and sex as appropriate to the phantoms represented by the RADAR dose factors. The

resulting data subsets were further matched by tissue to intermediate source regions (InSRs - Table 11), which were then mapped to available RADAR source regions (RASRs). Some InSRs (i.e., soft tissues, and uncertain) do not have matching RASRs, and others (i.e., Bone_Group, Gonads, and Total Body) could not be directly matched to a RASR without additional imputation to map them into an appropriate RASR. Missing tissue data were then imputed from existing measurements.

Tissue results were only available for a few longer-lived progeny within decay series, requiring imputation of existing results through each decay series. Finally, tissue concentration results for each radionuclide were imputed between phantoms as necessary. The RASR activities were calculated from the concentration measurements using ICRP (1975) organ and tissue masses.

Absorbed dose calculations were made for each RASR and RADAR target tissue (RATT) combination using the RASR activities and RADAR dose factors. The RATTs were mapped to lists of target tissues (TarTs) having ICRP tissue weighting factors (ICRP 1977, ICRP 1990, ICRP 2007). When ICRP TarTs had no corresponding RATTs, they were mapped to an appropriate surrogate RATT. Equivalent doses to tissues and organs were calculated and combined to produce a 1977 effective dose equivalent, or 1990, or 2007 effective dose using ICRP tissue weighting factor recommendations from those years (ICRP 1977, ICRP 1990, ICRP 2007).

Data entry

If available in tabular form, data were hand-keyed from the original literature into a relational database created specifically for this study. All data were keyed in original (historical) units, with unit conversions performed by the software. Data fields in the database's concentration data table are summarized in Table 12. If data were only available as points on a graph, the individual values were digitized from the graph, and then transferred to the database. Anderson (1959) and Hallden (1963) provided individual results as points on a graph. Holtzman (1963) provided ^{210}Po concentrations in trabecular and cortical bone as points on a graph, but these data could not be correlated with the individual results in tabular form and were rejected.

Each record was assigned a unique alphanumeric identifier (UID). Measurement records from a single person contained an additional, individual-specific, UID to facilitate grouping data by individual. Each record also contained an article code identifying the source of the data. These three identifiers allowed traceability of the data back to their source and identifying groups of data needing aggregation. If the measurement type (e.g., mean concentration) and uncertainty (e.g., standard deviation) were noted in the study, that information was recorded. Age and gender of individual subjects were entered when available; age was recorded as –1 and gender recorded as "unk" when unavailable. Records containing average concentrations from a population also contain the number of subjects in the population. Measured tissue name, subject location, and smoking history were also recorded when available.

Quality assurance

Quality assurance is a systematic, planned regimen of checking the data used in, and software created for, the current work. Quality assurance ensures that data were transcribed to electronic form correctly and that the software operates as intended.

Data were visually checked against the original articles and further checked through graphic exploration. When available, isotopic ratios in the data were examined to ensure the data show no enrichment.

A software code was written to normalize and perform statistical analyses on the data and to calculate absorbed tissue doses, equivalent tissue doses, and effective dose. The code imports RADAR dose factors, ICRP (1975) reference man mass values and formatted concentration data. Its graphical user interface displays the results of each calculation stage, which can be exported to a variety of formats for further analysis. Any data errors or anomalies encountered during loading and calculation are automatically recorded for troubleshooting. The software was tested following a test plan shown in Appendix A prior to use.

Data normalization

The variety of concentration units found in the original literature required converting data to MBq kg^{-1} wet tissue activity concentration. Associated uncertainty and variability were transformed with the

same conversion prior to converting them to standard deviation. A judgment was made for some multi-person averages where the authors did not specify whether the uncertainty statistic was a sample standard deviation or a standard deviation of the mean. The latter was converted to a sample standard deviation by multiplying by $\sqrt{N}$, where N is the number of data points. Furthermore, it is highly doubtful that authors of earlier papers fully accounted for measurement uncertainty as well as variability within the available samples. When no uncertainty statistic was given in the original paper, a coefficient of variation of 0.5 was arbitrarily chosen. Figure 2 shows the method used to load and convert the tissue concentration data collected from the literature.

Additional data transformations were required depending on the measurement units. Bone measurements reported relative to mass of bone ash were converted relative to mass of wet tissue by

$$C_{\text{bone}} = C_{\text{ash}}\left(\frac{m_{\text{ash}}}{m_{wet}}\right) \tag{2}$$

where, C_{ash} is the reported bone ash concentration, m_{wet} is the wet bone mass in the skeleton of Reference Man (ICRP 1975) and m_{ash} is bone ash mass in the skeleton of Reference Man (ICRP 1975). Cortical and trabecular bone ash ratios were calculated by similar methods.

Hursh and Gates (1950), Hursh (1957) and Palmer and Queen (1958) provided whole-body radium activities measured in ash from cremated cadavers. Palmer and Queen (1958) also reported the mass of the ash from each cremated cadaver. In this case, the data were normalized using

$$C = C_{\text{ash}}\left(\frac{m_{\text{ash}}}{m_{\text{wet}}}\right) \tag{3}$$

where, C_{ash} is the reported whole-body ash concentration, m_{wet} is the Reference Man (ICRP 1975) whole-body mass and m_{ash} is the reported whole-body ash mass. When no ash weight was provided (e.g., Hursh and Gates 1950 and Hursh 1957), the data were normalized using a ratio of Reference Man ash mass to Reference Man whole-body mass.

Hallden et al. (1963) reported their bone activity measurements per gram of calcium. In this case, the data were normalized using a ratio of the mass of calcium in bone as reported by IRCP (1975), divided by the mass of bone in Reference Man (IRCP 1975).

The NCRP (1987) provided plots, originally in an UNSCEAR report (1972), of total body potassium concentration by age for both women and men. The curves represented 10,000 measurements, but the number of measurements for each age was not indicated. The 1970 U.S. census data (U.S. Bureau of the Census 1975) was used to estimate the number of subjects in each RADAR phantom represented in the curve. Population data from the 1970 census (the year closest to the report date) are organized by age and gender. The census data are organized in age ranges, so equal age distribution in each range was assumed. The number of subjects of each RADAR phantom age in the NCRP (1987) ^{40}K results was calculated by

$$n_{\text{phan}} = \frac{\left(\frac{n_{\text{pop}}(a)}{N_{\text{Tot}}} \right)}{y}, \tag{4}$$

where, n_{phan} is the number of subjects of a RADAR phantom age, n_{pop} is number of people in the U.S. in age range a, N_{Tot} is the total U.S. population, and y is the number of years in the age range.

Correlating subject age and gender to phantom age and gender

Articles reported on various ages and sexes depending upon subject availability or study parameters. Reported subject ages were correlated to RADAR phantom ages. When an age range was given in an article, the average of the range extents was used to match to a RADAR phantom. When no age was reported, the tissue measurement was considered to be that of an adult.

Once subject ages were adjusted as needed, a method was developed to realistically match each datum to a RADAR phantom based on age. An obvious method would be to use the midway point between phantom ages to create age bins for assigning phantoms (e.g., data from subjects younger than three years old would be assigned to the 1-year-old phantom and data from subjects older than three years

old would be assigned to the 5-year-old phantom). Plots of growth rates over time (ICRP 1975) show growth rates are larger early in life and level off in a person's 20s. Therefore, using a geometric mean as a division between age bins is more appropriate than using the midway point. The age used to divide between the newborn and 1-year-old phantoms is the age when 50% of the 1-year-old mass is attained (4.5 months [ICRP 1975]). Table 13 shows the ages used to divide data between phantoms.

Data matched to an adult phantom were assigned based on the reported gender. If no gender was reported, the datum was assumed to represent an adult male.

Elemental data

If tissue concentration data were absent for radionuclides with natural abundance, then elemental tissue concentrations and isotopic ratios were used. Commonly, elemental studies focus on uranium, but potassium and rubidium studies were also found. Radionuclide-specific activities were calculated by

$$A_{\mathrm{sp}} = \frac{\lambda f_{\mathrm{nat}} N_{\mathrm{a}}}{m_{\mathrm{a}}}, \tag{5}$$

where, f_{nat} is isotopic natural abundance, N_{a} is Avogadro's number, and m_{a} is the atomic mass.

Left-censored data

Censoring is only reporting data precisely within a certain range. For instance, left-censored data is data that falls below a reporting threshold, and is reported as less than that threshold (e.g., "< 0.01 Bq g^{-1}"). Left-censored tissue concentration data (e.g., < 0.91 Bq g^{-1}) were converted to one-half the reported maximum value. Since left-censored concentrations were reported without uncertainties, a standard deviation was calculated for the adjusted concentration such that the tissue concentration value had less than a 5% chance of being above the maximum reported value. This calculation was made using

$$s = \frac{C_{\mathrm{adj}}}{\mathrm{NORMSINV}(0.95)}, \tag{6}$$

where, s is standard deviation, C_{adj} is the adjusted concentration and the NORMSINV() function converts a probability (in this case 95%) into a standard normal deviate—in this case, 1.645.

Imputing across phantoms

Scarce data required imputing juvenile and adult female tissue concentrations from abundant adult male tissue concentration data to determine age and sex dependency of effective doses. Adult male concentrations were applied to the adult female phantom when no tissue data existed with which to perform cross-tissue imputation. When no data existed in a juvenile RASR, adult male and adult female values for the same RASR were used. In all cases, the standard deviations of the concentrations were increased to account for the uncertainty associated with using adult male values for juveniles and adult females. Figure 3 illustrates the methods used to impute missing tissue data across phantoms, which is described in the following text.

The standard deviations were increased by the equivalent of an s_G of 1.5 using

$$s = C_n \sqrt{e^{(\ln s_G)^2} - 1}, \tag{7}$$

where, $s_G = 1.5$.

Tissue masses were required for aggregating concentration data from studies containing repeated measurements of the same or related tissues from the same individual. Tissue masses for juvenile and adult female phantoms were imputed when the tissue concentration data were imputed. The ICRP (1975) organ and tissue mass values by age were used when available.

The USTUR autopsy data contained mass measurements for individual bones—most of which were not listed in ICRP (1995)—from adult subjects, requiring bone mass imputation for juvenile phantoms. Bone masses were required for mass-weighted averaging of the concentration data. The major regions of the body (e.g., skull, lower limbs, etc.) make up different fractions of total bone mass as an individual ages. For that reason, imputing juvenile individual bone masses required a calculation more complex than simply multiplying the juvenile total bone mass by a mass ratio of an individual bone to total bone in an adult. The USTUR analysis protocol calls for analyzing the tissues from one side of the body and it was observed that not all bones in a skeletal region were analyzed. Therefore, the sum of bone mass in the subject's skeletal regions was unavailable, and the total ICRP (1995) skeletal region mass was

used instead for calculating individual bone mass fractions for use in the juvenile bone imputation. The USTUR bone names were matched to ICRP bone names (e.g., "metacarpal 5" to "hands"), which were in turn matched to one of the four major divisions of the skeleton for which ICRP (1995) had estimates of total bone mass percentages by age. The masses of the major divisions of the skeleton for juvenile phantoms were calculated by multiplying the region's mass fraction (ICRP 1995) by the reference total bone mass (ICRP 1995) for each phantom age. Individual bone masses for each phantom were then calculated using

$$m_b(k) = m_b(\mathrm{A}) \times \frac{m_{R_{\mathrm{skel}}}(k)}{m_{R_{\mathrm{skel}}}(\mathrm{A})}, \tag{8}$$

where, m is mass, b is bone, R_{skel} is skeletal region, k is juvenile phantom and A is adult male phantom.

As with the USTUR bone data, autopsy data for non-bone tissues from the USTUR often contained tissue measurements of portions of an organ. Again, a tissue's mass fraction had to be established to impute tissue mass for a juvenile phantom prior to aggregation using mass weighted averaging. As with the USTUR bone data, a ratio of analyzed soft tissue mass to ICRP (1975) organ mass was used in the calculations. Juvenile organ masses were obtained from ICRP (1975). The mass of a given portion of a juvenile organ was then calculated by

$$m_v(k) = m_v(\mathrm{A}) \times \frac{m_o(k)}{m_o(\mathrm{A})}, \tag{9}$$

where, m is mass, v is a specified portion of a tissue or organ, o is organ, k is juvenile phantom and A is adult male phantom.

Data imputation

Figure 4 diagrams the methods used to aggregate and disaggregate tissue concentration data, as appropriate, within a TIVAD. These methods are further described in the following text. Aggregation or disaggregation started with a set of LitTIVADs, which are TIVAD measurements directly from the literature. The result of aggregation or disaggregation was a set of iTIVADs, which are TIVAD measurements representing the original sample population.

The radioactivity tissue concentration data from the literature were in one of several forms:

- repeated measurements of the same or related tissues (e.g., different bones) from the same individual;
- single measurements of tissues or organs from individuals;
- or averages of measurements from two or more individuals.

In the first case, results were reduced to the second case by mass- and inverse variance-weighted averaging. If the standard deviation of the *i*th concentration measurement within the same organ or tissue of an individual, $s_i(C_i)$, was predominantly due to measurement uncertainty rather than to variability within the individual, combining mass weighting with inverse variance weighting gives the best mass-averaged concentration

$$\overline{C}^* = \sum_i w_i C_i \tag{10}$$

where,

$$w_i = \frac{\frac{m_i}{s_i^2}}{\sum_j \frac{m_j}{s_j^2}} \tag{11}$$

This approach was used to combine data from multiple samples from the same individual, such as bone, muscle, kidneys, and lymph nodes. The unbiased estimator of the weighted population variance (Wikipedia 2009) is

$$s^2\left(\overline{C}^*\right) = \frac{1}{1-\sum w_i^2} \sum w_i \left(C_i - \overline{C}^*\right)^2 \tag{12}$$

This variance includes components of intra-individual variability and measurement uncertainty.

Bone was the predominant tissue requiring aggregation of subtypes. The data were observed to contain a number of bone types for adult, but only femur for 5- and 10-year-olds and only femur and humerus for 15-year-olds. The ICRP (1995) did not provide individual bone masses, but provided the

percent contribution of selected bones to the overall skeletal mass. Adult bone masses were calculated from the data in ICRP (1995) using

$$m_b = f_b m_{\text{skel}}, \tag{13}$$

where, m_b is the mass of bone b, f_b is the percentage of total fresh skeletal weight contributed by bone b and m_{skel} is total skeletal bone mass. Calculating individual bone masses for juveniles is slightly more complicated because ICRP (1995) only presented the mass contribution of major divisions of the skeleton rather than for individual bones. Since ICRP (1995) data for juveniles were separated by gender and RADAR juvenile phantom dose factors apply to combined genders, the arithmetic mean of the two sets of ICRP (1995) values for each juvenile age was used to determine bone masses. Bone masses for juveniles were calculated using

$$m_b(\mathrm{k}) = \left(\frac{f_b(\mathrm{k})}{f_b(\mathrm{a})} \right) \overline{m}_b(\mathrm{a}), \tag{14}$$

where, $\overline{m}_b(\mathrm{a})$ is the arithmetic mean of the adult male and female masses for bone b as calculated in Eq. (13), f_b is the percentage of total fresh skeletal weight contributed by the bone b, a is adult and k is juvenile.

Once repeated measurements of the same or related tissues from an individual were reduced to single measurements of tissues or organs from an individual, the multi-person averages in the data set were disaggregated. This left the problem of correctly preserving the variability information in multi-person averages while combining those averages with single measurements of tissues or organs from individuals.

The problem was one of disaggregating a concentration value from the literature that is an average over N persons into N positive numbers that have the same mean and standard deviation as the concentration value from the literature. The approach taken here was to convert multi-person average data

(along with their standard deviations) to lognormal distributions having the same arithmetic mean and standard deviation as reported in the literature using the following:

$$\ln s_G = \sqrt{\ln\left(\frac{s^2}{\overline{C}^2} + 1\right)} \tag{15}$$

and

$$C_{50} = \overline{C}\exp\left(-\left(\ln s_G\right)^2 / 2\right), \tag{16}$$

where, C_{50} is the geometric mean and s_G is the geometric standard deviation (Strom and Stansbury 2000). From this lognormal distribution, a sample of N concentration values was drawn, one from the center of each of N probability intervals. The cumulative probabilities (quantiles) of each of the N concentration values q_i, $n \in \{1, 2, \ldots, N\}$, generated in this way are

$$q_i = \frac{i - 0.5}{N}, \tag{17}$$

corresponding to standard normal deviate ("z-scores") of

$$z_i = \text{NORMSINV}\left(q_i\right) \tag{18}$$

where, the NORMSINV() function converts a probability into a standard normal deviate. For each z_i, a concentration value for the nth individual, C_i, was generated using

$$C_i = \exp\left(\ln C_{50} + z_i \ln s_G\right). \tag{19}$$

This procedure was followed for each multi-person radioactivity concentration average for a given radionuclide j and tissue type v, maintaining separate values by age, sex, and geographic region as data permitted.

For $N < \infty$, the C_i values generated by Eq. (19) have a mean that is less than $\overline{C}$ and a standard deviation that is less than s because, while the procedure creates a value in the center of each of N probability intervals, it fails to sample the extreme values well enough. It can be shown that there is no value of s_G that produces a lognormal distribution with mean $\overline{C}$, for which C_i values generated by Eq.

(19), have the correct value of s. However, by replacing the 0.5 in Eq. (17) with a smaller number f_{KN}, each sampled value is shifted to the right in the probability interval:

$$q_i = \frac{i - f_{KN}}{N}, \tag{20}$$

as reported by Kumazawa and Numakunai (1981, 1991). For each N and s_G, a value of f_{KN} can be found by iteration that preserves $\overline{C}$ and improves the agreement of the standard deviation of the sample with the value of s from the original literature. This method was used here.

Aggregating or disaggregating the sample data resulted in a dataset comprised of iTIVADs, which are radioactivity concentration values for j radionuclides in one or more tissues, v, in N individuals. For each radionuclide, these iTIVADs needed to be aggregated by ages and tissues corresponding to those of the RADAR phantoms. Figure 5 illustrates the procedure for aggregating these data into concentration values for RADAR source regions (RASRs).

The disaggregated C_i values were combined with the previously aggregated and individual values and the arithmetic mean and standard deviation of this complete set of iTIVADs was calculated using

$$\overline{C}_{j,v} = \frac{1}{n}\sum_i C_{i,j,v} \quad \text{and} \tag{21}$$

$$s(\overline{C}) = \sqrt{\frac{1}{N-1}\sum_i \left(C_i - \overline{C}\right)^2} \quad , \tag{22}$$

where, $\overline{C}$ is the arithmetic mean of iTIVAD concentrations, n is the number of iTIVADs, C_i is the ith iTIVAD concentration and $s(\overline{C})$ is the standard deviation of the arithmetic mean of iTIVAD concentrations. Thus, the values of $\overline{C}$ and $s(\overline{C})$ found in this way are stored as the radioactivity concentration values and standard deviations for each RASR v, radionuclide j, age group, and sex.

Negative results

Values less than zero in observed activity or concentration arise when counting small amounts of radioactive materials in a sample, and by chance the background is larger than the sample count. Negative

values cannot be used with many of the equations described in this study because the logarithm of a negative number is undefined. Furthermore, a negative concentration value is not a “possibly true” result. To manage the problem of negative values, a new lognormal distribution was created using the arithmetic mean and standard deviation from the population. This distribution represents a set of “possibly true” data values (Hofer 2008), albeit with both measurement uncertainty and variability contributing to the variance. This method preserves the most important statistics from the population—the arithmetic mean and standard deviation—and provides usable values from a population having the same characteristics as the one originally measured. The new non-negative distribution of "possibly true" values was then sampled to produce the same number of data as were in the original population, thus avoiding rejection of data with negative values. This sample replaced the original data.

Figure 6 illustrates this method by superimposing a lognormal distribution of possibly true values over the distribution of data from Lynch (2009). The arithmetic mean and standard deviation have been preserved between the two distributions, but the new distribution of possibly true values contains no negative values.

Bone surface and bone volume seeking radionuclides

Bone was separated into four distinct source regions: 1) trabecular bone surface, 2) trabecular bone volume, 3) cortical bone surface, and 4) cortical bone volume. Once concentration values for bones were aggregated into an average bone concentration, it was applied to the bone surface or bone volume source region based on the radionuclide's affinity for either region. The present analysis used a simplifying assumption that a radionuclide is exclusively non-bone-seeking, exclusively bone-surface-seeking or exclusively bone-volume-seeking.

Radionuclides were categorized using elemental data provided by ICRP (1979, 1980, 1981). Primordial series radionuclides in equilibrium were assumed to be formed in situ from decay of the parent radionuclide and, therefore, the activity from these progeny was considered to be partitioned in bone the same as activity from the parent radionuclide regardless of ICRP (1979, 1980, 1981) data. Activity from non-series radionuclides, those at the head of a primordial chain or those in disequilibrium was treated

based on the data in ICRP (1979, 1980, 1981). Table 14 lists radionuclides and their classifications in the current analysis as 1) non-bone seeking, 2) bone surface seeking or 3) bone volume seeking.

Imputing data into source regions lacking data

Three approaches can be considered to account for the correlation in activity concentrations in the various organs and tissues within an individual who is exposed to radioactive materials in the environment:

1. Deterministic biokinetic models such as those of the ICRP predict a linear relationship between organs and tissues, so that the correlation between concentrations is one.
2. The degree of correlation can be assessed by examining published data from single individuals, such as USTUR cases.
3. Data from different geographic regions when two or more tissues have been analyzed can be compared.

The last two approaches were outside of the scope of this study. Therefore, for the assessment of variability, a correlation coefficient of one was assumed.

Figure 7 illustrates the method used to impute tissue concentrations for RASRs which are missing concentration values.

For every phantom, a mass-weighted average of tissue concentration values was calculated to apply to tissues lacking concentration data. The approach was to combine the aggregated activity concentration data for each tissue from the same phantom into a mass-weighted average using equations (10) and (11). The population variance of the mass-weighted average was estimated using Eq. (12). The set of tissues used to calculate the average values excluded kidneys, liver, lungs, and bone because they can preferentially accumulate some radionuclides and including these tissues could have biased the average upwards.

Once RASR concentrations were compiled from the data, the activity contained in a RASR was calculated using

$$A_\zeta(\zeta, j, a, g) = C_\zeta(\zeta, j, a, g) m_\zeta, \quad (23)$$

where, A_ζ is the activity in the RASR, C_ζ is the activity concentration in the RASR, m_ζ is the RASR mass, ζ is the RASR, j is the radionuclide, a is the phantom age and g is the phantom gender (when applicable). The RASR masses were those used by Stabin and Siegel (2003) to calculate the RADAR dose factors.

Radium-228 was the only radionuclide in disequilibrium with its parent without sufficient data to impute activities between RASRs. Only ^{228}Ra concentrations in bone were available in the literature. Radium-228 activities in other tissues were imputed by applying the ratio of ^{226}Ra and its parent, ^{230}Th, to tissue activities of ^{228}Ra's parent, ^{232}Th. This was justified because both radium isotopes have long-lived thorium parents and both have additional intake routes from diet so that uptake of ^{228}Ra and ^{226}Ra from diet should have similar fractions. Figure 8 shows the procedure used for imputing ^{228}Ra activities.

Imputing "remainder of the body" activity

In vivo measurements and some whole-body ash studies present results for the whole-body. The RADAR total body source region encompasses those tissues remaining after the other RASRs have been removed. This method avoids double-counting of radionuclide contributions. Since total-body activity results include all tissues and organs, the remainder of the body activity was imputed to accommodate the RADAR total-body dose factor. Figure 9 illustrates the method used to calculate the remainder of the body activity for each RADAR phantom.

When total-body activity existed for a given phantom and radionuclide combination, the remainder of the body activity was calculated by

$$A_{\text{remainder}}(j, a, g) = A_{\text{TotalBody}}(j, a, g) - \sum A_v(j, a, g) \quad (24)$$

where, v is tissue or organ, A is activity, j is radionuclide, a is age, and g is the phantom gender (if applicable). When total body measurements were unavailable, the soft tissue source region was used as a surrogate for the remainder of the body RASR. The remainder of the body activity was estimated using

$$A_{\text{remainder}}(j, a, g) = \left(m_{\text{RemainingTissue}}(j, a, g) - m_{\text{Muscle}}(j, a, g)\right) C_{\text{ST}}(j, a, g), \quad (25)$$

where, ST is the soft tissue source region, A is activity, C is activity concentration, m is mass, j is radionuclide, a is age, and g is the phantom gender (if applicable). Stabin and Siegel (2003) described the remaining tissue mass as that which is left after removing the mass of all defined organs from the whole-body mass. Since the present analysis considered muscle activity separately, the muscle mass was removed from the remaining tissue mass to calculate the activity in the remainder of the body.

Hollow-organ contents

The RADAR dose factors are available for RASRs (contents of organs, or RASCOs) to accommodate absorbed dose calculations for hollow-organ walls from ingested radionuclides (e.g., stomach contents, urinary bladder contents) or those in systemic circulation (e.g., heart contents).

Since no hollow-organ contents data were available in the data set, a method of estimating hollow-organ content activities was developed for the current analysis. Figure 10 illustrates the procedure for imputing hollow-organ content activities, which is described in the following text.

Unlike radionuclides in tissues and organs, radionuclides in organ contents are transitory and move through the organ at a defined rate. Primordial radionuclides, series isotopes in disequilibrium, and cosmogenic radionuclides were assumed to be ingested and were, therefore, considered in the hollow-organ content analysis. Table 15 shows the radionuclides for which intake data were obtained.

Activities of hollow-organ contents in the urinary bladder (UB) contents, upper large intestine (ULI) contents, lower large intestine (LLI) contents, stomach, and small intestine (SI) contents RASCOs were calculated using

$$A_j = t_\zeta \dot{I}_j \tag{26}$$

where, A_j is the activity of radionuclide j in MBq, t_ζ, is the mean residence time of RASCO ζ in days from ICRP (1979), and $\dot{I}_j$ is the intake rate of radionuclide j in Bq day^{-1} from ICRP (1975).

Since ICRP (1975) presented intake rates for ^{210}Po and ^{226}Ra in pCi day^{-1}, other radionuclides of interest were calculated from the elemental intake rates presented by ICRP (1975) using f_{nat} the specific activity of the radionuclide of interest using

$$\dot{I}_{\mathrm{a}} = \dot{I}_{\mathrm{m}} f_{\mathrm{nat}} A_{\mathrm{sp}} \tag{27}$$

where, $\dot{I}_{\mathrm{a}}$ is the activity intake rate, $\dot{I}_{\mathrm{m}}$ is the elemental mass intake rate, f_{nat} is the natural abundance of the radionuclide and A_{sp} is the specific activity of the radionuclide. Radionuclides without natural abundances were not considered in the analysis, with the exception of ^{228}Ac, which is a significant gamma emitter.

For each region of the gastrointestinal tract, some of radionuclide *j* was assumed to be absorbed by the previous region (that is, the activity of radionuclide *j* will be lower in the small intestine because some was absorbed by the stomach). Since ICRP (1975) did not provide "intake" rates for urinary bladder or lower large intestines, it was assumed that the loss from those RASCOs equaled the intake. Thus, $\dot{I}_j$ was different for each RASCO. Using this method, the concentrations of all radionuclides in the ULI contents and LLI contents were less than or equal to the contents of the stomach and small intestine contents. Some were greatly depleted (e.g., ^{14}C was 2% and ^{3}H was 4% of the values in the upstream compartments). Similarly, ^{40}K (11%) and ^{87}Rb (14%) were depleted. With the exception of ^{210}Pb (68%), all other radionuclides were between 84% and 100% of the upstream values. The values of $\dot{I}_j$ for phantoms other than adult male were scaled by a ratio calculated by intake or loss data, as appropriate, provided by ICRP (1975).

In its 1996 report, UNSCEAR presented specific activity for tritium in surface water. In the current analysis, daily water intake was considered to have the same tritium content as surface waters. Additionally, the specific activity reported by UNSCEAR (1996) for ^{14}C is for food, eliminating the need for additional assumptions.

The gastro-intestinal (GI) tract-related organ content source regions include stomach contents, small intestine contents, upper large intestine contents, lower large intestine contents, urinary bladder contents, and gall bladder contents. In its 1979 report, ICRP provided residence times for all but the urinary bladder and gall bladder. Since the gall bladder does not obtain contents directly from ingestion, its content data were imputed separately. Urinary bladder residence time was estimated using

$$t_r = \frac{t_w}{\left(\frac{(V - V_o)}{V_p}\right)}, \tag{28}$$

where, t_r is the residence time in days, t_w is the time awake each day in days (assumed to be 15 hours), V is the volume of urine voided per day (ICRP 1975), V_o is the estimated urinary bladder overnight capacity, and V_p is the average urinary bladder physiological capacity (ICRP1975). It was assumed that voiding occurs at the first sensation to void—defined by ICRP (1975) as the physiological capacity—and that the bladder is at its maximum physiological capacity upon waking in the morning.

Since ICRP (1975) only reported elemental intake, fecal loss, and urinary loss rates for adult male, these rates were estimated for the other phantoms in the current analysis. The ICRP (1975) presented total mass intake, fecal loss, and urine loss rates for adult males, adult females, and 10- and 1-year-old children. Isotopic intake and loss rates can be scaled by using ratios of adult male total intake or loss rates to those of other phantoms. Total mass intake and loss rates for 5- and 15- year-old children and newborns were not reported. They were developed by performing a linear regression using the rates reported by ICRP (1975). Plots of mass intake rates of principal nutrients by age in ICRP (1975) allow a better estimation of the intake rates of 5- and 15- year old children and newborns than the linear regression method employed for fecal and urine loss rates.

Organ contents for gall bladder and heart were imputed by

$$(v' \in V') \Rightarrow (A_{v'}(j,a,g) = m_{v'}(j,a,g) C_{ST}(j,a,g)), \tag{29}$$

where, v' is organ contents, V' is the set of organ contents in heart or gall bladder, ST is soft tissue, A is activity, C is activity concentration, m is mass, j is radionuclide, a is age, and g is the phantom gender (if applicable).

Apportioning activity into cortical and trabecular bone

As noted previously, bone was segregated into four distinct RASRs. Calculated bone activity was averaged over the entire bone, so the value had to be partitioned among the four RASRs. The ICRP's 1995 report defines a total bone reference mass ratio as 80% cortical and 20% trabecular. Activity was

apportioned into the four RASRs by multiplying the total bone activity by 0.8 to obtain the activity in the cortical bone surface and cortical bone volume, and by 0.2 to obtain the activity in the trabecular bone surface and trabecular bone volume. Figure 11 shows the procedure used to apportion activity into trabecular and cortical bone.

Imputing through series

Following data imputation between tissues within a phantom, missing tissue data were imputed in decay series. Figure 12 shows the method used to impute tissue concentration data in decay series.

Starting with the first radionuclide in the chain, missing tissue activities for the progeny radionuclides were imputed using

$$\left(R_j \in \varepsilon\right) \Rightarrow \left(A_{R_j} = A_{R_1}\right) \tag{30}$$

where, R_j is the j^{th} radionuclide in a chain, R_1 is the 1st radionuclide of the chain, ε is the set of radionuclides in equilibrium with R_1 and A is the activity of the radionuclide. Radionuclides in disequilibrium and radon were then used as R_1 for subsequent progeny imputation using Eq. (30).

Radionuclides assumed to be in disequilibrium (Table 16) are generally well characterized in the literature, with the exception of 32,800-y ^{231}Pa, 21.8-y ^{227}Ac and 5.75-y ^{228}Ra. No tissue concentration data were found in the literature for ^{231}Pa or ^{227}Ac. It is not possible for ^{231}Pa to grow into radioactive equilibrium with its parent, ^{231}Th, in a human lifetime, nor is it likely that there is no tissue accumulation of ^{231}Pa at all. This also holds true for ^{231}Pa's progeny, ^{227}Ac. Accordingly, two sets of calculations were made to test the sensitivity of the final effective dose to unknown tissue activity variabilities for these radionuclides: one assuming both equilibrium between ^{231}Th, ^{231}Pa and ^{227}Ac and the other assuming no ^{231}Pa and ^{227}Ac activities.

Radon presented a special problem as a portion of it diffuses out of the tissue containing it prior to decaying into a non-gaseous element. Radon-219 and ^{220}Rn have sufficiently short half-lives (3.96 s and 55.6 s, respectively) to assume minimal escape prior to decay and the fractional retention factors from NCRP (1987) were used for these radionuclides. A portion of ^{222}Rn, with a half-life of 3.823 days, was

assumed to absorb into the bloodstream to be carried to the lungs and exhaled. Srivastava (1986) noted that 100% of radon formed in soft tissues will escape and 70% formed in bone will escape. To account for this loss, it was assumed that the remaining ^{222}Rn activity in bone is 0.3 times the activity of the immediate parent. The fraction of ^{222}Rn activity remaining in soft tissues was calculated using

$$f_A = 1 - \left(\frac{f}{f + \lambda} \right) \tag{31}$$

where, f_A is fraction of remaining activity, f is release fraction for ^{222}Rn from soft tissue to blood (100 day^{-1} [ICRP 1994]), and λ is the decay constant for ^{222}Rn (0.181 day^{-1}). Using this equation, the fraction of remaining ^{222}Rn activity in soft tissue is 1.81×10^{-3}.

Fractional retention for other selected radionuclides was considered when imputing between radionuclides in a series. Fractional retention factors used came from NCRP (1987) and are shown in Table 17.

Imputing weighting factors for tissues in the RADAR list that are not in ICRP

The RADAR target regions, *z,* did not always match one-for-one with tissues for which the ICRP has published risk-based tissue weighting factors w_T. An appropriate surrogate tissue was used whenever possible, for instance, activity in the thymus was used for the esophagus, for which there is no RADAR target region. The dose contribution from ICRP tissues without credible surrogates was calculated by applying a scale factor to the final effective dose using

$$SF = \frac{1}{1 - \sum_T w_{UT_y}}, \tag{32}$$

where, w_{UT_y} is tissue weighting factor from ICRP recommendations of year *y* without a match to a RADAR target tissue. The scale factor did not include gender-inappropriate organs. Therefore the scale

factor for the adult male did not include the tissue weighting factor for uterus and the scale factor for adult female did not include the tissue weighting factor for prostate.

The ICRP's 2007 report listed 13 remainder organs and applied a collective tissue weighting factor of 0.12 to the group. The present analysis used a tissue weighting factor for each of these remainder organs, calculated by

$$w_T = \frac{w_T(r)}{G}, \tag{33}$$

where, $w_T(r)$ is the collective tissue weighting factor for the remainder organ group and G is the number of tissues in the remainder organ group.

Calculating equivalent doses

The complete sets of activities for each phantom were converted to equivalent dose rates using

$$\dot{H}(\tau, j, a, g) = \sum_{\zeta} A(\zeta, j, a, g) F_{\mathrm{D}}(\zeta, \tau, j, a, g), \tag{34}$$

where, A is activity, F_{D} is RADAR dose factor, j is radionuclide, a is age, g is gender, ζ is RASR, and τ is RATT.

Calculating effective doses

Effective doses were calculated for each year for which ICRP (1977, 1990, 2007) issued tissue weighting factor recommendations using the equivalent dose rates calculated with Eq. (34). Effective doses were calculated using

$$E_y(a, g) = (3.16 \times 10^7 \,\mathrm{s}) \sum_T w_{T_y} \sum_j \dot{H}_T(j, a, g), \tag{35}$$

where, w_{T_y} is tissue weighting factor from ICRP (1977, 1990, 2007) recommendations of year y. The resultant effective dose only included contributions from ICRP (1977, 1990, 2007) target tissues that had corresponding RADAR target tissues (RATTs). The ICRP tissue weighting factors for gender-inappropriate organs were changed to zero in this calculation, thus the effective dose to uterus in the male

and prostate in the female are both 0 mSv. Multiplying the effective dose by the scale factor calculated in Eq. (32) provided the effective dose accounting for TarTs without RATT equivalents.

Propagating variability

The data used in this study have variances that are a combination of measurement uncertainty and inter- and intra-individual variability. Ideally, variance due to measurement uncertainty would be removed so that all variance is due to variability (Hofer 2008). In this study, variability was propagated by calculating an upper bound assuming all variance was due to variability and assuming that all activities in every tissue and organ for every radionuclide were highly correlated. Estimating the average coefficients of variation approximated the variability of the effective dose. This was calculated using

$$CV(E_j) \approx \frac{\sum_T w_T H_{T,j} CV(H_{T,j})}{\sum_T w_T H_{T,j}} \text{ and} \tag{36}$$

$$CV(E) \approx \frac{\sum_j E_j CV(E_j)}{\sum_j E_j} \tag{37}$$

where, $CV(E_j)$ is the coefficient of variation of the effective dose E from radionuclide j, w_T is the ICRP tissue weighting factor, $H_{T,j}$ is the equivalent dose H to ICRP TarT T from radionuclide j, $CV(H_{T,j})$ is the coefficient of variation of the equivalent dose H to ICRP TarT T from radionuclide j, $CV(E)$ is the coefficient of variation of the annual effective dose E, and E_j is the effective dose from radionuclide j.

Results

Average annual effective doses from internally deposited ubiquitous radionuclides were calculated for members of the U.S. public. These effective doses were calculated using 11,741 tissue concentration measurements from 42 articles, data provided by the United States Uranium and Transuranium Registries (USTUR) and data from Pacific Northwest National Laboratory's (PNNL) in

vivo counting facility. When tissue concentration data were absent, they were imputed from concentration values from other tissues, other radionuclides or other phantoms as appropriate.

Table 18 contains the average annual effective doses to the seven populations studied, based on the RADAR phantoms used in this study, along with the coefficient of variation for each estimate, representing the upper bound of variability. Table 18 also presents the geometric standard deviation and average annual effective doses at the 1^{st}, 5^{th}, 50^{th}, 95^{th} and 99^{th} percentiles for each population studied.

Juvenile average annual effective doses generally increase with decreasing age, except for the 1-year-old using 2007 and 1990 ICRP tissue weighting factors and the 15- and 10-year-old are higher than the other juveniles using 1977 tissue weighting factors. The adult female average annual effective dose was lower than expected (Figure 13). Annual effective doses to all populations studied decreased as more recent ICRP tissue weighting recommendations were used in the dose calculations. The overall effective dose decrease results from decreased weighting for gonads in each successive set of recommendations.

Figure 14 shows the contribution of each radionuclide in the study to overall average annual effective dose to the adult male using 2007 ICRP tissue weighting recommendations. Potassium-40 provides the highest effective dose, which is 49% of the overall effective dose. Polonium-210 and ^{226}Ra provide 27% and 7% of the annual effective dose, respectively. All other radionuclides contributed 2% or less of the total annual effective dose.

In the adult male, and using 2007 ICRP weighting factors, non-series primordial radionuclides account for the highest percentage (50%) of the average annual adult male effective dose, primarily due to equivalent doses from ^{40}K. The uranium series provide the next highest percentage of overall dose, contributing 38% of the average annual effective dose. The thorium series contributes 10% of the average annual effective dose. All other radionuclide categories (i.e., anthropogenic, cosmogenic, and the actinide series) collectively contribute less than 2% of the total average annual effective dose. Dose contributions from high- and low-LET radiations are nearly evenly split. Alpha-emitting radionuclides provide 47.5% of the dose, the majority of which (37.7%) comes from the uranium series. Beta- and gamma-emitting radionuclides account for 52.5% of the average annual effective dose, the majority of which (50.3%)

comes from non-series primordial radionuclides. Table 19 shows the contribution of each radionuclide category and each type of radiation to the overall average annual effective dose to the adult male using 2007 ICRP tissue weighting factors.

Using 2007 ICRP tissue weighting factors, lung makes up the largest percentage of average annual effective dose (Table 20), followed by red bone marrow and gonads. However, when using 1990 and 1977 tissue weighting factors, gonads make up about a quarter of the average annual effective dose due to the higher tissue weighting factors for gonads in these years' recommendations.

Potassium-40 contributes the highest annual equivalent dose to all RATTs except the osteogenic cells. In the adult male, ^{40}K contributes between 42% and 77% of the total annual equivalent dose to all RATTs except for the pancreas, thyroid and osteogenic cells. In the pancreas and thyroid, ^{40}K accounts for 34% and 22% of the total annual equivalent dose, respectively. In the osteogenic cells ^{210}Po contributes 43% of the total annual equivalent dose, which is a higher percentage than that from ^{40}K (8%).

As with the adult male, and using 2007 ICRP tissue weighting factors, the adult female's and 15-year-old's lungs receive the highest annual weighted equivalent doses, followed by bone marrow. In the newborn, 1-, 5- and 10-year-old, the order is reversed, with bone marrow receiving the highest annual weighted equivalent dose. Table 21 displays, by population studied, the annual weighted equivalent doses to TarTs whose annual weighted equivalent doses are about 10% or greater of the average annual effective dose.

Two separate analyses were performed to establish bounding dose values from ^{231}Pa and its progeny because of an absence of data for these radionuclides. One analysis assumed that ^{231}Pa is in secular equilibrium with its parent ^{231}Th and the other assumed no ^{231}Pa activity. Assuming secular equilibrium for ^{231}Pa and its progeny increases the average annual effective dose estimate for the adult male using 2007 ICRP tissue weighting factors by 2 µSv, from 418 µSv to 420 µSv. Another set of analyses examined the contribution of hollow-organ contents to average annual effective dose. Removing hollow-organ contents from the analysis decreases the average annual effective dose using 2007 ICRP tissue weighting factors to the adult male by 4% from 418 µSv to 402 µSv. Figure 15 shows how adult

male average annual effective doses are affected when either organ contents are removed from, or ^{231}Pa and progeny are added to, the analysis.

Discussion

Uncertainty and variability

There are many sources of uncertainty in the average effective dose results. Radioactivity concentration measurements themselves are often uncertain, with coefficients of variation of tens or hundreds of percent not uncommon. The data are so sparse that, for many radionuclides and many ages of people, there are no values in the literature. Imputation of values from measurements in adult males, and to a lesser extent, from adult females, is a highly uncertain process. The degree of radioactive equilibrium between parent and progeny has to be assumed for many radionuclides. For ^{222}Rn and ^{220}Rn formed from the decay of ^{226}Ra and ^{224}Ra in the body, the fraction of activity remaining in various tissues and organs in the body is uncertain. Dosimetric phantoms used in the RADAR dose calculations are approximations of real people, and individuals vary systematically from those phantoms. Since those variations are unknown, they become uncertainties in this analysis.

Detailed propagation of uncertainty is beyond the scope of this project because it would require many lengthy Monte Carlo simulations. Instead, the combination of variability and uncertainty is treated as an upper bound of inter-individual variability. These upper bounds correspond to geometric standard deviations of lognormally-distributed effective doses in the range of 1.7 to 2.0, depending on the phantom. This leads to ranges of effective doses that vary by a factor of 10 or more as shown in Table 18.

Comparisons with the NCRP's estimates

The NCRP's Report No. 93 estimates an annual effective dose equivalent of 390 μSv to an adult male from internally deposited radionuclides (NCRP 1987). The NCRP does not detail its calculation methods, but the tissue concentrations used in its estimate are presented in NCRP Report No. 94 (1987). Directly comparing the results from the current analysis to those of the NCRP requires modifying the current analysis to use the previously described methods but only include data for radionuclides

considered in the NCRP's analysis (i.e., the ^{238}U and ^{232}Th series, ^{3}H, ^{40}K, ^{87}Rb and ^{14}C). Tritium, ^{87}Rb and the actinium series are minor contributors to overall annual effective dose. Removing them from the analysis produces no appreciable change in the annual effective dose to the adult male using 2007 tissue weighting recommendations. Using the same tissue weighting recommendations (ICRP 1977) as the NCRP (1987) in this modified analysis results in a 37% higher annual effective dose to the adult male when compared to NCRP's (1987) estimate. However, using 2007 ICRP tissue weighting factors in this modified analysis produces only a 7% higher annual effective dose estimate. The bone marrow annual equivalent dose differs by only 1 μSv between the two analyses, but the other tissue estimates are higher in this current analysis (using 1977 weighting factors), with the annual equivalent dose estimate for gonads 49% greater than that of NCRP, and the bone surface estimate nearly triple. Table 22 compares the NCRP's (1987) equivalent dose estimates by tissue with those of the modified analysis previously described using both 2007 and 1977 ICRP tissue weighting factors.

NCRP Report No. 94 (1987) is a source for the data used in the NCRP's analysis (1987). Table 23 compares the activity concentrations from NCRP Report No. 94 with those used in the current analysis for the 3 radionuclides with the largest contributions to annual effective dose.

The present work estimates a 58% higher weighted annual equivalent dose to an adult male lung compared to the NCRP's (1987) estimate, despite the apparent good agreement between the activity concentrations in lung tissue used in both analyses for the three major dose contributing radionuclides. This wide separation indicates there are differences between the dose calculation methods used by these analyses. The NCRP's (1987) dose calculation methods and the current analysis are indeed fundamentally different. The current method obtains a dose equivalent rate for each target region by summing the absorbed dose—obtained by multiplying activity in the source by a dose factor—from each source region over all radionuclides. NCRP calculates dose equivalent rates by multiplying the activity concentration in a tissue or organ by a dose conversion factor. To determine how the difference in the two calculation methods might affect the annual effective dose estimate, the current analysis was modified to use only data used in NCRP Report No. 93 to calculate an annual effective dose to an adult male using 1977 ICRP

weighting factors. The result is 26% higher than the NCRP's (1987) estimate. Table 24 compares the equivalent doses presented in NCRP Report No. 93 with the current analysis modified to use the NCRP's activity concentration data.

Figure 16 compares the average annual effective doses calculated using the current methods and data set with both the NCRP's (1987) annual effective dose equivalent estimate and the annual equivalent dose calculated using the current methods and NCRP's (1987) data.

The NCRP (2009) derived its dose estimates for the radionuclides in the present study from data published by UNSCEAR (2000), limited to those data for U.S. residents. The NCRP was able to develop dose numbers for the U and Th series (excluding inhalation of ^{222}Rn and ^{220}Rn decay products) only for adults. It adopted the NCRP Report No. 94 values for the minor radionuclides (^{3}H, ^{14}C, ^{87}Rb). It calculated ^{40}K values from new data. The NCRP (2009) results are compared to those of this study in Table 25. Overall, the new results are 134 μSv higher (47% higher) for men, and 47 μSv higher (16% higher) for women. NCRP did not calculate dose to women. The increase in the present work is attributable to more data, data on more radionuclides, and complete imputation of activity to tissues and organs that the NCRP-UNSCEAR analysis did not include.

Comparison with UNSCEAR's estimate

UNSCEAR (2000) reports an annual effective dose of 310 μSv to an adult male from internally deposited ^{40}K and radionuclides from the uranium and thorium series using internationally obtained data. The present work estimates an average annual effective dose to an adult male, using 1990 ICRP tissue weighting factors, to be 444 μSv, which is 43% higher than the UNSCEAR estimate. The present work includes radionuclides not considered by UNSCEAR and a more appropriate comparison is achieved by modifying the current analysis to include only those radionuclides included in the UNSCEAR analysis. Doing so produces an average annual effective dose of 405 μSv (31% higher) to the adult male using 1990 ICRP tissue weighting factors. Table 26 compares the results of this modified analysis with those of UNSCEAR (2000).

Table 27 compares the tissue activity concentrations used in the current analysis with those used in UNSCEAR (2000).

There is a considerable discrepancy between the tissue activity concentrations used and the results obtained when comparing the current analysis with that of UNSCEAR (2000). The difference in effective dose estimates between the two studies cannot be explained entirely by tissue activity concentration differences. For instance, the ^{210}Po activity concentration in bone used in the current analysis is 34% lower than the activity concentration used in UNSCEAR (2000), yet the average annual effective dose from ^{210}Po calculated by the current analysis is 71% higher than that calculated in UNSCEAR (2000). Since the maximum equivalent dose in the current analysis is delivered to the osteogenic cells from ^{210}Po, and 17% of that dose is from self-irradiation, a decrease in ^{210}Po activity concentration in bone would be expected to decrease the overall average annual effective dose. Clearly, differences in the methods of the two studies account for the differences in results. UNSCEAR (2000) lists absorbed dose rate per unit concentration of the radionuclides included in its analysis, however, it is unclear how applying these factors to the tissue activity concentrations presented in the same table yields the reported effective dose rates. If UNSCEAR calculates effective dose by multiplying concentration by the absorbed dose rates per unit concentration of radionuclide, and then by a tissue-weighting factor, then its analysis appears to be much like the NCRP (1987) method. However, this is supposition since there is insufficient information in the UNSCEAR report to reproduce its calculations.

The UNSCEAR methods are compared with those of the current analysis by modifying the current analysis to use only the tissue activity concentration data published in UNSCEAR (2000). Table 28 compares the average annual effective doses by radionuclide to an adult male calculated by this modified analysis with those calculated by UNSCEAR (2000).

Even using UNSCEAR's (2000) data, there are considerable annual effective dose estimate differences between the current analysis and UNSCEAR. The average annual effective dose to an adult male using ICRP 1990 tissue factors and the UNSCEAR data with the methods and dose factors of the current analysis is 135 μSv, 56% lower than UNSCEAR's (2000) estimate. The average annual effective

dose from ^{210}Po is 22% higher than UNSCEAR's (2000) estimate, while ^{40}K and $^{228/224}$Ra estimates are much lower, being 89% and 99.6% lower respectively. These dramatic differences between the results when using the same data indicate vastly different dose calculation techniques. Figure 17 illustrates the average annual effective dose differences between the current analysis, UNSCEAR (2000) and the current analysis modified to use UNSCEAR's (2000) data.

Adult female average annual effective dose estimate

The current analysis produces an adult female average annual effective dose estimate that is lower than anticipated. The effects of RADAR dose factors on each population's average annual effective dose estimate is examined by using a modified analysis using only the adult male data from the current data set and preserving the uncertainty when imputing concentration data into other phantoms. This method removes age- and sex-related variability and illustrates how dose factors affect the average annual effective dose estimate.

Figure 18 compares the average annual effective doses to all populations calculated using the adult-male-only data set with those calculated using the entire dataset (i.e., the average annual effective dose estimates of the present work). Average annual effective dose estimates calculated using the entire data set are lower for each juvenile, but within 5%. Compared with average annual effective doses to juveniles, the adult female average annual effective dose shows a larger decrease (15%) from the adult-male-only data set.

The thyroid shows the largest decrease in annual weighted equivalent dose to a TarT in the adult female (48% decrease) when comparing between the results obtained using the complete data set and using the adult-male-only data. All other annual weighted equivalent doses to TarTs in the adult female are between 6% and 34% lower. Dose reduction across all TarTs is caused by reduced tissue activity concentrations and resulting activities of ^{40}K and ^{210}Po—which are the biggest contributors to overall effective dose—in all adult female RASRs. A large difference in thyroid activity concentrations of ^{228}Th and its progeny drives the thyroid annual weighted equivalent dose disparity between the adult-male-only and complete data sets. Using the adult-male-only data set, ^{228}Th and progeny account for 48% of the

thyroid dose; using the entire data set they account for 8% of the thyroid dose. Since TIVADs are not available for ^{228}Th progeny in either data set, tissue activity concentrations for progeny in equilibrium with ^{228}Th are imputed from ^{228}Th tissue activity concentrations. Only one ^{228}Th TIVAD is available for the thyroid in each sex; for the female, the value is obtained from Wrenn, et al. (1981) and for the male the value is obtained from USTUR (2008). Both values have a high coefficient of variation (1.25 for the male concentration, 1.51 for the female concentration). The large difference between dose estimates stemming from such a scarcity of data underscores the need for more tissue activity concentration data to reduce effective dose estimate uncertainties.

Juvenile average annual effective dose estimates

Data scarcity also produces unexpected results with the juvenile annual weighted equivalent dose estimates. Bone marrow is expected to recieve the highest annual weighted equivalent dose in newborns and 1-year-olds, while lung recieves the highest dose in the other juveniles. RADAR dose factors are inversely proportional to the mass of the target organ and the ratio of lung mass to red bone marrow mass decreases as age increases with the most substantial ratio decrease occurring between the 5- and 10-year-olds. Therefore, the ratio of lung dose factor to red bone marrow dose factor for a given radionuclide increases with age, such that an equivalent dose to the lung is expected to exceed that to the red bone marrow starting with the 5-year-old. The results of the adult-male-only analysis confirms this expectation. In the present work, the lung in the 5- and 10-year-olds unexpectedly recieves a lower annual weighted equivalent dose relative to that recieved by bone marrow. Polonium-210 activity concentrations in the lung are an order of magnitude lower than in the other phantoms resulting in diminished ^{210}Po activity and therefore a lower overall lung to lung equivalent dose. The reason for this difference in activity is because one LitTIVAD exists for ^{210}Po in the lung in both the 5- and 10-year-olds, while the other juveniles' ^{210}Po lung concentrations are imputed from adult male values. Whether this represents the true state of nature or not is uncertain.

Lymph nodes

RADAR dose factors do not account for lymph nodes as either source or target tissues. The ICRP, however, lists lymph nodes as a remainder tissue in its 2007 tissue weighting recommendations. Remainder tissues are collectively assigned a tissue weighting factor of 0.12. Contribution to annual effective dose from radionuclides deposited in lymph nodes is of great interest since lymph nodes are a concentratior tissue for many radionuclides. Several articles found in the literature review had lymph node tissue activity concentrations, but these are not used in the present work. All lymph node tissue activity concentrations found in the literature are measurements from single individuals and have coefficients of variation ranging from 0.5 to 1.19. These data are arithmetically averaged for comparison with the lung RASR values used in the present work. Table 29 compares the lymph node and lung activity concentrations for radionuclides for which lymph node data is found.

Activity concentrations of thorium isotopes in lymph nodes are an order of magnitude higher than those in lung, and activity concentrations of uranium isotopes are two orders of magnitude higher. A way to estimate the impact of these lymph node activity concentrations is using

$$H_l = H_L \times \left(\frac{C_l}{C_L} \right) \tag{38}$$

where H is equivalent dose, C is tissue activity concentration, L is lung and l is lymph node. Table 30 shows the equivalent and annual weighted equivalent doses to lymph nodes using this approximation.

This approximation essentially uses the RADAR dose factors for lung as surrogate factors for lymph nodes. Having actual dose factors calculated specifically for lymph nodes would result in different results than those shown in Table 29. Still, the 19.8 μSv average annual effective dose estimate obtained by this approximation indicates that neglecting the contributions of radionuclides deposited in lymph nodes results in artificially lower average annual effective dose estimates. This approximation was not included in the present work because of the uncertainties arising from using lung dose factors as surrogates for lymph nodes.

Effects of smoking on average annual effective doses

Tobacco plants are known to have elevated levels of ^{210}Pb and ^{210}Po. Sticky hairs, called trichromes, on both sides of tobacco leaves trap decay products (e.g., ^{210}Po and ^{210}Pb) of radon emanating from soils and fertilizer (U.S. Environmental Protection Agency 2009). The compound coating the trichromes is not water soluble, preventing rainwater or irrigation from washing the radon progeny off the leaves, allowing the decay products to accumulate (U.S. Environmental Protection Agency 2009). Additionally, the two-year curing time for cigarette tobacco allows ^{210}Po to grow into equilibrium with ^{210}Pb (Ferri and Baratta 1966). Accordingly, the tissues of smokers have shown elevated activity concentrations of ^{210}Po and ^{210}Pb. Ferri and Baratta (1966), Baratta and Ferri (1967) and Blanchard (1967) recorded the smoking histories of the subjects in their studies in an effort to correlate ^{210}Po and ^{210}Pb tissue concentrations with smoking. The other articles with ^{210}Po or ^{210}Pb concentrations obtained during the literature search had no smoking histories recorded and were classified in the present work as "unknown". Tables 31 and 32 present ^{210}Po and ^{210}Pb tissue activity concentrations, respectively, used in the present work and organized by subjects' smoking history.

The concentrations of both ^{210}Po and ^{210}Pb are generally higher in smokers than non-smokers, with the largest differences occurring in the liver, testes and lung. The large difference in ^{210}Po concentrations in the testes results from imputing the non-smoking concentration from other non-concentrator organs. There were no measurements of ^{210}Po concentrations in the testes of non-smokers, and the imputation may be an under estimation. Similarly, ^{210}Pb concentrations in bone for both smokers and non-smokers are imputed from non-concentrator organ concentrations and are more than an order of magnitude lower than the measured concentration in the "unknown" group. This underestimation of concentration does not have an effect on the average annual effective dose because of the low dose factors for ^{210}Pb. The data with unknown smoking histories come from different articles than the data identified as being from smokers or non-smokers. Lead-210 concentrations for subjects with unknown smoking histories fall between the values for smokers and non-smokers except for bone (as previously mentioned) and pancreas, where the value is slightly below non-smokers' value. Polonium-210 values for subjects

with unknown smoking histories are only between smoker and non-smoker values for lungs, liver and thyroid, while kidneys, muscle and pancreas concentrations are higher than either the smokers or non-smokers values. Soft tissue ^{210}Po activity concentrations in smokers and non-smokers are imputed from non-concentrator organ values, while soft tissue ^{210}Po activity concentrations in subjects with unknown smoking histories are measured values. The imputed soft tissue values are almost an order of magnitude lower than the measured values.

Having ^{210}Po and ^{210}Pb data organized by smoking history presents the opportunity to examine the effects of smoking on average annual effective doses. Three modified analyses were performed: one in which only ^{210}Po and ^{210}Pb from smokers were included with the rest of the data set, one in which only ^{210}Po and ^{210}Pb from non-smokers were used and one in which only ^{210}Po and ^{210}Pb from subjects with unknown smoking histories were used. Table 33 presents the average annual effective doses to the adult male estimated from these three analyses using 2007 ICRP tissue weighting recommendations.

The estimated average annual effective dose to an adult male using data with unknown smoking histories is 13% higher than that estimated using data from smokers and 28% higher than that estimated with non-smokers' data. This increase is attributable to ^{210}Po bone, red bone marrow and total body concentrations being substantially higher in the "unknown" data set than in the smokers-only data set. The bone and red bone marrow concentrations in the smokers' and non-smokers' data are imputed from non-concentrator tissue concentrations while the data from subjects with unknown smoking histories have measured values for these tissues. While the total body concentration is imputed from the soft tissue RASR concentration in all three cases, the soft tissue concentrations from subjects with unknown smoking histories are measured values and are imputed values from non-concentrator organ concentrations for the smoking and non-smoking subjects. The higher concentrations and resulting activities in the bone, red bone marrow and total body RASRs of the subjects with unknown smoking histories results in much higher doses to bone surface and red bone marrow, driving the overall dose upward relative to the overall doses estimated with the data from smokers and non-smokers.

Removing the data from subjects with unknown smoking histories and comparing the average annual effective doses from the analyses using only the data sets from smokers and non-smokers provides the most direct comparison since these two data sets both have measurements from the same tissues (except testes were not measured in non-smokers). The average annual effective dose decreases 12% from 376 μSv to 332 μSv between the smokers-only data set and non-smokers-only data set, indicating increased ^{210}Po and ^{210}Pb concentrations in tobacco have a marked effect on average annual effective dose. Tissue concentrations of ^{210}Po in the lungs and gonads of smokers are much higher than those of non-smokers. The lungs receive the highest weighted equivalent dose in both groups, so the 68% increase in ^{210}Po concentration in the lungs of smokers results in a 15.4 μSv increase in annual weighted effective dose over non-smokers. Similarly, the large increase in the ^{210}Po concentration in gonads of smokers results in a 10.4 μSv increase in annual weighted effective dose over non-smokers. All other ICRP TarTs except kidneys show increased dose in smokers compared to non-smokers, and all RASRs except kidneys, muscle and heart contents show elevated ^{210}Po concentrations in smokers compared to non-smokers.

Table 34 shows the annual weighted equivalent dose to TarTs receiving 10% or more of the total average annual effective dose, organized by smoking history. In all three cases, the lungs receive the highest annual weighted equivalent dose, with bone marrow receiving the next highest. Gonads receive the third highest annual weighted equivalent dose in smokers and in subjects with unknown smoking histories, but non-smokers have the breast receiving the third highest dose. This is due to the low imputed ^{210}Po concentration in testes in non-smokers, which makes the annual weighted equivalent dose to testes lower than that to the breast.

Conclusions

The average annual effective dose from internally-deposited ubiquitous radionuclides to an adult male in the United States is 418 μSv with a coefficient of variation (CV) of 0.68 (geometric mean = 346 μSv, s_G = 1.85). The average annual effective dose an adult woman with the same exposures is 332 μSv

with a coefficient of variation of 0.79 (geometric mean = 261 μSv, s_G = 2.01). Average annual effective doses to juveniles in the United States under the same exposure conditions increase with decreasing age and are 430 μSv (*CV* = 0.78, geometric mean = 339 μSv, s_G = 1.99), 434 μSv (*CV* = 0.73, geometric mean = 351 μSv, s_G = 1.92), 443 μSv (*CV* = 0.76, geometric mean = 353 μSv, s_G = 1.96) and 442 μSv (*CV* = 0.67, geometric mean = 367 μSv, s_G = 1.84) to the 15-, 10-, 5- and 1-year-old respectively. The newborn receives the highest average annual effective dose, 465 μSv (*CV* = 0.59, geometric mean = 400 μSv, s_G = 1.73). The coefficients of variation and s_Gs are upper bounds on variability as explained above. It is clear that a quantitative treatment of uncertainty in these results could only be done approximately, due to the absence of uncertainty values for many of the original data. Uncertainty characterization in the presence of substantive variability would require a large Monte Carlo simulation.

The estimate of average annual effective dose to an adult male presented in this study is 146 μSv higher (37% higher) than that presented in NCRP Report No. 93 when using 1977 ICRP tissue weighting factors, and 133 μSv higher (47% higher) than that presented in NCRP Report No. 160. The present work's adult male average annual effective dose estimate could not be directly compared to the estimate of average annual effective dose presented by UNSCEAR (2000), but a modified analysis using the same tissues and radionuclides is 95 μSv higher (31% higher).

When compared to estimates by the NCRP and UNSCEAR, the higher average annual effective doses presented in this study are partly attributable to a larger body of data supporting the calculations. The intricate dose calculations accounting for irradiation between organs also contributes to the differences when compared to the NCRP and UNSCEAR studies. Given the difficulties described above, we recommend that UNSCEAR and NCRP commission new studies using the methods described here. Such studies would better characterize the uncertainty and variability of doses due to ubiquitous radionuclides in the body. Future work should include all usable data from the scientific literature.

Despite the large amount of data used in this study, the scarcity of data for some tissues and radionuclides underscores the need for more tissue activity concentration studies to further reduce uncertainty in the dose estimates. The absence of data for juveniles is a particular concern. Even when

data exist, a lack of detail about the subjects in the study diminishes the usefulness of the data for studying effects of variability on effective doses. Researchers should consider being more precise and complete when presenting data in a journal article; often a table with the characteristics of each subject in the study (e.g., height, weight, age, sex, geographic location, smoking history, etc.) is helpful.

The body of data compiled for this study lacked activity measurements for radionuclides for which whole-body measurements are possible, such as ^{208}Tl and ^{214}Bi. Momcilovic and Lykken (2007) present equations with which the ^{214}Bi whole-body concentration variations in both genders can be estimated over the course of a year. These equations were not used in the present work as the results cannot be apportioned to specific tissues and organs. Developing sets of whole-body activity measurements of ^{208}Tl and ^{214}Bi correlated with age, sex, body mass index, and geographical location should be investigated. The relative ease of these measurements could allow a large body of data to be created which would reduce uncertainty in the effective dose estimates from the uranium series progeny.

Using a crude scaling procedure, we estimate that accounting for ubiquitous radionuclides in the lymph nodes would increase the effective dose in adult males by about 20 μSv. Given this contribution to overall average annual effective dose presented by the lymph nodes, creating a lymph node source region, a lymph node target region and dose factors for calculating equivalent doses to other tissues and organs from radionuclides deposited in the lymph nodes should be considered. Similarly, adding source regions and dose factors for the 2007 ICRP TarTs without matching RASRs (i.e., extrathoracic region, oral mucosa, prostate and salivary glands) would also reduce uncertainty in the final average annual effective dose estimate.

While this study examined the effects of age and gender on average annual effective dose, there remain several other variables in the data that remain unexplored. Geographic location and body mass index were the two most commonly encountered variables in the current data set that were not considered in the present work. Further work identifying and examining the effects of other variables besides gender and age on average annual effective doses to the U.S. public from internally-deposited, ubiquitous radionuclides is highly recommended.

Acknowledgements—The authors would like to thank Dr. Paul S. Stansbury, Dr. R. Gene Schreckhise and Mr. Bruce A. Napier for insightful discussions and guidance, Dr. Michael G. Stabin for providing dose factors and advice, Mr. Timothy P. Lynch for providing ^{40}K and ^{137}Cs whole body-data, Dr. Anthony C. James and Dr. Sergei Y. Tolmachev for graciously providing uranium and thorium data, Dr. Isabelle M. Fisenne for locating and digitizing one of her reports, Dr. Samuel E. Glover for discussions, and Dr. Fred A. Mettler for providing UNSCEAR data. The findings and conclusions in this report are those of the authors and do not necessarily represent the views of any funding agency. Pacific Northwest National Laboratory is operated by Battelle for the U.S. Department of Energy under Contract DE-AC05-76RL01830.

References

Anderson EC, Langham WH. Average potassium concentration of the human body as a function of age. Science 130:713–4; 1959.

Baratta EJ, Ferri ES. Strontium-90, cesium-137, and polonium-210 in human tissues. Radiol Health Data Rep 8: 298–9; 1967.

Baratta EJ, Apidianakis JC, Ferri ES. Cesium-137, lead-210 and polonium-210 concentrations in selected human tissues in the United States. Am Ind Hyg Assoc J 30: 443–8; 1969.

Black SC. Low-Level Polonium and Radiolead Analysis. Health Phys 7:87–91; 1961.

Blanchard RL. Correlation of lead-210 with strontium-90 in human bones. Nature. 211:995–6; 1966

Blanchard RL. Concentrations of ^{210}Pb and ^{210}Po in human soft tissues. Health Phys 13: 625–32; 1967.

Bogen DC, Welford GA, Morse RS. General population exposure of stable lead and ^{210}Pb to residents of New York City. Health Phys 30: 359–362; 1976.

Broadway JA, Strong AB. Radionuclides in human bone samples. Health Phys 45: 765–8; 1983.

Cember H, Johnson TE. Introduction to health physics. 4th ed. New York: McGraw Hill Medical; 2009.

Cohn SH, Abesamis C, Zanzi I, Aloia JF, Yasumura S, Ellis KJ. Body elemental composition: comparison between black and white adults. Am J Physiol 232:E419–22; 1977.

Ferri BA and Baratta EJ. Polonium 210 in tobacco, cigarette smoke, and selected human organs. Public Health Rep. 81: 121–127; 1966.

Fisenne IM, Keller HW, Harley NH. Worldwide measurement of ^{226}Ra in human bone: estimate of skeletal alpha dose. Health Phys 40: 163–71; 1981.

Fisenne IM, Welford GA. Natural U concentrations in soft tissues and bone of New York City residents. Health Phys 50: 739–46; 1986.

Fisenne IM, Perry PM. Stable calcium and potassium in tissues from New York City residents. EML-455 1986.

Fisenne IM, Perry PM, Harley NH. Uranium in humans. Radiat Prot Dosimetry 24: 127–131; 1988.

Fox-Wasylyshyn SM, El-Masri, MM. Handling missing data in self-report measures. Res Nurs Health 28: 488–495; 2005.

Gelman A, Hill J. Data analysis using regression and multilevel/hierarchical models. New York: Cambridge University Press; 2006.

Hallden NA, Fisenne IM, Harley JH. Radium-226 in human diet and bone. Science 140: 1327–9; 1963.

Harley JH. HASL procedures manual, New York: U.S. Atomic Energy Commission; HASL-300; 1972.

Harley NH, Fisenne, IM. Distribution and alpha radiation dose from naturally occurring U, Th, and Ra in the human skeleton. Health Phys 58: 515–8; 1990.

Hofer E. Hypothesis testing, statistical power, and confidence limits in the presence of epistemic uncertainty. Health Phys 92: 226–235; 2007.

Hofer E. How to account for uncertainty due to measurement errors in an uncertainty analysis using Monte Carlo simulation. Health Phys 95:277–290; 2008.

Holtzman RB. Measurement of the natural contents of RaD (Pb210) and RaF (Po210) in human bone-estimates of whole-body burdens. Health Phys 9: 385–400; 1963.

Hursh JB, Gates AA. Body radium content of individuals with no known occupational exposure. Nucleonics 7: 46–59; 1950.

Hursh JB. The natural occurrence of radium in man and in waters in food. Brit. J. Radiol. 7: 45–53; 1957.

Hursh JB. Natural lead-210 content of man. Science 132: 1666–7; 1960.

Hursh JB, Lovaas A. Radium-226 in bone and soft tissues of man. Nature 198: 265–8; 1963.

Hunt VR, Radford EP Jr, Segall AJ. Comparison of concentrations of alpha-emitting elements in teeth and bones. Int J Radiat Biol Relat Stud Phys Chem Med. 7:277–87; 1963.

Hunt VR, Radford EP, Segall A. Naturally occurring concentrations of alpha-emitting isotopes in a New England population. Health Phys 19: 235–43; 1970.

International Commission on Radiological Protection. Report of the task group on reference man. Oxford: Pergamon Press; ICRP Publication 23; 1975.

International Commission on Radiological Protection. Recommendations of the International Commission on Radiological Protection. Oxford: Pergamon Press, ICRP Publication 26. Ann ICRP, 1(3), 1977.

International Commission on Radiological Protection. Limits for intakes of radionuclides by workers. Oxford: Pergamon Press, ICRP Publication 30, Part 1. Ann ICRP 2(3/4); 1979.

International Commission on Radiological Protection. Limits for intakes of radionuclides by workers. Oxford: Pergamon Press, ICRP Publication 30, Part 2. Ann ICRP 4(3/4); 1980.

International Commission on Radiological Protection. Limits for intakes of radionuclides by workers. Oxford: Pergamon Press, ICRP Publication 30, Part 3. Ann ICRP 6(2/3); 1981.

International Commission on Radiological Protection. 1990 Recommendations of the International Commission on Radiological Protection. Oxford: Pergamon Press; ICRP Publication 60; Ann ICRP 21(1/3); 1991.

International Commission on Radiological Protection. Age-dependent doses to members of the public from intake of radionuclides: part 2. ingestion dose coefficients. Oxford: Pergamon Press; ICRP Publication 67; Ann ICRP 23(3/4); 1994.

International Commission on Radiological Protection. Basic anatomical and physiological data for use in radiological protection: the skeleton. Oxford: Pergamon Press; ICRP Publication 70; Ann ICRP 25(2); 1995.

International Commission on Radiological Protection. Recommendations of the ICRP. Oxford: Pergamon Press; ICRP Publication 103; Ann ICRP 37(2/4); 2007.

Iyengar V, Woittiez, J. Trace elements in human clinical specimens: evaluation of literature data to identify reference values. Clin Chem 34: 474–81; 1988.

Kathren RL. Uranium in the tissues of two whole body donations to the USTUR. Richland, WA: United States Uranium and Transuranium Registry; USTUR-0072-97; 1997.

Kaul, A. Interne Strahlensxposition durch ^{40}K. In: Aurand K. et al., eds. Die natruliche strahlen-exposition des menschen. Stuttgart, Germany: Georg Theime Verlag; 1974: 103–111.

Krebs, AT. Untersuchungeii zum problem der radiumvergiftung. Strahlentherapie 72: 164; 1942.

Kumazawa S, Numakunai T. A new theoretical analysis of occupational dose distributions indicating the effect of dose limits. Health Phys 41: 465–475; 1981.

Kumazawa S, Numakunai T. Why do we need dose distribution models? Radiat Prot Dosimetry 36: 269–273; 1991.

Lovaas AI, Hursh JB. Radium-226 and lead-210 in human teeth and bones. Health Phys 14: 549–55; 1968.

Lucas HF, Holtzman RB, Dahlin DC. Argonne National Laboratory Radiological Physics Division summary report. July 1962–June1963. Chicago: Argonne National Laboratory; ANL-6769; 1963.

Lucas HF, Holtzman RB, Dahlin DC. Radium-226, radium-228, lead-210 and fluorine in persons with osteogenic sarcoma. Science 144: 1573–5; 1964.

Lucas HF, Edgington DN, Markun F. Natural thorium in human bone. Health Phys 19: 739–42; 1970.

Martin, A. Content and distribution of stable strontium and ^{226}Ra in human skeletons from Wisconsin decedents 1957-61. Br J Radiol 42: 295–8; 1969.

McInroy JF, Boyd HA, Eutsler BC, Romero D. The U.S. Transuranium Registry report of the ^{241}Am content of a whole body. Part IV: Preparation and analysis of the tissues and bones. Health Phys 49:587–621; 1985.

Momcilovic B, Lykken GI. Seasonality of ^{214}Bi activity in the human body and of ^{222}Rn concentration in home ambient air. Health Phys 92:484–487; 2007.

National Committee on Radiation Protection and Measurements. Ionizing radiation exposure of the population of the United States. Bethesda: National Council on Radiation Protection and Measurements; NCRP 94; 1987.

National Committee on Radiation Protection and Measurements. Ionizing radiation exposure of the population of the United States. Bethesda: National Council on Radiation Protection and Measurements; NCRP 160; 2009.

Novak LP, Hamamoto K, Orvis AL, Burke EC. Total body potassium in infants. Determination by whole-body counting of radioactive potassium (^{40}K). Am J Dis Child 119:419–23; 1970.

Novak LP. Total-body potassium during the first year of life determined by whole-body counting of 40K. J Nucl Med 14:550–7; 1973.

Palmer RF, Queen FB. Normal abundance of radium in cadavers from the Pacific Northwest. Am J Roentgenol Radium Ther Nucl Med 79: 521–9; 1958.

Segall A. Radiogeology and population exposure to background radiation in Northern New England. Science 140: 1337–1339; 1963.

Singh NP, Lewis LL, Wrenn ME. Uranium, thorium and plutonium in bones from the general population of the United States. In: Priest ND , ed. Metals in bone. Lancaster, England: MTP Press; 1985: 231–241.

Singh NP, Lewis LL, Wrenn, ME. Utilization of femoral head for estimating the skeletal burden of U and Pu in humans. Health Phys 56: 341–3; 1989.

Spiers FW, Radionuclides in the human body: physical and biological aspects. New York : Academic Press; 1968.

Srivastava GK, Raghavayya M, Kotrappa P, Somasundram S. Radium-226 body burden in U miners by measurement of Rn in exhaled breath. Health Phys 50: 217–221; 1986.

Stabin MG, Siegel JA. Physical models and dose factors for use in internal dose assessment. Health Phys 85: 294–310; 2003.

Strom DJ, Stansbury PS. Determining parameters of lognormal distributions from minimal information. PNNL-SA-32215. Am Indust Hyg Assoc J 61:877–880; 2000.

Strom DJ, Lynch TP, Weier DR. Radiation doses to Hanford workers from natural potassium-40. Richland, WA: Pacific Northwest National Laboratory; PNNL-18240; 2009.

United Nations. Ionizing radiation: levels and effects - a report of the United Nations scientific committee on the effects of atomic radiation to the General Assembly, with annexes New York: United Nations. 1972.

United Nations. Ionizing radiation: sources and biological effects United Nations scientific committee on the effects of atomic radiation 1982 report to the General Assembly, with annexes. New York: United Nations. 1982.

United Nations. Sources, effects and risks of ionizing radiation. United Nations scientific committee on the effects of atomic radiation 1988 report to the General Assembly, with annexes. New York: United Nations. 1988.

United Nations. Sources and effects of ionizing radiation: United Nations scientific committee on the effects of atomic radiation 1996 report to the General Assembly, with scientific annex. New York: United Nations. 1996.

United Nations. Sources and effects of ionizing radiation: United Nations scientific committee on the effects of atomic radiation report to the General Assembly,with scientific annexes . New York: United Nations. 2000.

U.S. Bureau of the Census. Mobility of the population of the United States: March 1970 to March 1975. Washington DC: U.S. Government Printing Office; Current Population Reports, Series P-20, Number 285. 1975.

U.S. Environmental Protection Agency. Tobacco smoke [online]. Available at: http://www.epa.gov/rpdweb00/sources/tobacco.html. Environmental Protection Agency. Accessed 01 July 2009.

Walton A, Kologrivov R Kulp JL. The concentration and distribution of radium in the normal human skeleton. Health Phys 1: 409–16. 1959.

Wikipedia. Weighted mean [online]. Available at: http://en.wikipedia.org/wiki/Weighted_mean. Accessed 15 January 2009.

Wrenn ME, Singh NP, Cohen N, Ibrahim SA, Saccomanno G. Thorium in human tissues. Washington, DC: U.S. Nuclear Regulatory Commission. 1981.

Appendix A Software Quality Assurance

A software code is written to perform the imputations and calculations described in the methods of the present work. A series of tests designed to ensure the code correctly reads input files, imputes data as described in the methods, calculates equivalent and effective doses and reports results is shown in Table A.1.

Appendix B Contributions of each manuscript author

Table B.1 details the number of hours worked by each manuscript co-author in the preparation of this study.

Footnotes

*Battelle, Richland, WA 99352-0999.

For correspondence contact: Daniel J. Strom strom@pnl.gov.

† Lynch, TP. Personal Communication. Pacific Northwest National Laboratory. March 30, 2009.

‡ United States Transuranium and Uranium Registries. Personal Communication. December 11, 2008.

§ United States Transuranium and Uranium Registries. Personal Communication. February 11, 2009.

** http://www.doseinfo-radar.com/

Figure 1. Illustration of data processing steps. Italic text represents concentration data and bold text represents activity data.

Figure 2. Methods used to load and convert tissue concentration data. Italic text represents concentration data.

Figure 3. Methods used to impute missing tissue concentration data across phantoms. Italic text represents concentration data.

Figure 4. Methods used to aggregate and disaggregate tissue concentrations within tissue (in vivo or autopsy) data (TIVADs).

Figure 5. Procedure for aggregating intermediate TIVAD (iTIVAD)concentrations into RASR concentrations. Italic text represents concentration data.

Figure 6. Lognormal distribution of possibly true values created from the arithmetic mean and standard deviation of the set of data from Lynch (2009) superimposed over the distribution of original data. The new distribution contains no negative values.

Figure 7. Method for imputing tissue concentrations in RASRs lacking such data. Italic text represents concentration data and bold text represents activity data

Figure 8. Procedure for imputing ^{228}Ra activities for RASRs lacking ^{228}Ra data. Bold text represents activity data.

Figure 9. Method for calculating the remainder of the body activity for each RADAR phantom. Bold text represents activity data.

Figure 10. Procedure for imputing hollow-organ content activities. Bold text represents activity data.

Figure 11. Method used to apportion bone activity into trabecular and cortical bone.

Figure 12. Method used to impute tissue concentration data in decay series. Bold text indicates activity data.

Figure 13. Changes in annual effective doses to the populations studied from using the ICRP tissue weighting factors from 1977, 1990 and 2007.

Figure 14. Contribution to the adult male annual effective dose (418 μSv) by radionuclide using 2007 ICRP tissue weighting factors.

Figure 15. Effects of including hollow-organ contents and ^{231}Pa (+ progeny) on adult male annual effective dose estimates using 2007 ICRP tissue weighting recommendations.

Figure 16. Comparison of annual effective doses to an adult male calculated by the current analysis, NCRP Report No. 93, and the current analysis modified to use only data from NCRP Report No. 94. Numbers in parentheses indicate the year of the ICRP tissue weighting recommendations used in the estimate

Figure 17. Annual effective dose estimates calculated in the current analysis, by UNSCEAR (2000) and by the current analysis modified to use UNSCEAR (2000) data.

Figure 18. Effects of data variability on annual effective dose estimates. Each data point in the figure represents a ratio of the effective dose for the phantom to the effective dose of the adult male phantom. The adult male data only analysis removes age- and sex- variability from the results to illustrate effects of RADAR dose factor on annual effective dose. The entire data set is the data used for this analysis and includes age- and sex- variability.

Table 1. Tissues analyzed for uranium series radionuclides by study – numbers in table identify article data were collected from.

	^{238}U	^{234}U	^{230}Th	^{226}Ra	^{210}Pb	^{210}Po
Adrenals	31	31	31			
Bladder					6	6
Blood			18			10, 16
Bone	24, 25[b], 26, 28, 29, 30, 31	24, 25[b], 26, 28, 29, 30, 31	22, 25[d], 27, 30, 31	4, 8[a], 9, 10, 11[c], 12, 17[a], 20, 23, 27, 30	5, 6, 7, 10, 12, 14,17[a], 20, 21, 27	15, 27
Brain	31	31	31			
Breasts			27	27		
Gonads			22, 27, 31	27	15, 27	15
Heart	30		22	9	15,18,27	13,15,16,18,27
Kidney	31	31	22, 27, 31	9	15, 27	13,15,16,27
Liver	26, 31	26, 31	22, 31	9	15,18,27	13,15,16,18,27
Lung	26, 31	26, 31	22, 27, 31	27	7,15,18,27	13,15,16,18,27
Lymph nodes			22			
Muscle	31	31	31	9		13,16
Pancreas	31	31	31		15, 27	15,16,27
Spleen	31	31	22, 31	9	15, 27	15,16,27
Stomach						16
Testes	31	31		9		16

[1]Hursh and Gates (1950)
[2]Hursh (1957)
[3]Palmer and Queen (1958)
[4]Walton et al. (1959)
[5]Hursh (1960)
[6]Black (1961)
[7]Blanchard (1961)
[8]Segall (1963)
[9]Hursh and Lovaas (1963)
[10]Holtzman (1963)
[11]Halliden et al. (1963)
[12]Lucas et al. (1964)
[13]Ferri and Barratta (1966)
[14]Blanchard (1966)
[15]Blanchard (1967)
[16]Baratta and Ferri (1967)
[17]Lovaas and Hursh (1968)
[18]Baratta et al.(1969)
[19]Martin (1969)
[20]Hunt (1970)
[21]Bogen, Welford and Morse (1976)
[22]Wrenn et al. (1981)
[23]Fisenne et al. (1981)
[24]Broadway and Strong (1983)
[25]Singh et al. (1985)
[26]Fisenne and Welford (1986)
[27]NCRP (1987)
[28]Fisenne, Perry and Harley (1988)
[29]Singh et al. (1989)
[30]Harley and Fisenne (1990)
[31]USTUR (2008)

[a]Tooth was used as an analogue for bone
[b]Only ileum was measured
[c]Only vertebrae was measured
[d]Rib, sternum and vertebrae

Table 2. Study parameters for articles containing usable uranium series data. "Result type" and "Reported Uncertainty" are based on the wording in the article.

Reference	No. of subjects	Location	Result type	Reported Uncertainty	Age correlation	Sex correlation
Hursh and Gates (1950)	31	Rochester, NY	Mass concentration g^{-1} ash	Standard Error	yes	yes
Hursh (1957)	14	Rochester, NY	Mass concentration g^{-1} ash	Unknown	yes	yes
Palmer and Queen (1958)	50	Pacific NW	Average mass concentration g^{-1} ash	90 % confidence limit	yes	yes
Walton et al. (1959)	140	New York City	Average mass concentration g^{-1} ash	Standard deviation	no	no
Hursh (1960)	18	New York	Activity concentration g^{-1} wet bone	Unknown	yes	no
Black (1961)	10	U.S.	Activity concentration g^{-1} wet tissue	Unknown	no	no
Holtzman (1963)	136	U.S.	Activity concentration g^{-1} ash	0.9 confidence level	yes	yes
Hursh and Lovaas (1963)	21	U.S.	Mass concentration g^{-1} wet sample	1 standard error (pooled samples)	yes	yes
Hallden et al. (1963)	135	San Fransisco, New York City	Activity concentration g^{-1} calcium	Standard deviation of the mean	no	no
Segall (1963)	Unk.	New England	Activity concentration g^{-1} tooth	Unknown	no	no
Lucas et al. (1964)	32	Midwest	Activity concentration g^{-1} ash	Unknown	no	no
Ferri and Baratta (1966)	3–8[a]	U.S.	Activity concentration g^{-1} wet tissue	Unknown	no	no
Blanchard (1966)	14	Cincinnati, OH	Activity concentration g^{-1} Ca	Unknown	yes	yes
Baratta and Ferri (1967)	1–8[a]	Boston	Average activity concentration 100 g^{-1} tissue	± 2σ counting error	no	yes
Blanchard (1967)	20	U.S.	Activity concentration kg^{-1} wet tissue weight	± 1σ counting error	yes	yes
Lovaas and Hursh (1968)	13	U.S.	Mean activity concentration g^{-1} wet tissue or g^{-1} calcium	standard deviation for the 0.90 confidence interval	no	no
Baratta et al.(1969)	9–22[b]	U.S.	Average activity concentration 100 g^{-1} wet tissue	± 2 standard deviations	yes	no
Martin (1969)	75	U.S.	Average activity concentration g^{-1} Ca	Unknown	no	no
Hunt (1970)	2–12[b]	Massachusetts	Activity concentration g^{-1} wet weight	Unknown	no	yes

Fisenne et al. (1981)	Unk.	New York City, U.S.	Mean and median activity concentrations per both gram of ash and gram of calcium	standard deviation (mean results), geometric standard deviation (median results)	no	yes (NYC) no (U.S.)
Wrenn et al. (1981)	33	Colorado, Washington D.C. and New York	Activity concentrations kg^{-1} wet tissue	standard deviation	yes	yes
Broadway and Strong (1983)	1–7[c]	U.S.	Average activity concentration kg^{-1} wet bone	± standard deviation of the mean	yes	no
Singh et al. (1985)	13	Colorado, Pennsylvania	Activity concentrations kg^{-1} wet bone	± standard deviation	no	no
Harley and Fisenne (1990)	75	Wisconsin	Activity concentration kg^{-1} bone ash	Unknown	yes	yes
USTUR (Case 0213)	1	U.S.	Activity concentration kg^{-1} wet tissue	± standard deviation	yes	yes
USTUR (Case 0425)	1	Boulder, CO	Activity concentration kg^{-1} wet tissue	± standard deviation	yes	yes

[a]Number of subjects varies by tissue
[b]Number of subjects varies by tissue and year collected
[c]Number of subjects varies by age group and year collected

Table 3. Tissues analyzed for thorium series radionuclides by study – numbers in table identify article from which data were collected

	^{232}Th	^{228}Ra	^{228}Th
Adrenals	6		6
Blood	2		
Bone	2, 3[a], 4, 5[b], 6	1	2, 6
Brain	6		6
Gonads	2		
Heart	2		
Kidney	2, 6		2, 6
Liver	2, 6		2, 6
Lung	2, 6		2, 6
Lymph nodes	2, 6		2
Muscle	6		6
Pancreas	6		6
Spleen	2, 6		6
Testes	6		6
Thyroid	2, 6		6
Other	6		6

[1]Lucas et al.(1964)
[2]Wrenn et al. (1981)
[3]Singh et al. (1985)
[4]Lucas et al.(1970)
[5]Harley and Fisenne (1990)
[6]USTUR (Case 0212)
[a]Rib, sternum and vertebrae
[b]Vertebrae, ribs and long bone shaft

Table 4. Study parameters for articles containing usable thorium series data. "Result type" and "Reported Uncertainty" are based on the wording in the article.

Reference	No. of subjects	Location	Result type	Reported Uncertainty	Age correlation	Sex correlation
Lucas et al. (1964)	32	Midwest	Activity concentration g^{-1} ash	Unk.	no	no
Wrenn et al. (1981)	33	Colorado, Washington D.C. and New York	Activity concentration kg^{-1} wet tissue	standard deviation	yes	yes
Singh et al. (1985)	13	Colorado, Pennsylvania	Activity concentration kg^{-1} wet bone	± standard deviation	no	no
Lucas et al.(1970)	38	U.S.	Mass concentrations g^{-1} bone ash	standard deviation of the results	yes	yes
Harley and Fisenne (1990)	75	Wisconsin	Activity concentration kg^{-1} bone ash	Unk.	yes	yes
USTUR (Case 0212)	1	Washington	Activity concentrations g^{-1} tissue ash	± 1 σ	yes	yes

Table 5. Study parameters for articles containing usable actinium series data. “Result type” and “Error” are verbatim from article

Reference	No. of subjects	Location	Result type	Error	Age correlation	Sex correlation
Broadway and Strong (1983)	1–7[a]	U.S.	Average activity concentration kg^{-1} wet bone	± standard deviation of the mean	yes	no
Singh et al. (1985)	13	Colorado, Pennsylvania	Activity concentration kg^{-1} wet bone	± standard deviation	no	no
Harley and Fisenne (1990)	75	Wisconsin	Activity concentration kg^{-1} bone ash		yes	yes

[a]Number of subjects varies by age group and year collected

Table 6. Tissues analyzed for elemental rubidium by study – numbers in table identify the article from which data were collected.

Tissue	Article	Tissue	Article
Adrenals	2	Other Tissues	3
Bone	1, 2	Pancreas	2
Brain	2	Red bone marrow	3
Breast	2	Spleen	2
Gall bladder	2	Stomach	2
Heart	2	Testes	1, 2, 3
Kidneys	2, 4	Thymus	2
Liver	2, 4	Thyroid	2, 3
Lungs	2, 3	Urinary bladder	2
Muscle	2	Whole body	5
Ovaries	1		

[1]UNSCEAR (1972)
[2]Iyengar et al. (1978)
[3]UNSCEAR (1982)
[4]NCRP (1987)
[5]UNSCEAR (1988)

Table 7. Tissues analyzed for elemental uranium by study – numbers in table identify the article from which data were collected

Tissue	Article	Tissue	Article
Adrenals	3	Lung	1, 3
Bladder	3	Lymph Nodes	3
Bone	1, 2[a], 3		
Brain	3	Muscle	3
Heart	3	Pancreas	3
Intestine	3	Spleen	3
Kidney	3	Stomach	3
Liver	1, 3	Thyroid	3

[1]Fisenne and Welford (1986)
[2]Fisenne et al. (1988)
[3]Kathren (1997)

[a]Vertebrae

Table 8. Study parameters for articles containing usable elemental uranium data. "Result type" and "Error" are verbatim from article

Reference	No. of subjects	Location	Result type	Error	Age correlation	Sex correlation
Fisenne and Welford (1986)	12-58[a]	New York City	average mass kg^{-1} wet tissue	± standard deviation of the mean	yes	no
Fisenne et al. (1988)	39	Illinois, Wisconsin	mass concentration kg^{-1} wet tissue	standard deviation (when available)	no	no
Kathren (1997)	2	New Mexico	mass concentration g^{-1} wet tissue, mass concentration g^{-1} ash	standard deviation	yes	yes

[a]Varies by tissue

Table 9. Lists of organs, tissues, and/or anatomical regions used in this study.

Acronym	Description
LitTIVADs	Literature Tissue (in vivo or autopsy) data (TIVAD)
iTIVADs	intermediate TIVADs
InSR	Intermediate Source Region
RASR	Radiation Dose Assessment Resource (RADAR) Source Region
RASTO	RASR (Tissue or Organ)
RASCO	RASR (Contents of Organs)
RATT	RADAR Target Tissue
ICRP1977 TarTs	Target Tissues found in International Commission on Radiological Protection (ICRP) 1977 recommendations
ICRP1990 TarTs	Target Tissues found in the ICRP 1990 recommendations
ICRP2007 TarTs	Target Tissues found in the ICRP 2007 recommendations

Table 10. Radionuclides for which doses are calculated.

Radionuclide	Radionuclide origin
U-Series (^{238}U + progeny[a])	Natural (Primordial)
Th-Series (^{232}Th + progeny[a])	Natural (Primordial)
Ac-Series (^{235}U + progeny[a])	Natural (Primordial)
^{40}K	Natural (Primordial)
^{87}Rb	Natural (Primordial)
^{3}H	Natural (Cosmogenic) and Anthropogenic
^{14}C	Natural (Cosmogenic) and Anthropogenic
^{137}Cs	Anthropogenic
^{90}Sr	Anthropogenic
^{129}I	Anthropogenic

[a]Includes all radioactive progeny.

Table 11. List of intermediate source regions (InSRs) and RADAR source region (RASR) counterparts. Tissues and organs listed in each article are matched to one of these 19 InSRs, most of which can be directly mapped to a RASR. InSRs which cannot be directly mapped to a RASR require additional imputation to match appropriate RASRs. The "undecided" InSR is not used.

InSR	RASR	InSR	RASR
Adrenals	Adrenals	Pancreas	Pancreas
Bone_Group[a]	TrabBoneV (Trabecular Bone Volume), TrabBoneS (Trabecular Bone Surface), CortBoneV (Cortical Bone Volume), CortBoneS (Cortical Bone Surface)	Red Mar. (Red Marrow)	Red Mar. (Red Marrow)
Brain	Brain	ND	SI Cont (Small Intestine Contents)
Breasts	Breasts	Soft Tissue	N/A[c]
ND[b]	GB Cont (Gallbladder Contents)	ND	StomCont (Stomach Contents)
Gonads[a]	Testes Ovaries	Spleen	Spleen
ND	HeartCon (Heart Contents)	Testes	Testes
Hrt Wall (Heart Wall)	Hrt Wall (Heart Wall)	Thyroid	Thyroid
Kidneys	Kidneys	TotBody (Total Body)	TotBody (Total Body)[d]
Liver	Liver	Undecided	N/A[e]
ND	LLI Cont (Lower Large Intestine Contents)	ND	ULI Cont (Upper Large Intestine Contents)
Lungs	Lungs	ND	UB Cont (Urinary Bladder Contents)
Muscle	Muscle	Uterus	Uterus

[a]No directly matching RASR is available. Additional imputation is required to match the listed RASRs
[b]No data. No organ content data exists in the data set.
[c]No directly matching RASR is available; soft tissue measurements are used in the "Remainder of the body" imputation
[d]The total body RASR represents the "remainder of the body" after all other RASRs are removed. The total body source group is the entire body, inclusive of all RASRs, thus additional imputation is required to match the source group to the RASR.
[e]Not used

Table 12. Database record fields and their descriptions.

Field Name	Data type	Description
Article_Code	string	Unique Identifier (UID) for source article
Individual_UID	string	UID for individual (if data are from one person)
Data_Point_UID	string	Record UID
Radioisotope	string	Radioisotope
Orig_Tissue_name	string	Tissue name as found in article
Orig_Concentration	real number	concentration value as found in article
Orig_Concentration_Units	string	concentration units as found in article
Meas_Type	string	(e.g., median concentration, mean concentration, etc.)
Uncertainty	real number	uncertainty as found in article
Uncertainty_Type	string	uncertainty type as found in article (e.g. "Standard Deviation")
Orig_Tissue_mass	real number	Tissue mass as found in article
Orig_Tissue_Mass_Units	string	Tissue mass units as found in article
Sex	string; 'M', 'F' or 'U'	gender listed in article, if available
Age	real number	age listed in article, if available
Individual_Measurement	boolean	If data came from an individual, field is TRUE; if data came from a population, field is FALSE
N	Integer	number of subjects if Individual_Measurement is FALSE
Location	string	geographic location as found in article, if available
Smoker	string; 'T', 'F' or 'U'	field only filled in if Individual_Measurement is TRUE; 'U' signifies 'unknown'
Notes	string	Notes for the record
Exclude	boolean	TRUE prevents record from being output to software input file

Table 13. Cutoff ages for matching data to RADAR phantoms.

RADAR phantom	Formula	Dividing age (years)
Newborn – 1-year-old	NA[a]	0.38
1-year-old – 5-year-old	$\sqrt{5}$	2.24
5-year-old – 10-year-old	$\sqrt{50}$	7.07
10-year-old – 15-year-old	$\sqrt{150}$	12.25
15-year-old – Adult	$\sqrt{300}$	17.32

[a]Determined to be the age at which 50% of the 1-year-old mass is attained, which is 4.5 months (ICRP 1975)

Table14. Assumed bone-seeking behavior of radionuclides in the current analysis.

Radionuclide	Assumed behavior	Radionuclide	Assumed behavior
^{3}H	Non bone-seeking	^{218}Po	Bone-volume-seeking
^{14}C	Non bone-seeking	^{219}Rn	Bone-surface-seeking
^{40}K	Non bone-seeking	^{220}Rn	Bone-surface-seeking
^{87}Rb	Non bone-seeking	^{222}Rn	Bone-volume-seeking
^{90}Sr	Bone-volume-seeking	^{223}Ra	Bone-surface-seeking
^{129}I	Non bone-seeking	^{224}Ra	Bone-surface-seeking
^{137}Cs	Non bone-seeking	^{226}Ra	Bone-volume-seeking
^{207}Tl	Bone-surface-seeking	^{227}Ac	Bone-surface-seeking
^{208}Tl	Non bone-seeking	^{227}Th	Bone-surface-seeking
^{210}Bi	Bone-volume-seeking	^{228}Ra	Bone-volume-seeking
^{210}Pb	Bone-volume-seeking	^{228}Th	Bone-surface-seeking
^{210}Po	Bone-volume-seeking	^{228}Ac	Bone-volume-seeking
^{211}Pb	Bone-surface-seeking	^{230}Th	Bone-surface-seeking
^{211}Bi	Bone-surface-seeking	^{231}Th	Bone-volume-seeking
^{212}Pb	Bone-surface-seeking	^{231}Pa	Bone-surface-seeking
^{212}Bi	Bone-surface-seeking	^{232}Th	Bone-surface-seeking
^{212}Po	Bone-surface-seeking	^{234m}Pa	Bone-volume-seeking
^{214}Po	Bone-volume-seeking	^{234}U	Bone-volume-seeking
^{214}Bi	Bone-volume-seeking	^{234}Th	Bone-volume-seeking
^{214}Pb	Bone-volume-seeking	^{235}U	Bone-volume-seeking
^{215}Po	Bone-surface-seeking	^{238}U	Bone-volume-seeking
^{216}Po	Bone-surface-seeking		

Table 15. List of radionuclides considered in the intake analysis for imputing activity in hollow-organ contents. Radionuclides not listed in this table are assumed to be not present.

Radionuclide	Reason for inclusion
^{3}H	Cosmogenic radionuclide
^{14}C	Cosmogenic radionuclide
^{40}K	Long-lived Primordial Radionuclide
^{87}Rb	Long-lived Primordial Radionuclide
^{232}Th	Long-lived Primordial Radionuclide
^{228}Ra	Long-lived Primordial Radionuclide
^{228}Ac	Significant gamma emitter in equilibrium with ^{228}Ra
^{238}U	Long-lived Primordial Radionuclide
^{234}U	Long-lived Primordial Radionuclide
^{226}Ra	Long-lived Primordial Radionuclide
^{210}Pb	Long-lived Primordial Radionuclide
^{210}Po	Long-lived Primordial Radionuclide
^{235}U	Long-lived Primordial Radionuclide

Table 16. Radionuclides assumed to be in radioactive disequilibrium with their parents.

Parent	Progeny assumed to be in disequilibrium	Series
^{232}Th	^{228}Ra	Thorium
^{228}Ac	^{228}Th	Thorium
^{212}Po	^{208}Tl	Thorium
^{226}Ra	^{222}Rn	Uranium
^{214}Pb	^{214}Bi	Uranium
^{214}Po	^{210}Pb	Uranium
^{210}Bi	^{210}Po	Uranium
^{231}Th	^{231}Pa	Actinium
^{231}Pa	^{227}Ac	Actinium

Table 17. Radionuclides assumed to have a fractional retention less than 100% and the fractional retention factors used (NCRP 1987).

Radionuclide	Fractional Retention of Radionuclide
^{220}Rn	0.9
^{216}Po	0.9
^{212}Pb	0.9
^{212}Bi	0.6
^{212}Po	0.6
^{208}Tl	0.3

Table 18. Average annual effective doses to the seven populations in this study. Doses were calculated using 2007 ICRP weighting factors and the coefficient of variation for each dose represents the upper bound of variability**.**

	Annual Effective Dose (μSv)							
Population	1st per-centile	5th per-centile	50th per-centile	Average	95th per-centile	99th per-centile	*CV*	s_G
Adult Male	82	125	346	418	953	1450	0.68	1.85
Adult Female	52	83	261	332	819	1316	0.79	2.01
15-year-old	68	109	339	430	1054	1686	0.78	1.99
10-year-old	77	120	351	434	1027	1603	0.73	1.92
5-year-old	73	116	353	443	1071	1697	0.76	1.96
1-year-old	89	135	367	442	1000	1514	0.67	1.84
Newborn	112	163	400	465	984	1428	0.59	1.73

Table 19. Percentage of adult male average annual effective dose by radionuclide type and radiation using 2007 ICRP tissue weighting factors. Bold text represents the maximum value in each column.

	Alpha	Beta/gamma	Total
Anthropogenic	0%	0.08%	0.08%
Cosmogenic	0%	1.46%	1.46%
Non-Series Primordial	0%	**50.48%**	**50.48%**
Uranium Series	**37.54%**	0.15%	37.69%
Thorium Series	9.7%	0.5%	10.23%
Actinide Series	0.05%	0%	0.05%
Totals	47.32%	52.68%	100.00%

Table 20. Annual weighted equivalent doses to ICRP Target Tissues (TarTs) by ICRP tissue weighting factor recommendation year. Tissues are in order of decreasing dose using 2007 ICRP tissue weighting recommendations. Values in bold are the highest annual weighted equivalent dose for the ICRP tissue weighting factor recommendation year and values in italics are the second highest. Values in parenthesis are percent contribution of the weighted equivalent dose to the total annual effective dose. Doses are in μSv.

		Annual equivalent dose					
ICRP Target Tissue (TarT)	H_T (μSv)	2007 ICRP Weighting Factors (E = 418 μSv) $w_T H_T$ (μSv)		1990 ICRP Weighting Factors (E = 444 μSv) $w_T H_T$ (μSv)		1977 ICRP Weighting Factors (E = 536 μSv) $w_T H_T$ (μSv)	
Lung	522.7	**62.7**	**(15%)**	*62.7*	*(14%)*	62.7	(12%)
Bone-marrow (red)	491.6	*59.0*	*(14%)*	59.0	(13%)	59.0	(11%)
Gonads	535.0	42.8	(10%)	**107.0**	**(24%)**	**134.0**	**(25%)**
Breast	290.2	34.8	(8.33%)	14.5	(3.27%)	43.6	(8.13%)
Thyroid	819.8	32.8	(7.85%)	41.0	(9.23%)	24.6	(4.59%)
Colon	258.2	31.0	(7.42%)	31.0	(6.98%)	15.5	(2.89%)
Bone surface	2930.0	29.3	(7.01%)	29.3	(6.60%)	*87.9*	*(16%)*
Liver	687.3	27.7	(6.63%)	34.7	(7.82%)	41.6	(7.76%)
Stomach	173.7	20.8	(4.98%)	20.8	(4.68%)	--	--
Esophagus	293.0	11.7	(2.80%)	14.7	(3.31%)	17.6	(3.28%)
Bladder	219.7	8.8	(2.11%)	11.0	(2.48%)	13.2	(2.46%)
Pancreas	626.0	5.8	(1.39%)	3.1	(0.70%)	--	--
Kidneys	578.2	5.5	(1.32%)	3.0	(0.68%)	35.4	(6.60%)
Adrenals	497.6	4.6	(1.10%)	2.5	(0.56%)	--	--
Heart	471.1	4.4	(1.05%)	--[a]	--[a]	--	--
Spleen	364.6	3.4	(0.81%)	1.8	(0.41%)	--	--
Brain	304.0	3.0	(0.72%)	1.5	(0.34%)	--	--
Muscle	294.6	2.7	(0.65%)	1.5	(0.33%)	--	--
Thymus	293.0	2.7	(0.65%)	1.5	(0.33%)	--	--
Gall bladder	225.8	2.1	(0.50%)	--	--	--	--
Small intestine	207.2	1.9	(0.46%)	1.0	(0.23%)	--	--
Skin	143.4	1.4	(0.34%)	1.4	(0.32%)	1.4	(0.27%)

Table 21. TarTs receiving annual weighted equivalent doses that are 10% or greater of the annual effective dose for the phantom containing them. TarTs are organized by phantom and are listed in descending order of annual weighted equivalent dose. Total annual effective dose for the phantom is provided in parentheses after the phantom name. Doses are calculated using 2007 ICRP tissue weighting factors.

ICRP TarT	Annual Weighted Equivalent Dose (μSv)	Percent of Annual Effective Dose
	Adult Male (418 μSv y^{-1})	
Lung	62.7	15%
Bone-marrow	59.0	14%
Gonads	42.8	10%
	Adult Female (332 μSv y^{-1})	
Lung	54.1	16%
Bone-marrow	44.4	13%
Gonads	31.4	9%
	15-yr-old (430 μSv y^{-1})	
Lung	61.9	14%
Bone-marrow	59.3	14%
Gonads	45.4	11%
	10-yr-old (434 μSv y^{-1})	
Bone-marrow	60.7	14%
Lung	55.8	13%
Gonads	46.0	11%
	5-yr-old (443 μSv y^{-1})	
Bone-marrow	65.6	15%
Lung	56.4	13%
Gonads	46.6	11%
	1-yr-old (442 μSv y^{-1})	
Bone-marrow	73.9	17%
Lung	61.2	14%
Gonads	44.2	10%
	Newborn (465 μSv y^{-1})	
Bone-marrow	89.0	19%
Lung	62.1	13%
Colon	59.1	13%

Table 22. NCRP estimates of annual weighted equivalent dose to selected tissues compared with those of the current analysis. For a direct comparison, only the radionuclides used in NCRP 93 (1987) were used to calculate the annual weighted equivalent doses in this table. Equivalent doses are in μSv.

	Lung	Gonads	Bone Surface	Bone Marrow	Other Tissues	Total[a]
NCRP 93 (1987)	40	90	30	60	170	390
Current Analysis (1977 ICRP weighting factors)	63	134	88	59	192	536
Current Analysis (2007 ICRP weighting factors)	63	43	29	59	224	418

[a]Effective dose for this study and effective dose equivalent in NCRP 93 (1987)

Table 23. Activity concentrations used by NCRP (1987) and in the current analysis for the 3 highest contributors to annual effective dose.

	NCRP 94	Current Analysis	NCRP 94	Current Analysis	NCRP 94	Current Analysis
	^{40}K (Bq kg^{-1})		^{210}Po (mBq kg^{-1})		^{226}Ra (mBq kg^{-1})	
Gonads	63	64	260	331	3	5
Breast	--[a]	44	--	21	3	3
Lungs	63	60	260	261	3	3
Bone	15	55	2,700	1,998	170	271
Red bone marrow	130	130	260	260	3	3
Thyroid	33	33	200	214	3	3
Kidney	56	79	480	330	--	4
Liver	74	85	560	515	--	9
Spleen	--	44	130	121	--	5
Heart	--	44	110	73	--	4
Other tissues	59	61	--	129	3	8

[a]Indicates data value was not provided

Table 24. NCRP estimates of annual weighted equivalent dose to selected tissues compared with those of the current analysis using the same data as NCRP. Equivalent doses are in μSv.

	Lung	Gonads	Bone Surface	Bone Marrow	Other Tissues	Total[a]
NCRP 93 (1987)	40	90	30	60	170	390
Current Analysis (NCRP 94 Data/1977 ICRP weighting factors)	62	113	85	54	179	493

[a]Effective dose for this study and effective dose equivalent in NCRP 93 (1987)

Table 25. Comparison of the average annual effective dose to an adult male estimated by the NCRP (2009) to annual effective doses to adult males and adult females estimated by the present work.

	This Study						NCRP 160	
	Men			Women				
Chain	Non-Primordial	Primordial	Total	Non-Primordial	Primordial	Total	Total	This Study/ NCRP 160
Other (^{3}H, ^{14}C, ^{87}Rb, ^{137}Cs-^{137m}Ba)	6.5	4.3	10.8	6.1	4.3	10.0	10.0	108%
^{40}K		206.9	206.9		181.7	181.7	149.0	139%
^{232}Th, ^{238}U, ^{235}U series		200.7	200.7		140.1	140.1	126.6	159%
Total	6.5	412.0	418.5	6.1	326.1	332.2	285.6	147%
		Difference	132.9		Difference	46.6		

Table 26. Comparison of UNSCEAR (2000) average annual effective doses with those of the current analysis, where only the radionuclides used in UNSCEAR (2000) were used. Doses are in μSv.

	$^{238/234}$U	^{230}Th	^{226}Ra	^{210}Pb/Po	^{232}Th	$^{228/224}$Ra	^{40}K	Totals
UNSCEAR	7	6	7	80	4	18	165	310[a]
Current analysis	10	5	31	130	3	16	211	405

[a]The UNSCEAR total used here is not a sum of the previous columns in the table, but rather the value quoted in the text of UNSCEAR (2000), which is that from ingestion and inhalation. UNSCEAR (2000) states that using tissue concentrations produces "...essentially the same result..."

Table 27. Tissue activity concentrations used by UNSCEAR (2000) and in the current analysis for the 3 highest contributors to annual effective dose.

	UNSCEAR	Current Analysis	UNSCEAR	Current Analysis	UNSCEAR	Current Analysis
	^{40}K (Bq kg^{-1})		^{210}Po (mBq kg^{-1})		^{226}Ra (mBq kg^{-1})	
Lungs	55	60	200	261	4	3
Bone	55	55	2,400	1,998	260	271
Kidney	55	79	600	330	4	4
Liver	55	85	600	515	4	9
Other tissues	55	107	100	129	4	3

Table 28. Comparison of UNSCEAR (2000) average annual effective doses with annual effective doses to an adult male using ICRP 1990 tissue weighting factors calculated by the current analysis using only UNSCEAR (2000) data. Doses are in μSv.

	$^{238/234}$U	^{230}Th	^{226}Ra	^{210}Pb/Po	^{232}Th	$^{228/224}$Ra	^{40}K	Totals
UNSCEAR	7	6	7	80	4	18	165	310[a]
Current analysis (w/UNSCEAR (2000) Data)	6	6	5	98	3	0.07	18	135

[a]The UNSCEAR total used here is not a sum of the previous columns in the table, but rather the value quoted in the text of UNSCEAR (2000), which is that from ingestion and inhalation. UNSCEAR (2000) states that using tissue concentrations produces "...essentially the same result..."

Table 29. Comparison of lymph node activity concentrations with lung activity concentrations for radionuclides for which lymph node data is found in the literature. Activity concentrations are in mBq kg^{-1}

	Adult Male			Adult Female		
	Lymph Nodes	Lungs	Ratio (LN/Lung)	Lymph Nodes	Lungs	Ratio (LN/Lung)
^{232}Th	250	19.2	13	258	23.2	1.18
^{228}Th	222	12.4	18	153	15.2	0.65
^{238}U	1,150	8.9	129	--	8.9	--
^{234}U	1,150	8.9	129	--	8.9	--
^{230}Th	327	33.9	10	334	44.6	0.92
^{210}Pb	1,100	192.0	6	--	368.0	--
^{210}Po	780	259.0	3	--	131.0	--
^{235}U	52	0.4	129	--	0.4	--

Table 30. Approximate contribution to average annual effective dose to an adult male from lymph nodes using ICRP 2007 tissue weighting factors. Lymph node weighted equivalent doses are approximated by multiplying the lymph node concentration by the ratio of lung equivalent dose to lung concentration for a given radionuclide. Lung concentrations and equivalent doses are provided here for comparison.

	Lungs		Lymph Nodes		
	Concentration (mBq kg^{-1})	Equivalent Dose (µSv)	Concentration (mBq kg^{-1})	Equivalent Dose (µSv)	Annual Weighted Equivalent Dose (µSv)[a]
^{210}Pb	191.8	0.1	1,100.0	0.3	0.0
^{210}Po	261.2	162.4	780.0	485.0	4.5
^{228}Th	12.4	7.0	222.3	126.0	1.2
^{230}Th	33.9	16.0	326.6	154.0	1.4
^{232}Th	19.2	8.1	249.6	105.0	1.0
^{234}U	8.9	5.1	1,147.7	662.0	6.1
^{235}U	0.4	0.2	52.8	27.7	0.3
^{238}U	8.9	4.5	1,147.7	580.0	5.4
				Total (µSv):	19.8

[a]Equivalent dose multiplied by ICRP 2007 tissue weighting factor of 0.0923

Table 31. Polonium-210 tissue activity concentration differences between smoking and non-smoking subjects. The "unknown" column contains tissue activity concentrations in subjects for which smoking history was not obtained. Concentrations are in mBq kg^{-1}.

	Non-Smokers	Smokers	Unknown	Difference (Smokers - Non-Smokers)
Heart Contents	111	30[b]	20	-81
Heart Wall	37	70	76	33
Kidneys	381	289	480	-92
Liver	328	565	539	236
Lungs	111	344	270	233
Muscle	27	22	36[c]	-5
Pancreas	91	128	144	37
Spleen	83	149	72	66
Testes	9[a]	244	419	235
Thyroid	118	268	200	150
Soft Tissue	23[a]	30[b]	129	7

[a]Tissue concentration for non-smokers is not available and is therefore imputed from non-concentrator organ concentrations
[b]Tissue concentration for smokers is not available and is therefore imputed from non-concentrator organ concentrations
[c]Tissue concentration for subjects with "unknown" smoking history is not available and therefore imputed from non-concentrator organ concentrations

Table 32. Lead-210 tissue activity concentration differences between smoking and non-smoking subjects. The "unknown" column contains tissue activity concentrations in subjects for which smoking history was not obtained. Concentrations are in mBq kg^{-1}.

	Non-Smokers	Smokers	Unknown	Difference (Smokers - Non-Smokers)
Kidneys	215	148	186	-67
Liver	237	468	328	231
Lungs	170	311	182	141
Pancreas	87	122	83	35
Bone	1,336	131[a]	2,145	-1,205
Spleen	54	178	167	125
Thyroid	126	315	280	189

[a]Bone concentration for smokers is not available and is therefore imputed from non- concentrator organ concentrations

Table 33. Average annual effective doses to smokers, non-smokers and subjects with unknown smoking histories. Differences in dose are caused by differences in tissue activity concentrations of ^{210}Po.

	Ann. Eff. Dose (μSv)
Smokers	376
Non-Smokers	332
Unknown smoking history	424

Table 34. TarTs receiving annual weighted equivalent doses that are 10% or greater of the average annual effective dose for the phantom containing them. TarTs are organized by subjects' smoking history and are listed in descending order of annual weighted equivalent dose. Total annual effective dose for the phantom is provided in parentheses after the phantom name. Doses are calculated using 2007 ICRP tissue weighting factors.

ICRP TarT	Annual Weighted Equivalent Dose (μSv)	Percent of Annual Effective Dose
	Smokers (376 μSv y^{-1})	
Lung	66.0	18%
Bone-marrow	40.1	11%
Gonads	37.4	10%
	Non-Smokers (332 μSv y^{-1})	
Lung	50.6	15%
Bone-marrow	38.1	11%
Breast	31.6	10%
	Unknown Smoking History (424 μSv y^{-1})	
Lung	63.3	15%
Bone-marrow	59.0	14%
Gonads	46.2	11%

Table A.1. Tests designed to verify the software code written in support of the present work performs the designed calculations correctly.

Test No.	Test item	Method	Pass
1	Software correctly imports phantom data.	Visual verification between source ASCII text file and software for all phantoms	Yes
2	Software correctly imports tissue mass data.	Visual verification between source ASCII text file and software for all tissues	Yes
3	Software correctly imports concentration input file.	Boolean check in a spreadsheet between input file and exported "concentrations" tab.	Yes
4	Software correctly imports dose factors from input file.	Boolean check in a spreadsheet between input text file and 10% of the dose factors loaded from binary file format. The check needs to include the first dose factors found at the beginning and end of the ASCII text input file and randomly selected factors in between.	Yes
5	Software correctly converts concentrations.	All concentrations are converted to units of MBq kg^{-1} in the database. A Boolean check will be made in a spreadsheet between these hand-calculated values and the values calculated and exported by the software.	Yes
6	Software correctly converts uncertainties.	All uncertainties are converted to units of MBq kg^{-1} in the database. A Boolean check will be made in a spreadsheet between these hand-calculated values and the values calculated and exported by the software.	Yes
7	Software correctly aggregates multiple tissue concentrations from an individual (LitTIVAD) to a single tissue group concentration (iTIVAD).	A single radionuclide encompassing both disaggregation and aggregation will be selected. All data for that radionuclide will need to be hand calculated and Boolean checked against the output results from the software.	Yes
8	Software correctly disaggregates individual concentrations (iTIVAD) from a sample set average concentration (LitTIVAD).		Yes
9	Software correctly aggregates all individual measurements (iTIVADs), into a correct average concentration for a given radionuclide, phantom and tissue combination (RASR)?		Yes
10	Software provides a concentration average for every radionuclide, phantom and tissue combination for which there is data.	A pivot table will be made of the export from the "LitTIVADs" tab of the software. Another pivot table will be made from the "iTIVADs" tab of the software. Each pivot table shows possible radionuclide, phantom and tissue combinations available in the data. When compared, the same table cells should be blank or have data between the two tables.	Yes
11	Software correctly imputes values for tissues	A mass weighted average (and standard deviation) of Adult Male RASR values will	Yes

	which have no measured data	be calculated for ^{14}C and ^{40}K. This weighted average will be compared against the one calculated by the software for imputing into tissues which have no measured data.	
12	Software correctly apportions activity into cortical and trabecular bone.	Adult male RASR concentrations for ^{232}Th in bone will be exported and used to calculate activities for cortical and trabecular bone. These activities will be multiplied by the applicable trabecular or cortical mass fraction and the result compared against that calculated by the software.	Yes
13	Software correctly calculates activity in the remainder of the body	Adult male compiled RASRs for ^{87}Rb will be exported from the software and used to hand calculated the remainder of the body activity and the result will be compared against that calculated by the software.	Yes
14	Software correctly models organ content activities.	Concentration data exported from the software and the Dietary Intake ini file will be used to calculate organ content activities as described in the methods. These results will be compared against that calculated by the software.	Yes
15	Software correctly imputes ^{228}Ra activities for tissues other than bone.	Adult male RASR activity data for ^{226}Ra, ^{230}Th, and ^{232}Th will be exported from the software. These data will be used to hand-calculate the ^{228}Ra values and the results will be compared against Adult Male RASR activity data calculated by the software for ^{228}Ra.	Yes
16	Software correctly imputes values for radionuclides that have no measured data.	Use the NewParents.ini file to determine which radionuclides are considered "new parents" and which should have values imputed ("imputed radionuclides"). Use concentrations exported from the software to determine if any of the imputed radionuclides have concentration data. Adult Male RASR data exported from the software will be used to determine if the activity values were imputed into imputed radionuclides lacking concentration data.	Yes
17	Software correctly imputes values for phantoms that have no measured data.	Using only non-imputed concentration data, identify radionuclide and RADAR source tissue combinations in the adult male data set that do not have counterpart data. For each phantom that is not adult male, use the lists of missing data developed in the previous step to verify that they were imputed by comparing them against exported imputed concentration data for each phantom.	Yes
18	Software correctly calculates absorbed dose.	Absorbed dose will be hand calculated for the adult male phantom using a selected set of RASRs and dose factors. These results will be compared to results exported from the "ICRP Doses" tab of the software.	Yes
19	Software correctly calculates equivalent doses.	Equivalent doses for the absorbed doses from test 18 will be hand calculated and compared to the software output.	Yes
20	Software correctly calculates and applies the correction factor for ICRP tissues without RADAR equivalents. Software correctly calculates annual effective dose.	Using 2007 ICRP weighting factors, hand calculate the Unmatched Organs Factor and the annual effective dose for adult male. Compare the results with those exported from the software.	Yes

Table B.1. Contributions of the co-authors of this manuscript. Contributions are measured in hours.

	Watson	Strom
Research Design & Discussion	100	130
Literature Search	120	10
Data Entry, Verification and Validation	80	20
Coding	907	0
Writing Literature Search	45	0
Writing Methods	35	10
Writing Results	12	0
Writing Discussion and Conclusions	45	1
Creating Figures	20	3
Creating Tables	30	5
Review	0	60

Figure 1. Illustration of data processing steps. Italic text represents concentration data and bold text represents activity data.

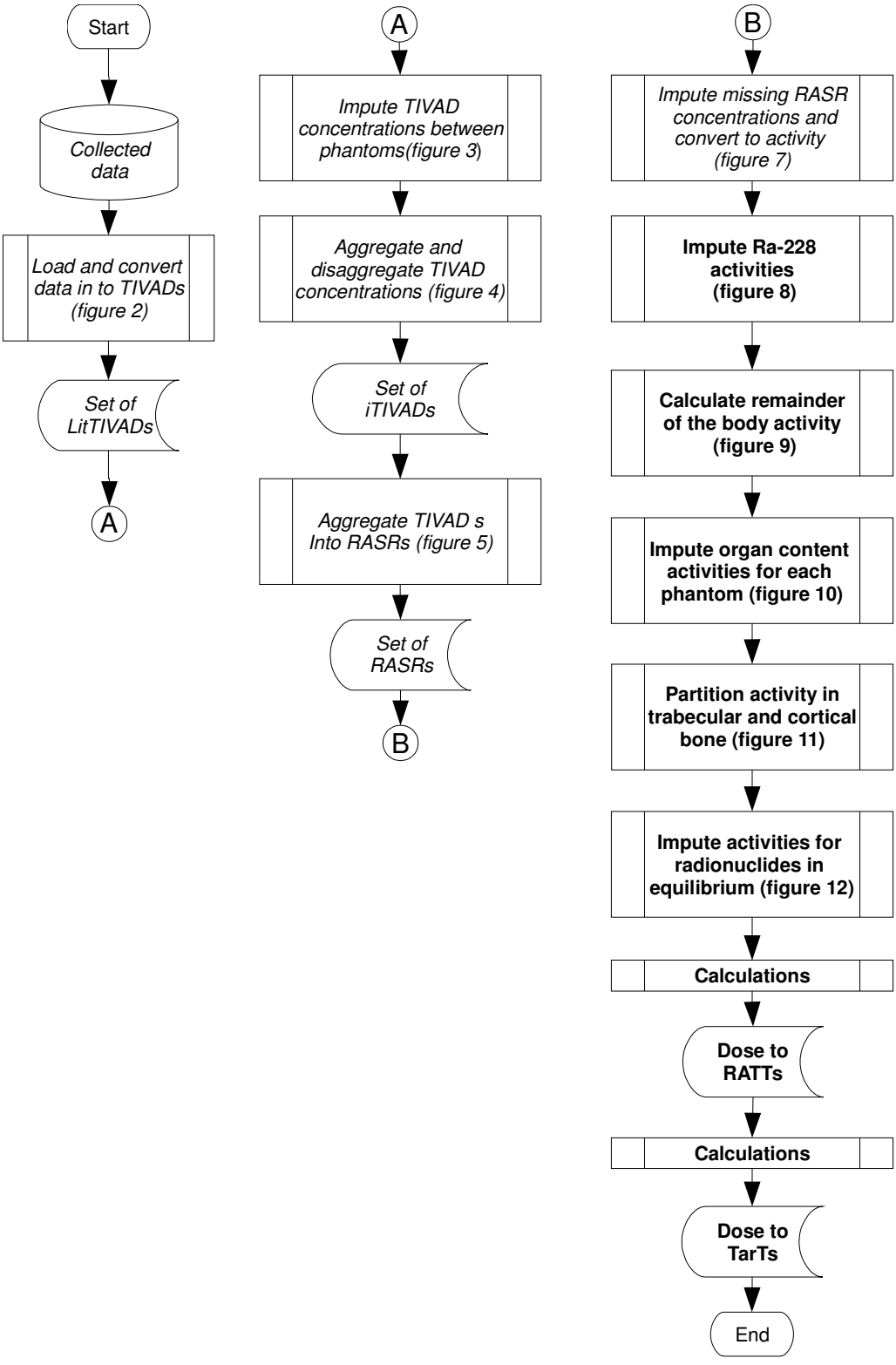

Figure 2. Methods used to load and convert tissue concentration data. Italic text represents concentration data.

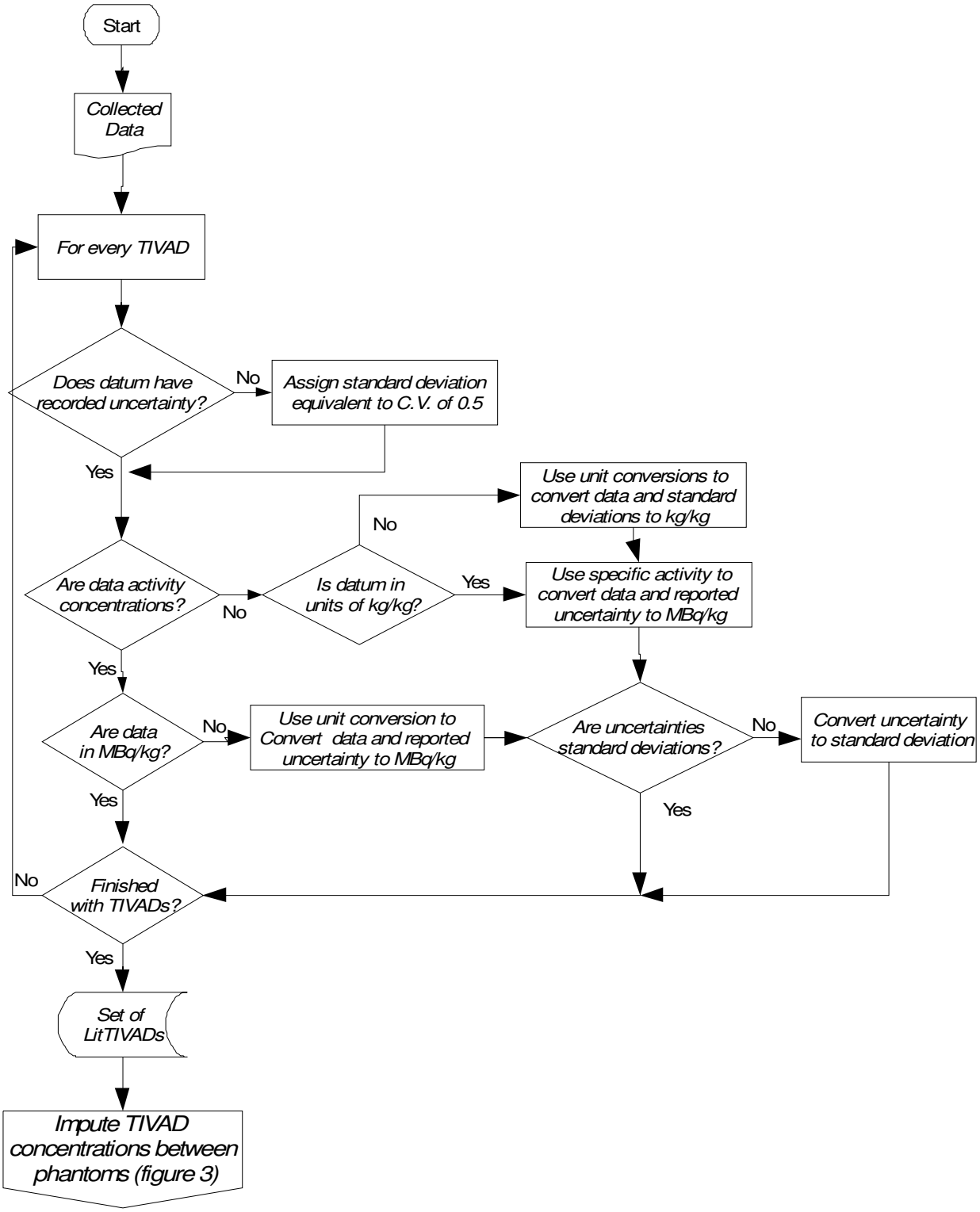

Figure 3. Methods used to impute missing tissue concentration data across phantoms. Italic text represents concentration data.

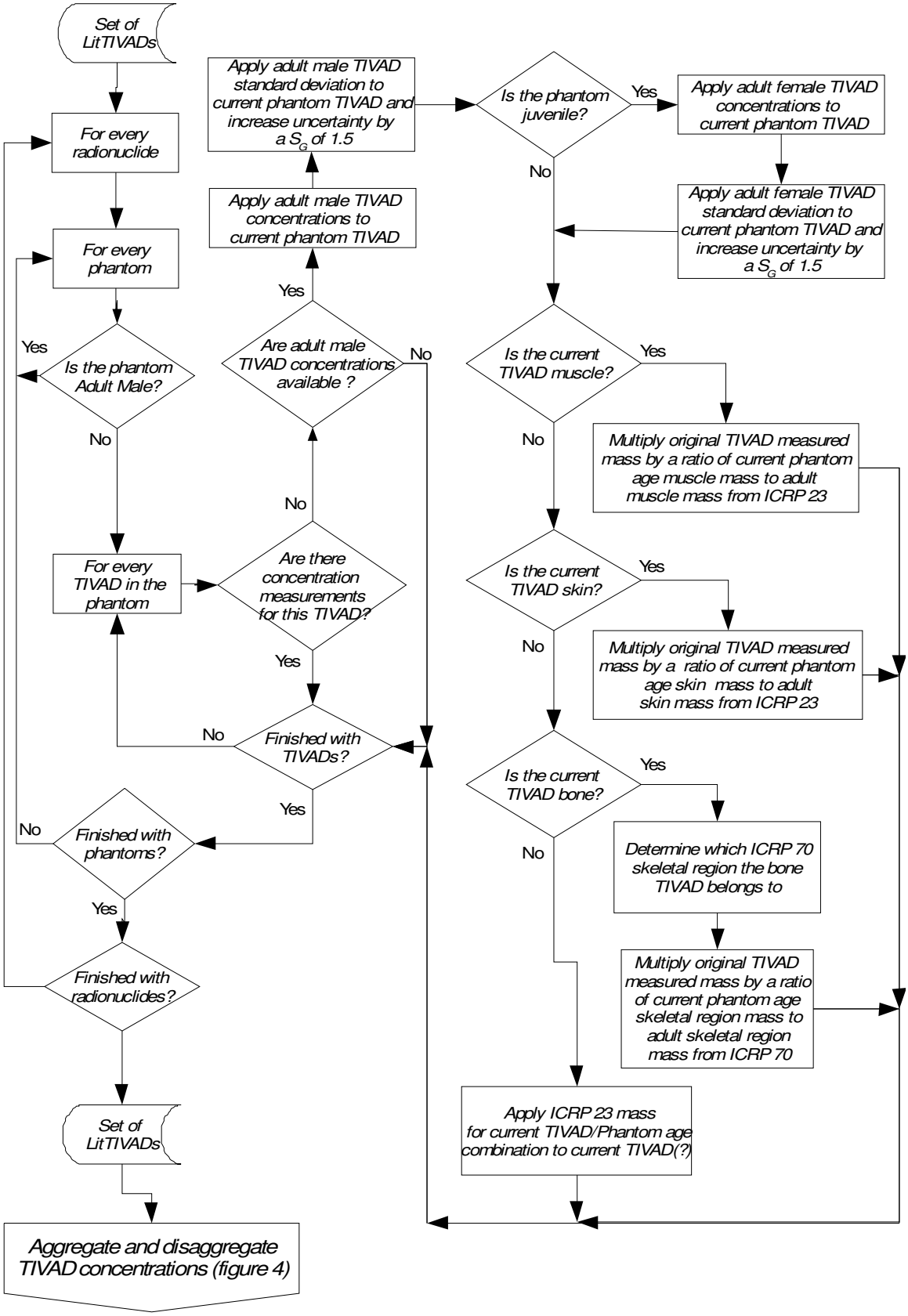

Figure 4. Methods used to aggregate and disaggregate tissue concentrations within tissue (in vivo or autopsy) data (TIVADs). Italic text represents concentration data.

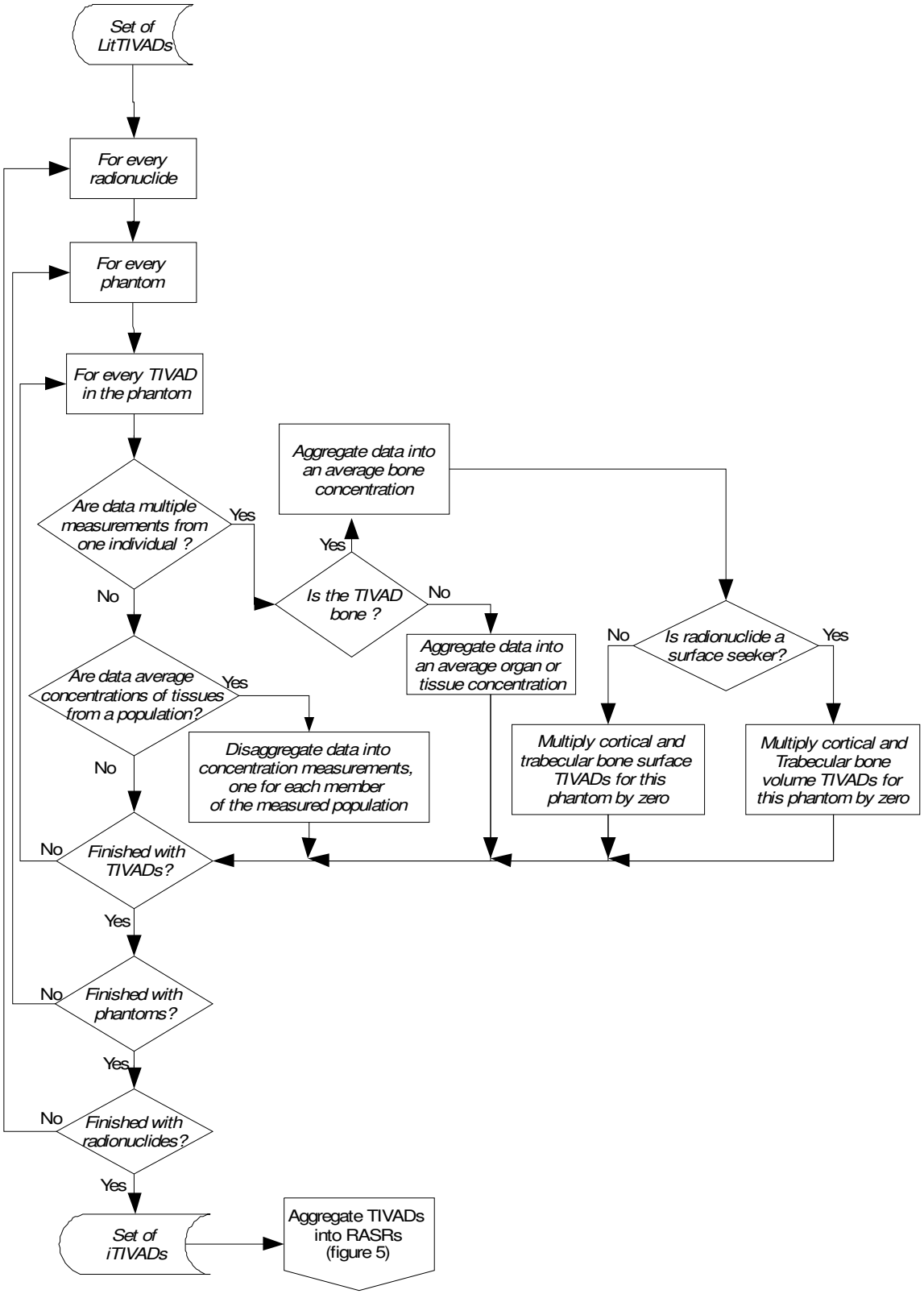

Figure 5. Procedure for aggregating iTIVAD concentrations into RASR concentrations. Italic text represents concentration data.

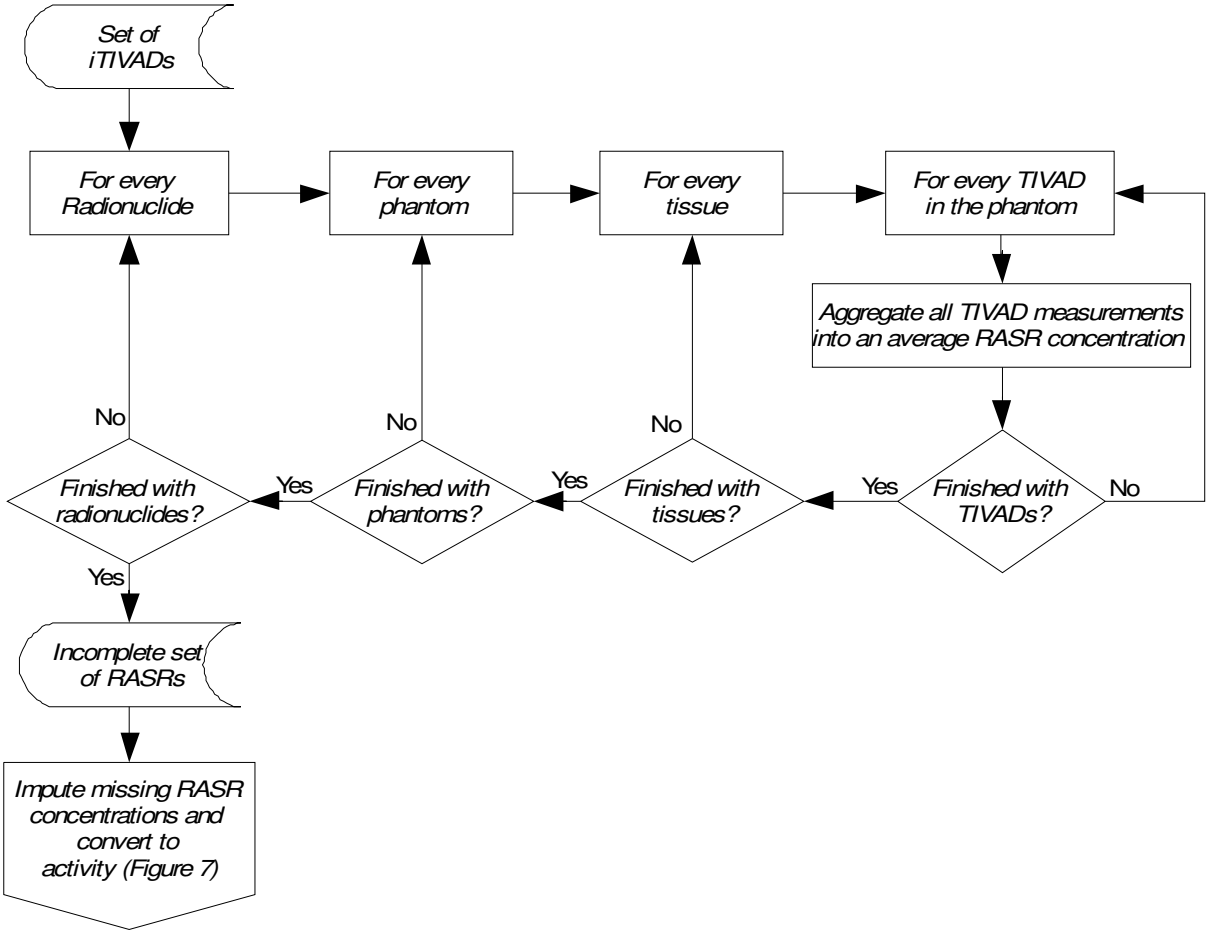

Figure 6. Lognormal distribution of possibly true values created from the arithmetic mean and standard deviation of the set of data from Lynch (2009) superimposed over the distribution of original data. The new distribution contains no negative values. The observed data are baseline ^{137}Cs measurements of 5,568 male Hanford workers (non-occupationally exposed), aged 18-85 (2000-2007 results) with an arithmetic mean of 92 mBq kg^{-1}, and a standard deviation of 205 mBq kg^{-1}. The possibly true lognormal concentration distribution has a geometric mean (C_{50}) of 25 mBq kg^{-1}, and a geometric standard deviation (s_G) of 5.02.

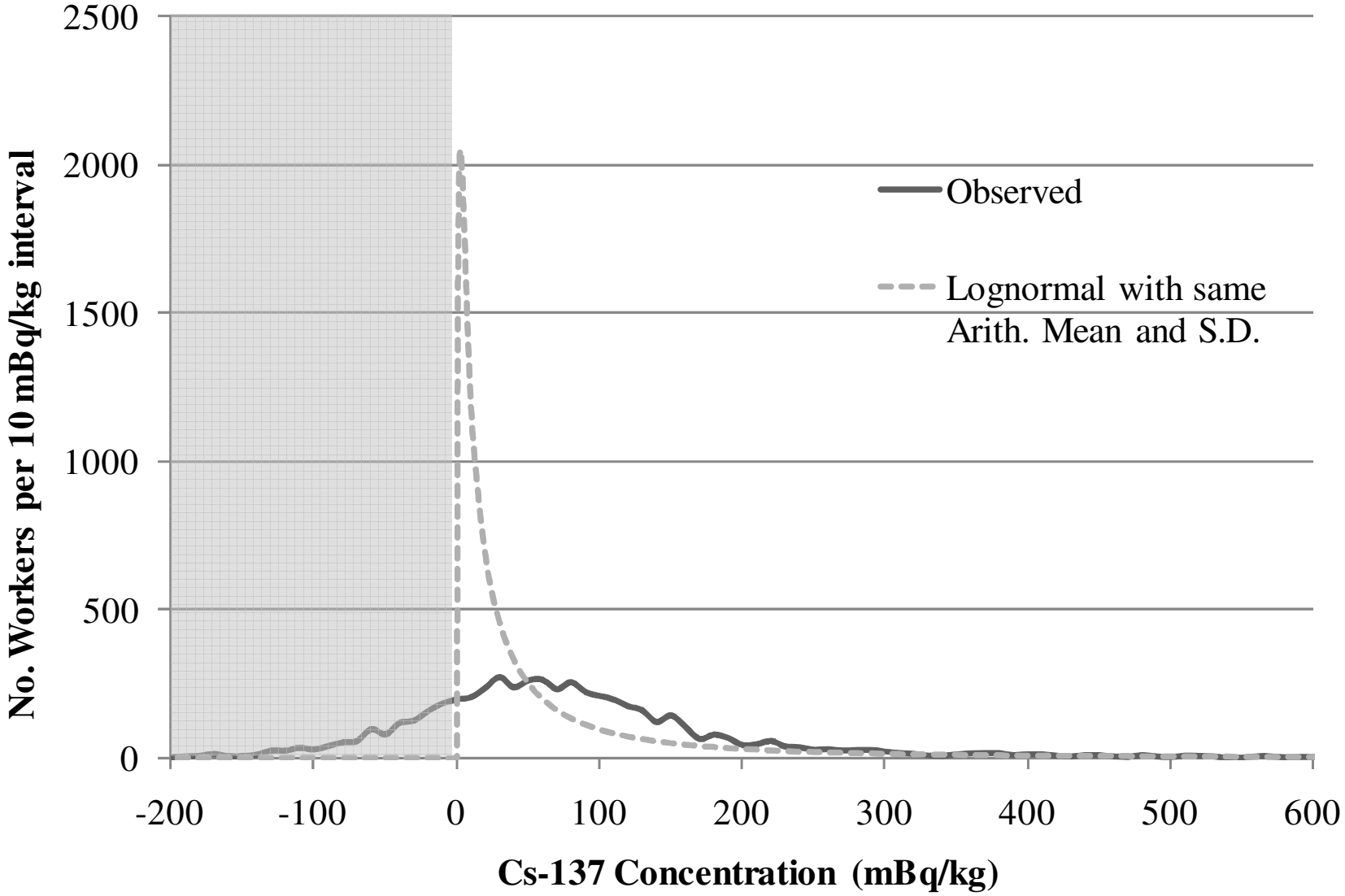

Figure 7. Method for imputing tissue concentrations in RASRs lacking such data. Italic text represents concentration data and bold text represents activity data

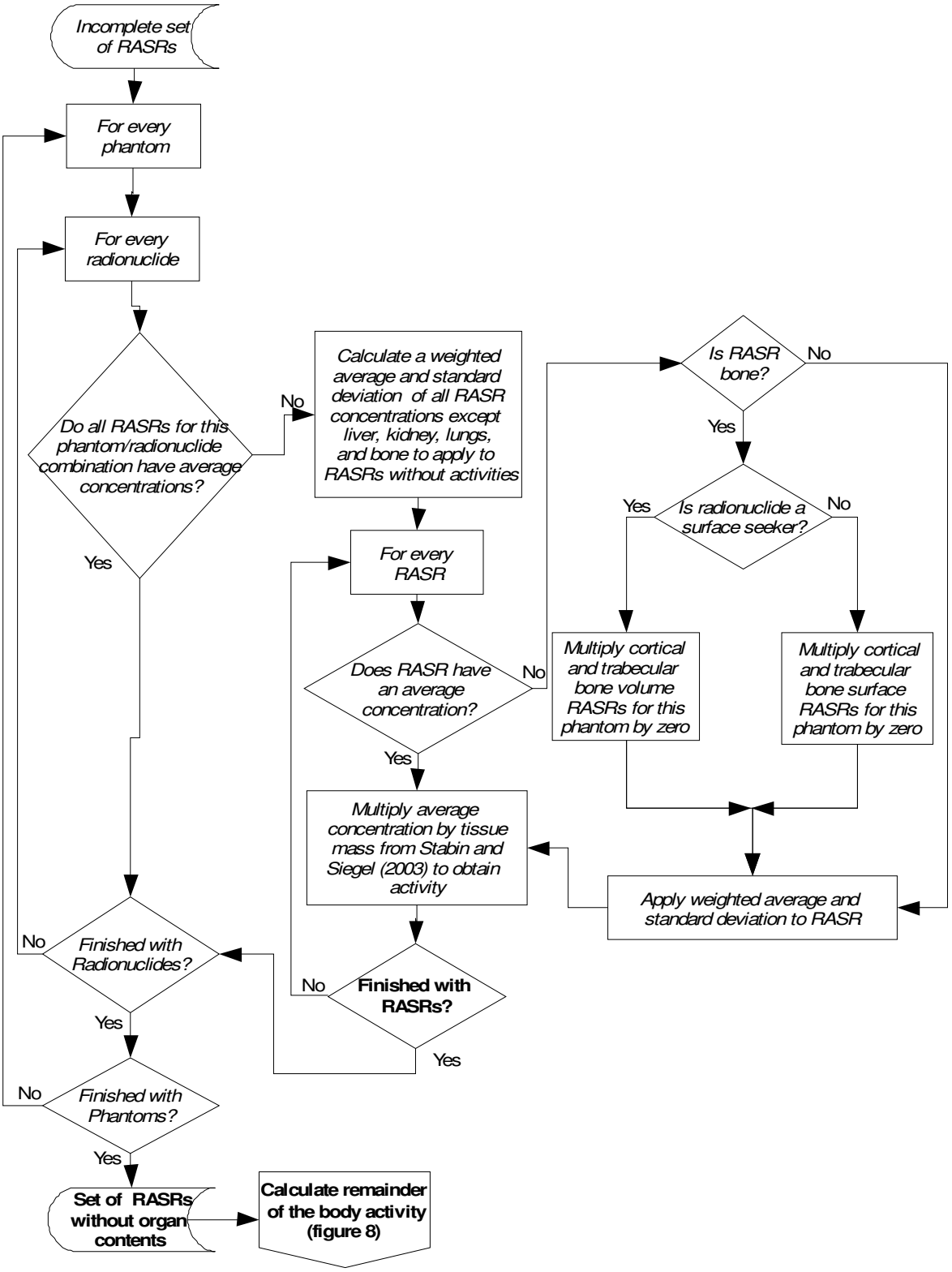

Figure 8. Procedure for imputing ^{228}Ra activities for RASRs lacking ^{228}Ra data. Bold text represents activity data.

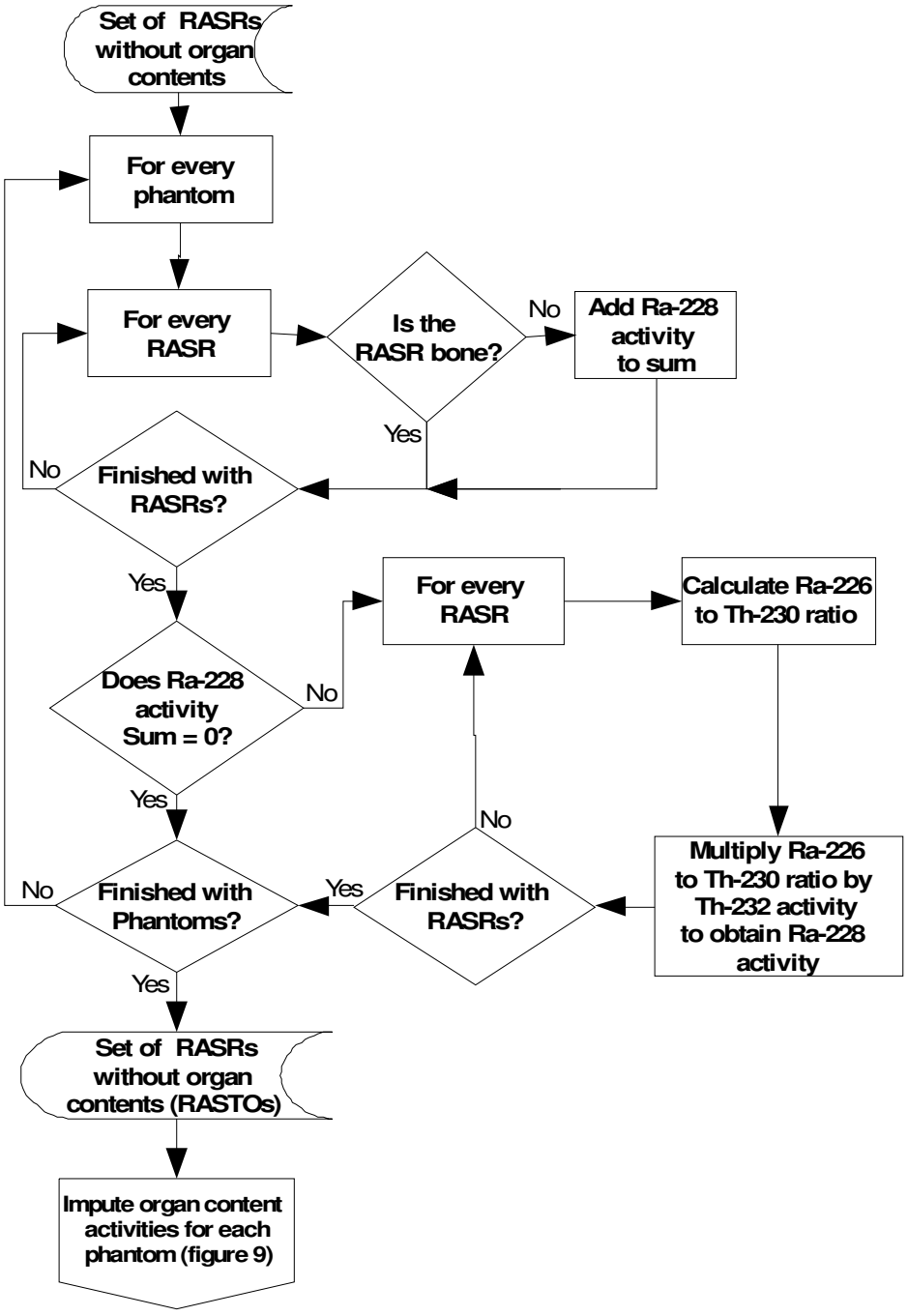

Figure 9. Method for calculating the remainder of the body activity for each RADAR phantom. Bold text represents activity data.

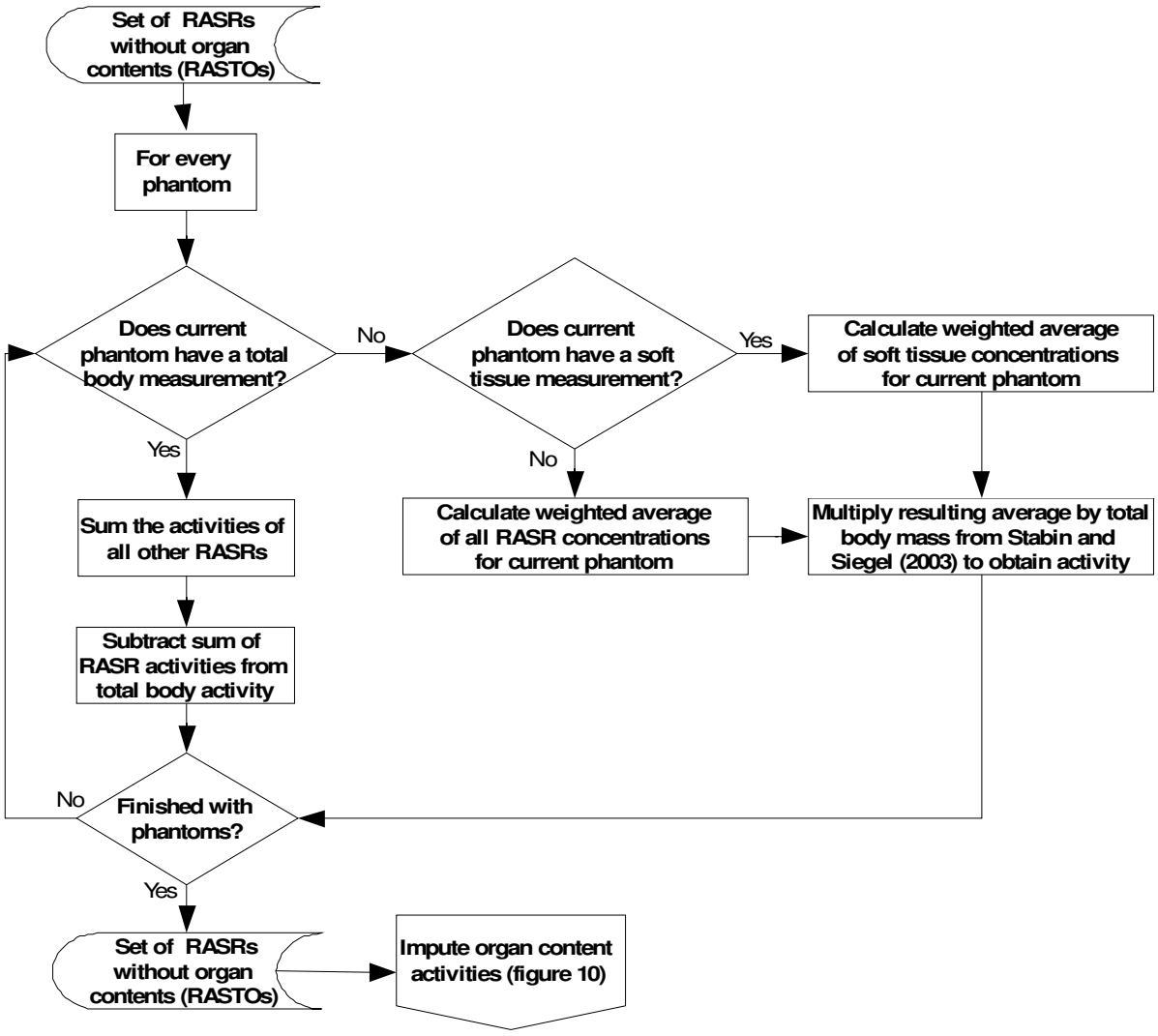

Figure 10. Procedure for imputing hollow-organ content activities. Bold text represents activity data.

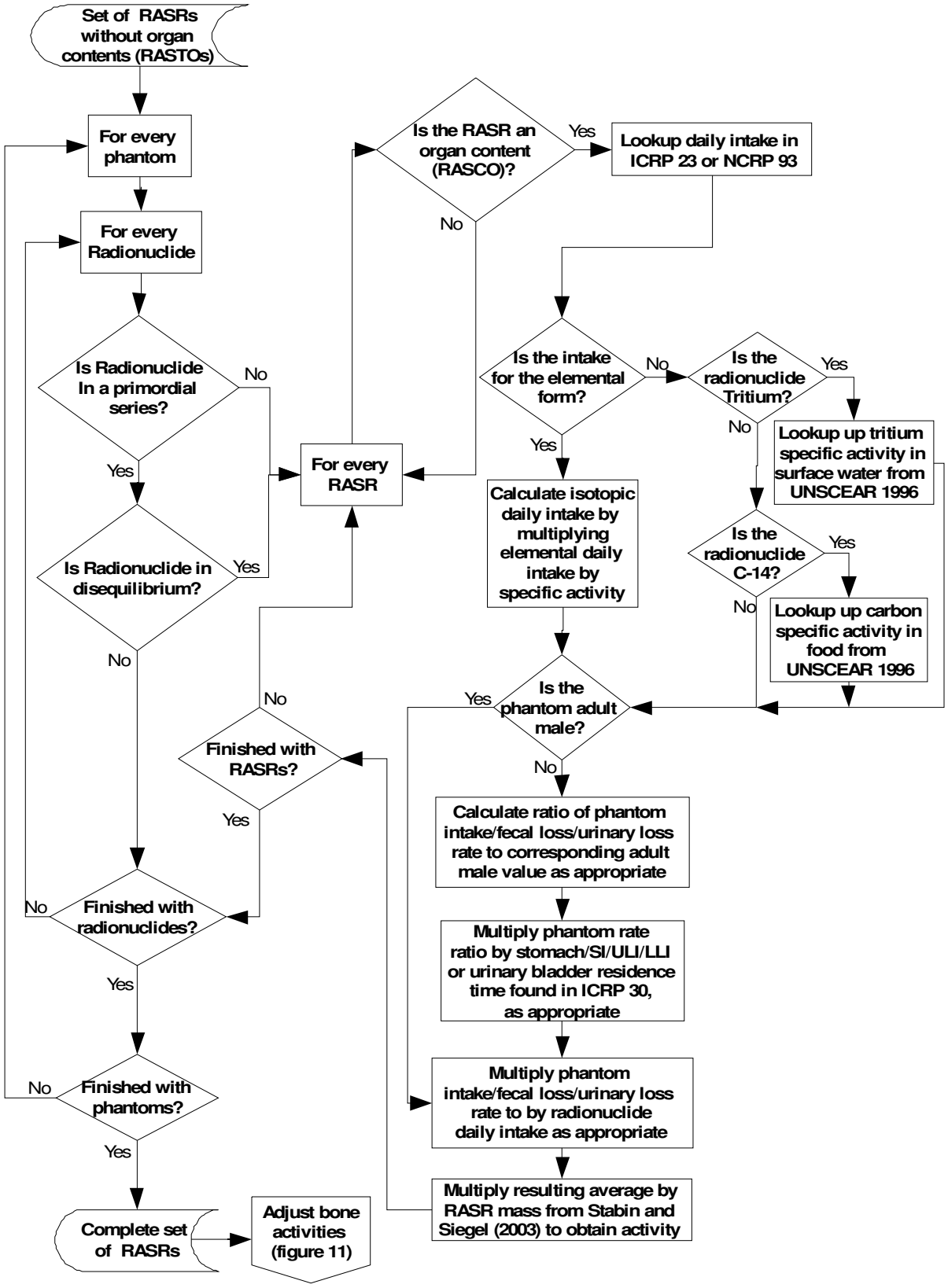

Figure 11. Method used to apportion bone activity into trabecular and cortical bone.

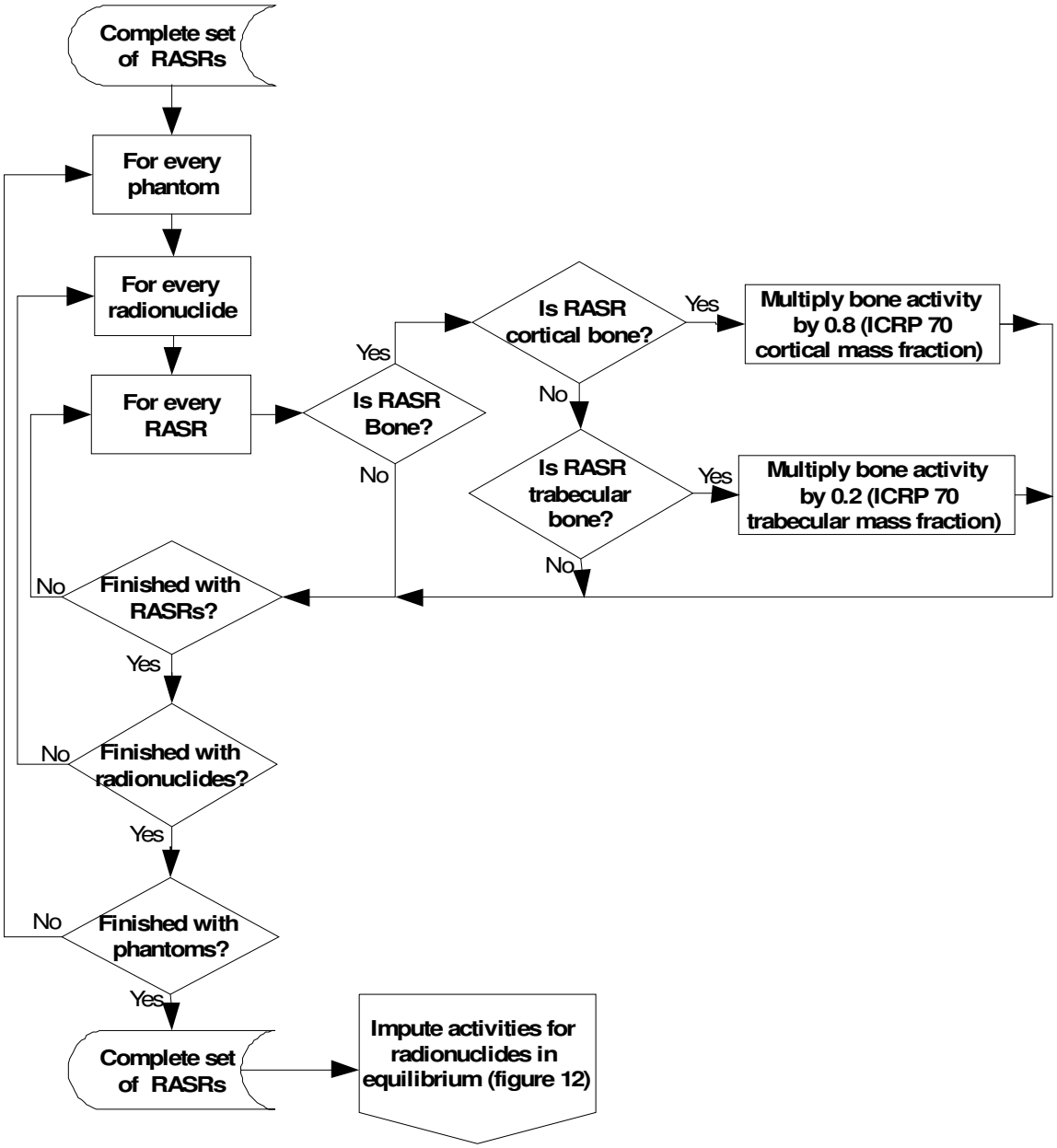

Figure 12. Method used to impute tissue concentration data in decay series. Bold text indicates activity data.

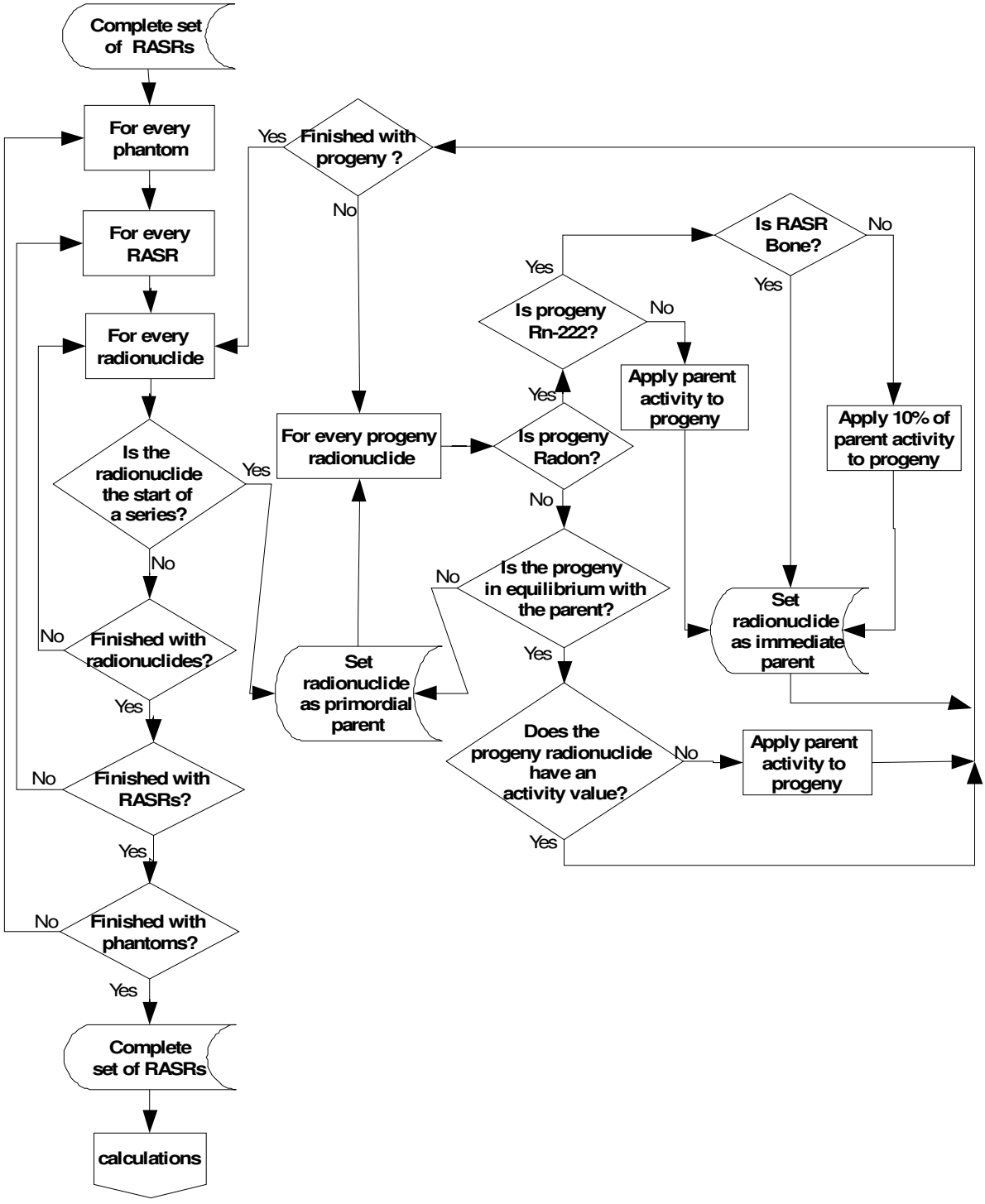

Figure 13. Changes in average annual effective doses to the RADAR phantoms from using the ICRP tissue weighting factors from 1977, 1990 and 2007.

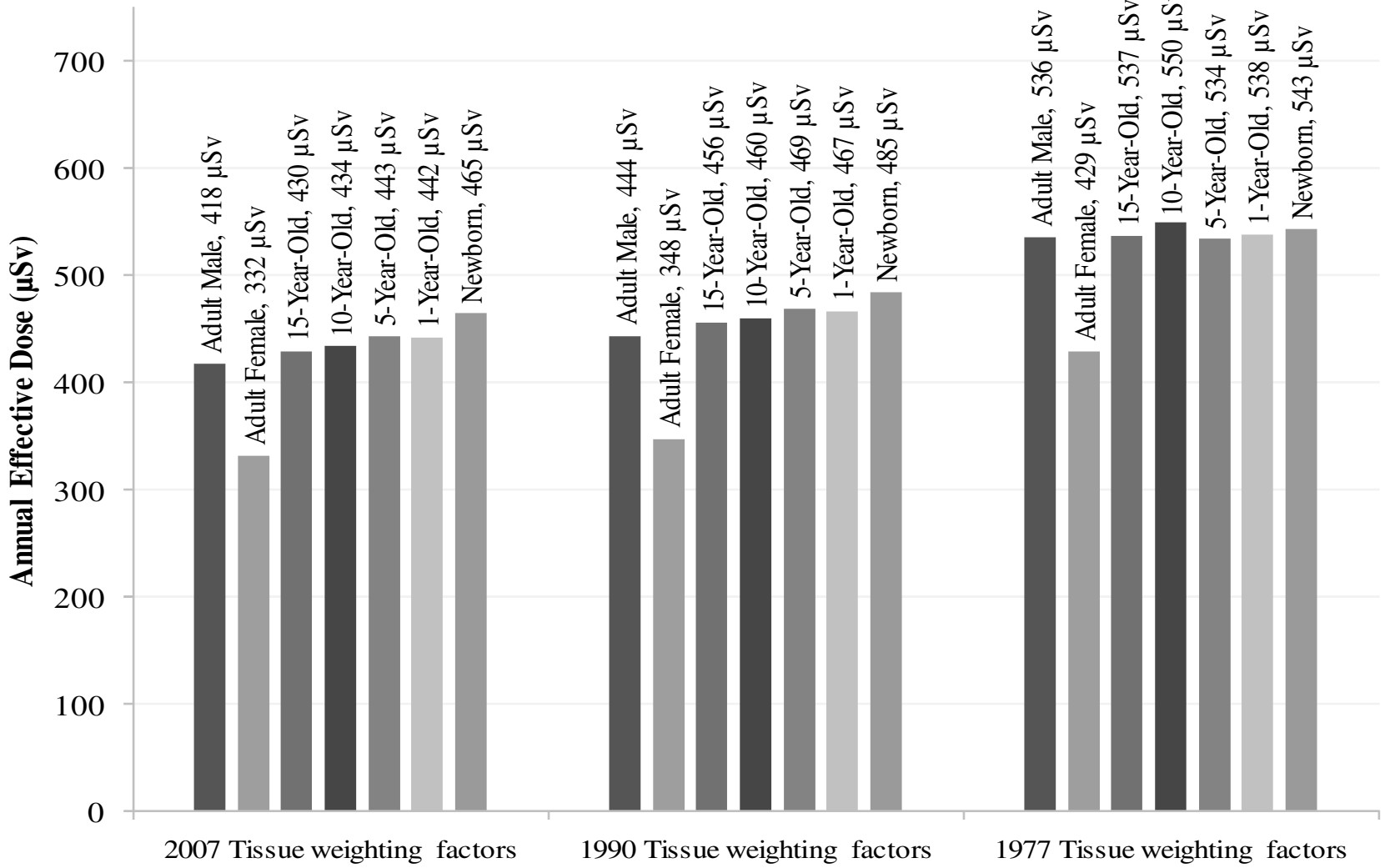

Figure 14. Contribution to the adult male average annual effective dose (418 µSv) by radionuclide using 2007 ICRP tissue weighting factors.

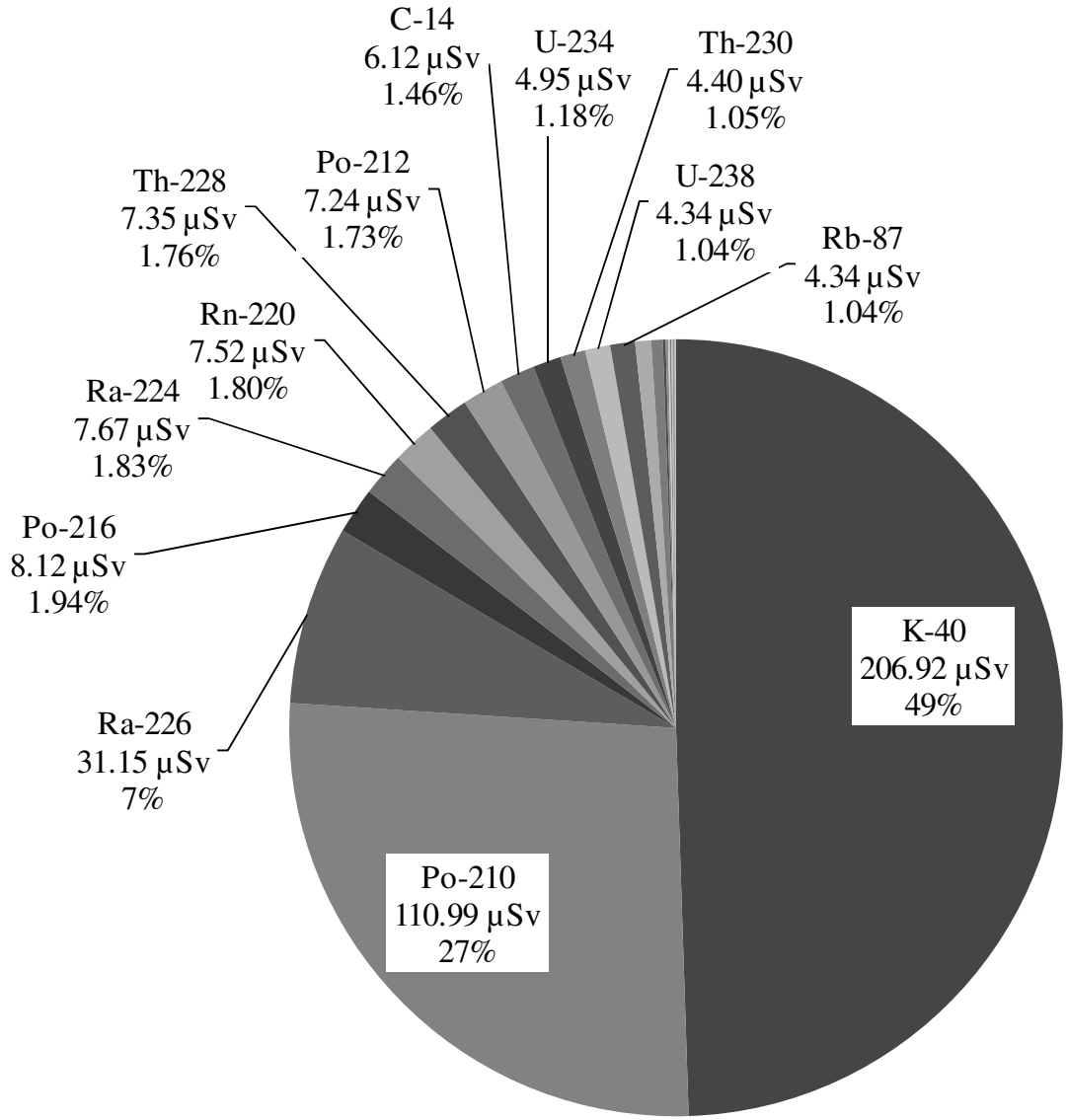

Radionuclides less than 1%	
Th-232	2.81 µSv (0.67%)
Bi-212	1.99 µSv (0.47%)
Bi-210	0.50 µSv (0.12%)
Po-214	0.46 µSv (0.11%)
Po-218	0.28 µSv (0.07%)
Rn-222	0.24 µSv (0.06%)
U-235	0.21 µSv (0.05%)
Ba-137m	0.21 µSv (0.05%)
Cs-137	0.15 µSv (0.03%)
Ac-228	0.11 µSv (0.03%)
Pb-210	0.05 µSv (0.01%)
Pa-234m	0.04 µSv (0.01%)

Figure 15. Effects of including hollow-organ contents and ^{231}Pa (+ progeny) on adult male average annual effective dose estimates using 2007 ICRP tissue weighting recommendations.

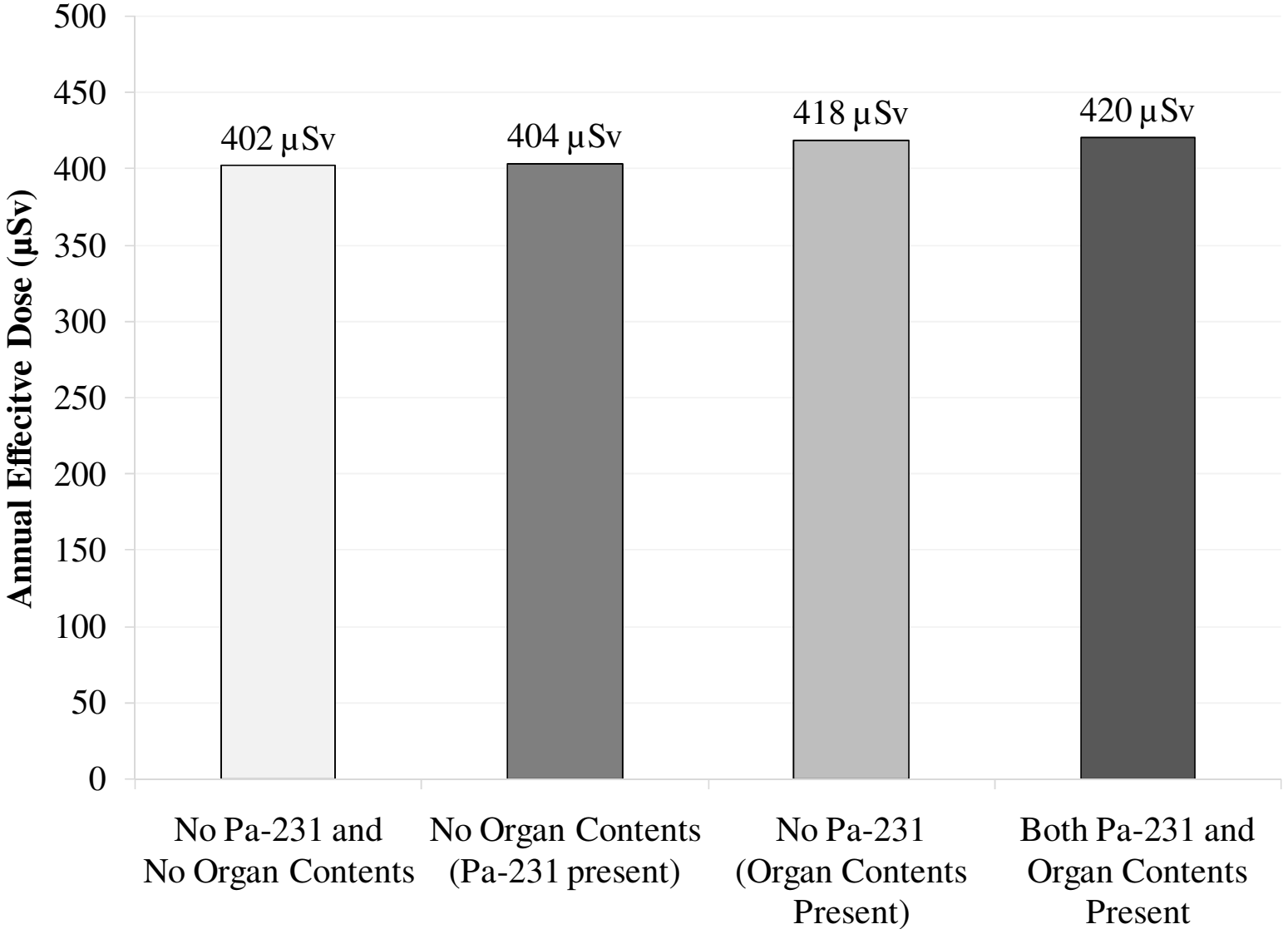

Figure 16. Comparison of average annual effective doses to an adult male calculated by the current analysis, NCRP Report No. 93, and the current analysis modified to use only data from NCRP Report No. 94. Numbers in parentheses indicate the year of the ICRP tissue weighting recommendations used in the estimate

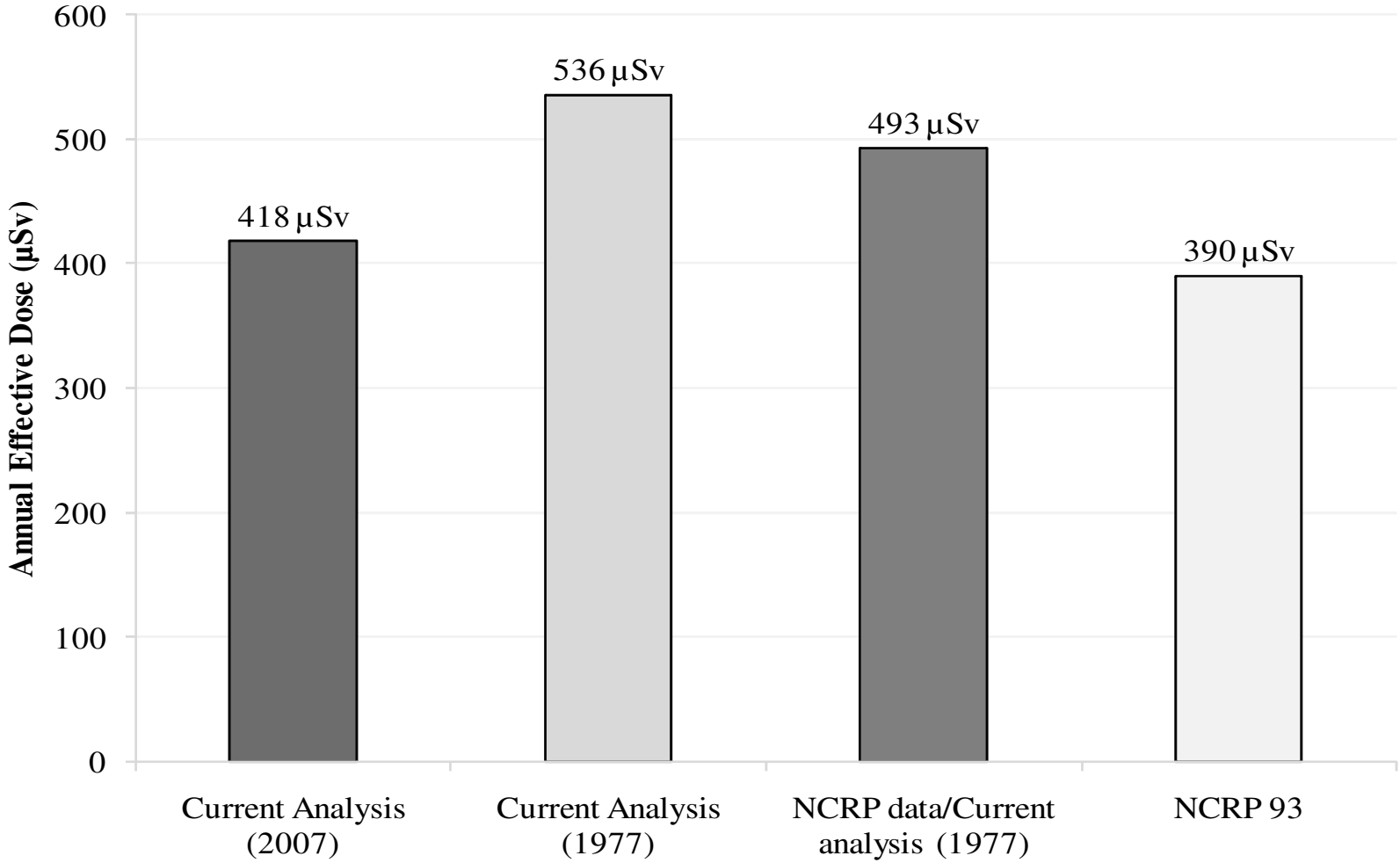

Figure 17. Average annual effective dose estimates calculated in the current analysis, by UNSCEAR (2000) and by the current analysis modified to use UNSCEAR (2000) data.

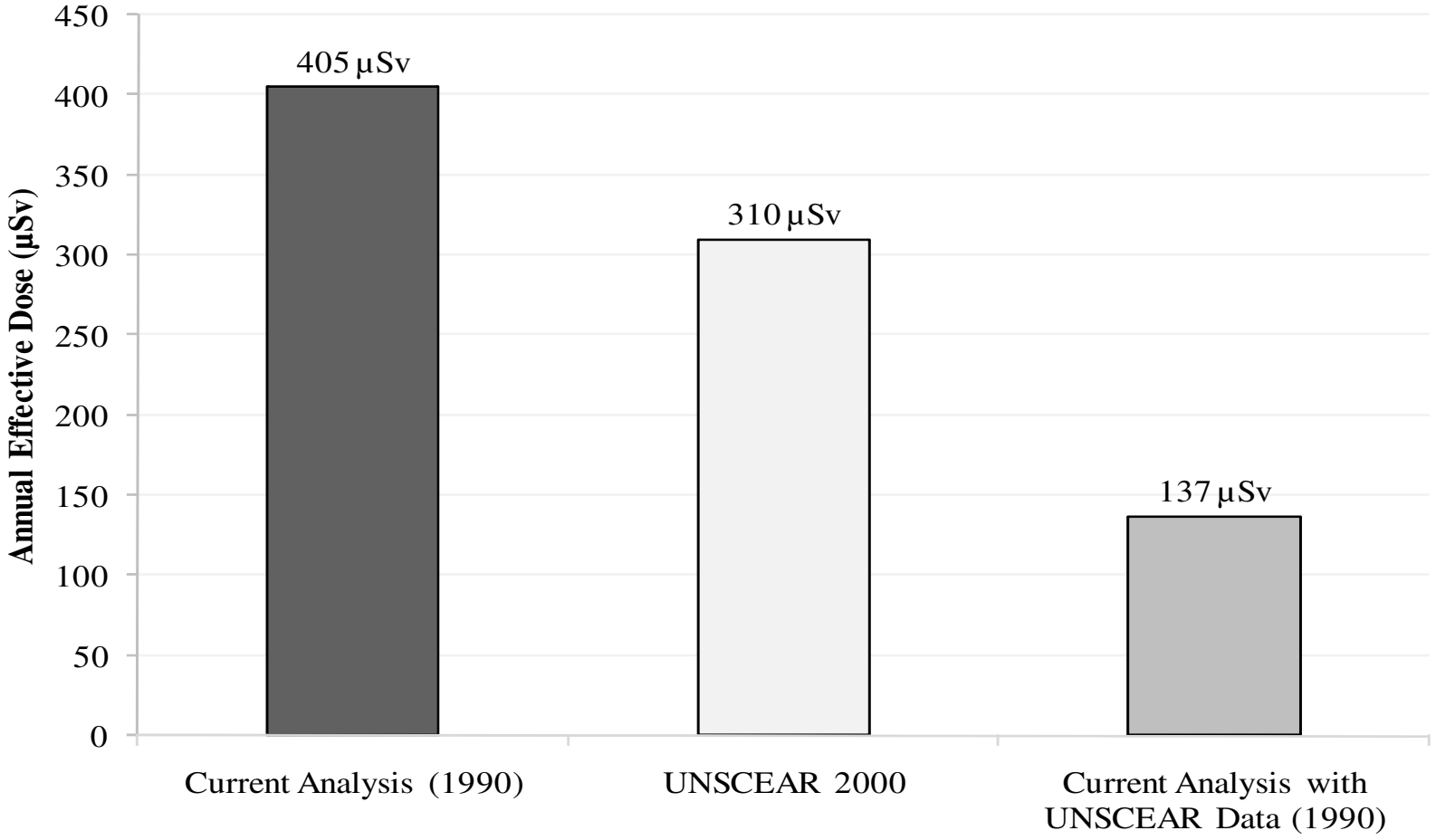

Figure 18. Effects of data variability on annual effective dose estimates. Each data point in the figure represents a ratio of the effective dose for the phantom to the effective dose of the adult male phantom. The adult male data only analysis removes age- and sex- variability from the results to illustrate effects of RADAR dose factor on annual effective dose. The entire data set is the data used for this analysis and includes age- and sex-variability.